This is to certify that the
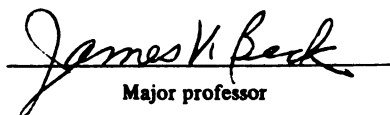
thesis entitled

On Application
of
unsteady surface element method to
thermal cavity problem

presented by

Wei-Chi Yang

has been accepted towards fulfillment
of the requirements for

Master of Science degree in *Mechanical Eng.*

James V. Beck
Major professor

Date *Jan. 10, 1986*

An APPLICATION

OF

UNSTEADY SURFACE ELEMENT METHOD TO

THERMAL CAVITY PROBLEM

BY

WEI-CHI YANG

A THESIS

Sbmitted to
Michigan State University
in partial fullfillment of the requirements
for the degree of

MASTER OF SCIENCE

Department of Mechanical Engineering

1985

ABSTRACT

An APPLICATION

OF

UNSTEADY SURFACE ELEMENT METHOD TO

THERMAL CAVITY PROBLEM

BY

WEI-GHI YANG

The unsteady surface element method (USEM) is a new numerical, systematic method for solution of transient, linear heat conduction problems. The method is developed from Duhamel's integral and the principle of superposition. It involves a set of Volterra integral equations, one for each element.

From the development of USEM, another method called the quasi-steady state method is obtained and is an unique contribution presented herein. It involves a set of linear algebraic equation, one from the energy conservation principle, others from interface conditions between connected geometries. The quasi-steady state thermal behavior can be obtained without the knowledge of the transient thermal behavior.

To show the advantages of the USEM, it is applied to the thermal cavity problem which is described in Chapter 2. In this thesis, one-,

three-, and five-node solutions of USEM are used to analyze the problem instead of several hundred elements required by finite difference. It is found that very high accuracy is attainable with a relatively small number of surface elements.

TABLE OF CONTENTS

LIST OF TABLES

v

LIST OF FIGURES

LIST OF SYMBOLS

c	Thermal capacity of the material
c_T	Thermal capacity of the thermocouple
erfc(.)	Completary error function
E	Distance between the top of thermocouple and the materail surface
$E_n(.)$	Exponential integral function
$J_i(.)$	Bessel function of first kind with order i
k	Thermal conductivity of materail
k_T	Thermal conductivity of the thermocouple
n	Number of surface elements
q_0	Constant heat flux
q_j	Heat flux through element j
r	Radial coordinate
R	Radius of the thermocouple
t	Time
t^+	Dimensionless time $(= \alpha t/E^2)$
T	Temperature
T^+	Dimensionless temperature $(= T/(q_0 R/k))$
T_0	Temperature at the top of thermocouple
$T_{0\infty}$	Temperature at the heated surface of a semi -infinite body due to a unit step heat flux on the surface

T_h	The temperature at the hot spot
z	Axial coordinate
z^+	Dimensionless z (= z/E)
ρ	Density of material
ρ_T	Density of the thermocouple
θ^i_{jk}	Influence function
α	Thermal diffusivity of material

CHAPTER 1

INTRODUCTION TO UNSTEADY SURFACE ELEMENT METHOD

1.1 Introduction

1.1.1 What is Unsteady Surface Element Method

The unsteady surface element method (USEM) is a new numerical, systematic method for the solution of transient, linear heat conduction problems. This method utilizes an integral formulation to describe the heat flow rather than a differential one. USEM will be used in this thesis to solve the thermal cavity problem which is described in Chapter 2. In the process of solving this problem, new aspects of the USEM will be developed.

1.1.2 Characteristics of USEM Compared with Other Related Method

1) In the USEM only the interface between two connected geometries needs discretization as opposed to discretization of the whole domain in the finite element (FE) and finite difference (FD) methods or discretization of the whole boundary in the boundary integral method (BIM). So the first characteristic of the USEM is that it is especially suitable for the bodies having infinite or semi-infinite domains. It can reduce both the size of the numerical calculations and the computer time.

2) The second characteristic is that it is suitable for problems

for which the area of contacting surface between two geometries is finite.

3) The third characteristic is that it is appropriate for the problem if the number of locations of interest is limited. In FD and FE methods the solution at all internal nodes is unavoidably generated, whether or not this information is needed.

4) A difficult part in the USEM is finding the influence function (kernel or building block) of the heat flow integral equation derived from the USEM. Many new influence functions are given herein.

5) It is appropriate for problems having temperature- independent thermal properties.

6) It is suitable for the linear heat conduction equation with linear or nonlinear boundary conditions.

1.1.3 Motivation

The usual type of problem solved by using USEM is two similiar or dissimiliar bodies contacting over part of their surface boundaries [1-4]. To extend the area of applications of this method the geometry considered in this thesis is a semi-infinite body in which a thermocouple is inserted as shown in Figure 1.1.

Another motivation is to compare the results given by the FD method [5] to show the characteristics of USEM.

a) The USEM can cover more extensive time domains of the transient solution than the FD method.

b) The quasi-steady state method is developed via the USEM. It is a unique contribution presented herein.
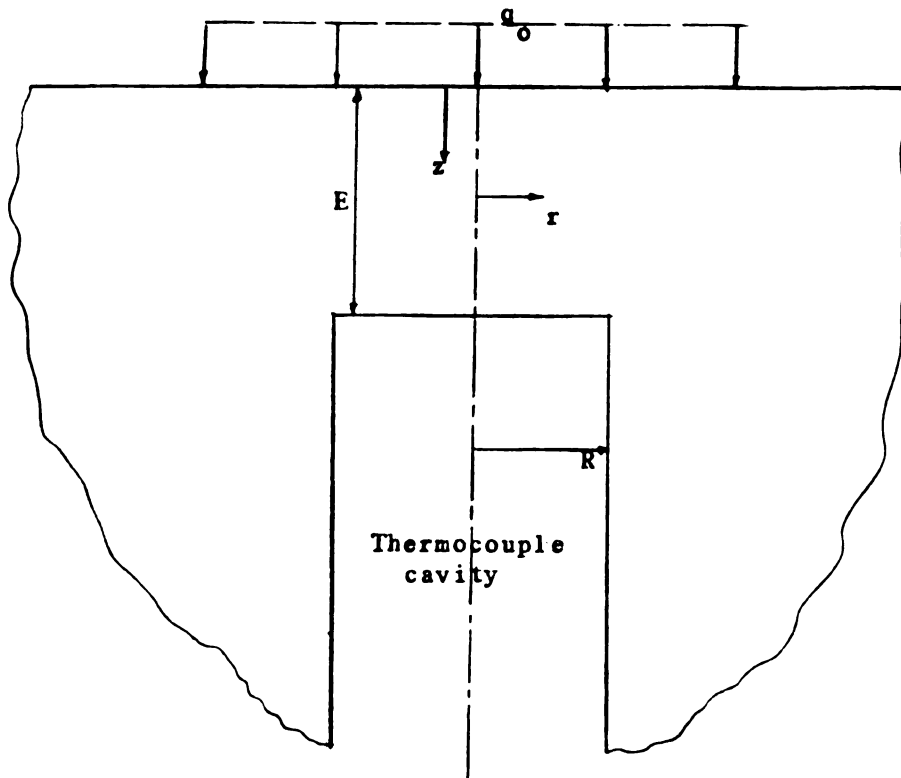
Figure 1.1 Geometry of the thermal cavity problem

1.2 Discussion Of USEM

1.2.1 Basic Equations

The USEM is developed from Duhamel's theorem. Duhamel's theorem provides a means for solving heat conduction problems with time-dependent boundary conditions by utilizing the corresponding solution of time-independent boundary conditions.

For example, a problem of heat conduction with one time-dependent boundary condition is

$$v^2 T(r,t) = (1/a)\partial T(r,t)/\partial t \qquad \text{in region R and } t>0 \qquad (1-1a)$$

$$k_i \partial T/\partial n_i + h_i T = \delta_{ji} f_i(t) \qquad \text{on boundary } S_i \text{ and } t>0 \qquad (1-1b)$$

$$T(r,t) = 0 \qquad \text{at } t=0 \text{ in region R} \qquad (1-1c)$$

where δ_{ji} is the delta function which is equal to 1 only when $i=j$.

The corresponding auxiliary problem is taken as

$$v^2 \theta(r,t) = (1/a)\partial\theta(r,t)/\partial t \qquad \text{in region R and } t>0 \qquad (1-2a)$$

$$k_i \partial\theta/n_i + h_i\theta = \delta_{ij} \qquad \text{on boundary } S_i \text{ and } t>0 \qquad (1-2b)$$

$$\theta(r,t) = 0 \qquad \text{for } t=0 \text{ in region R} \qquad (1-2c)$$

Then from Duhamel's theorem $T(r,t)$ can be expressed in terms of $\theta(r,t)$ [6] as

$$T(r,t) = \int_{\tau=0}^{t} f_i(\tau)(\partial\theta(r,t-\tau)/\partial t)d\tau \qquad (1-3)$$

where $f_i(t)$ is the forcing function in (1-1b).

If there is more than one time-dependent boundary condition, the principle of superposition can be used. The number of separate problems is equal to the number of time-dependent boundary conditions. If there are n time-dependent boundary conditions, the temperature can be expressed as

$$T(r,t) = \sum_{i=1}^{n}\int_{\tau=0}^{t} f_i(\tau)(\partial\theta_i(r,t-\tau)/\partial t)d\tau \qquad (1-4)$$

For each $\Theta_i(r,t)$ there are a corresponding field equation, boundary and initial conditions (1-2) to be satisfied.

The influence function of the corresponding heat conduction problem is denoted as Θ. If f_i represents temperature, Θ is called the temperature based influence function. If f_i represents heat fluxes, Θ is called the heat-flux based influence function. For many geometries the influence function are known or can be obtained simply by analytical or numerical procedures. In this thesis the influence functions are all based on the heat flux.

1.2.2 How to apply Duhamel's theorem in USEM

In applying the USEM, the interface condition between two connected geometries is used to combine the temperature integral equations for the point on the interface derived from Duhamel's theorem and the principle of superposition. In Figure 1.2, the thermal cavity problem, point 1 belongs to body 1 and body 2. Body 1 is a solid cylinder with radius R and height E. Body 2 is a semi-infinite body outside a cylindrical void with radius R. Body 3 is a semi-infinite cylindrical void with radius R.
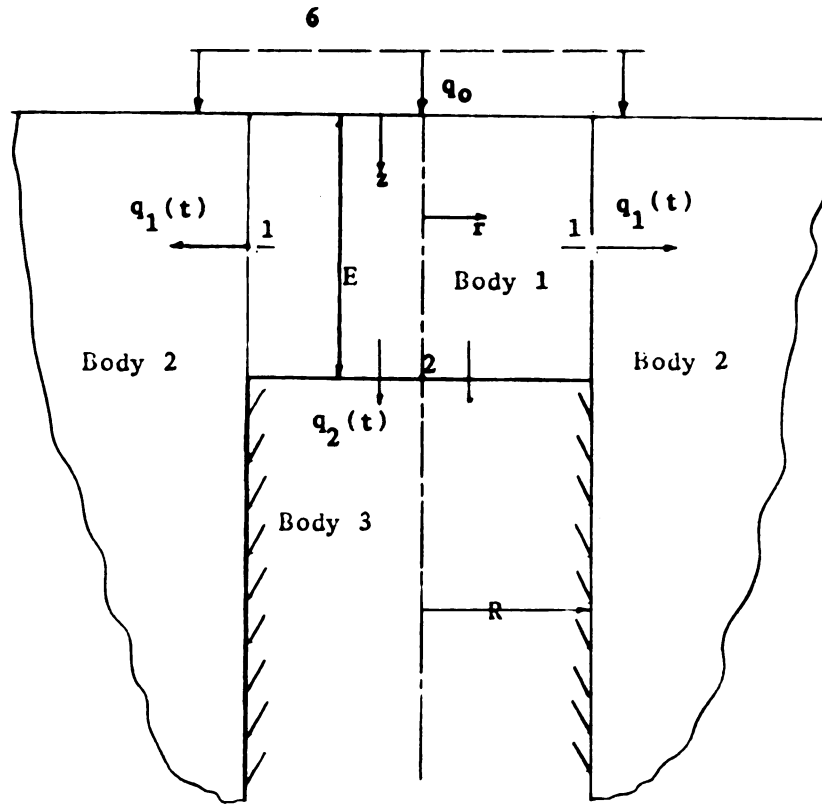
Figure 1.2 Possible discretization fot the thermal

cavity problem

For body 1 as shown in Figure 1.3, the temperature at point 1 can be expressed by Duhamel's theorem and the principle of superposition

$$T_1^1 = \int_0^t q_0 \partial\theta_{10}^1/\partial t \, d\lambda - \int_0^t q_1 \partial\theta_{11}^1/\partial t \, d\lambda - \int_0^t q_2 \partial\theta_{12}^1/\partial t \, d\lambda \qquad (1-5)$$

where q_0, q_1 and q_2 are heat flux histories and are assumed uniform in space, but may be function of time; $q_0(t)$ is known value.

For body 2 as shown in Figure 1.4, the temperature at point 1 can be expressed as

$$T_1^2 = \int_0^t q_0 \partial \Theta_{10}^2 / \partial t\, d\lambda + \int_0^t q_1 \partial \Theta_{11}^2 / \partial t\, d\lambda \qquad (1.6)$$

where the radial surface of body 3 is assumed to be insulated, Θ_{ji}^k is the temperature rise at point j of body k due to unit heat flux q_i and is called the heat-flux based influence function.
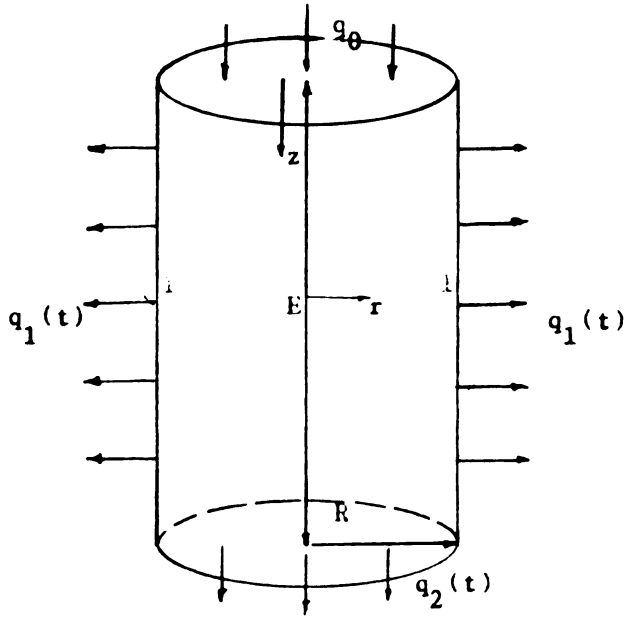
Figure 1.3 Geometry of body 1.   Figure 1.4 Geometry of body 2.
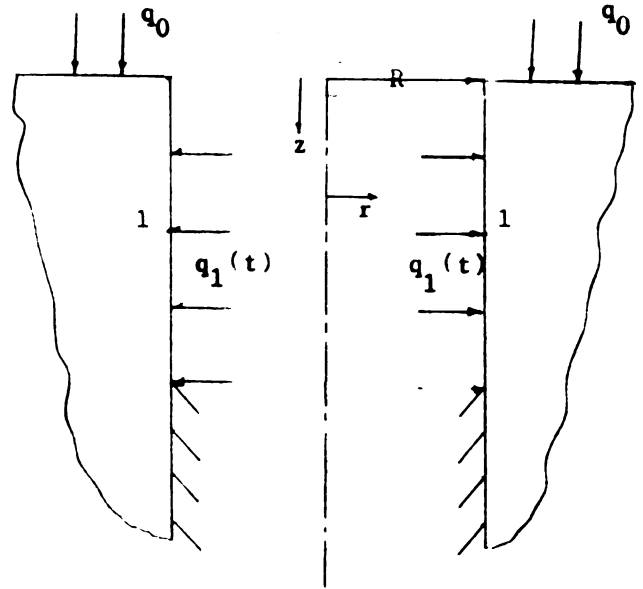
From the interface condition, equations (1.5) and (1.6) are the same because there is no physical boundary between body 1 and body 2. Then combine (1.5) and (1.6) to get

$$\int_0^t q_0 [\partial (\Theta_{10}^1 - \Theta_{10}^2) / \partial t]\, d\lambda = \int_0^t q_1 [\partial (\Theta_{11}^1 + \Theta_{11}^2) / \partial t]\, d\lambda + \int_0^t q_2 \partial \Theta_{12}^1 / \partial t\, d\lambda \quad (1.7)$$

where in some simple cases influence functions can be found in [7] and

[8]. For more complex boundary conditions Green's functions can be used to calculate the influence function. The use of Green's functions in the procedure of calculating influence functions are given in the Appendices. Equation (1.7) is an integral equation for heat flow for the thermal cavity problem. The heat fluxes $q_1(t)$ between bodies 1, 2 and $q_2(t)$ between bodies 1 and 3 are uniform in space, but are functions of time. Equation (1-7) is a one-node integral equation of heat flow. The left hand side of (1-7) is known and the right hand side contains $q_1(t)$ and $q_2(t)$, two unknown functions. If the thermocouple is insulated, $q_2(t)$ is equal to 0 and (1.7) is an integral equation with one unknown function, $q_1(t)$. This case will be dicussed in chapters 4 and 5. If the thermocouple is not insulated, another interface condition between body 1 and body 3 is needed. By using a similiar procedure, the temperature at point 2 can be expressed in two different forms. After the consideration of interface condition between body 1 and body 3, there are two equations with two unknowns (ie. $q_1(t)$ and $q_2(t)$). The influence of the thermal properties of thermocouple will be considered in Chapter 5.

Equation (1.7) can be simplifed by Laplace transform or Stolz's method. Both methods will be used in this thesis. Laplace transform will be introduced in Chapter 4 and Stolz's method will be given in Chapter 5.

1.3 Literature Review

N. R. Keltner and J. V. Beck [1] published the first paper discussing the USEM. The authors used USEM to solve the intrinsic thermocouple problem which is a semi-infinite cylinder (wire) attached perpendicular to the semi-infinite solid (subtrate) as shown in Figure 1.5. In this paper the transient thermal behavior of the interface between the thermocouple wire and the subtrate due to a unit temperature change in the subtrate was investigated by using the one-node USEM. This resulted in a single integral equation to solve. The authors used both the temperature based and heat-flux based USEM to get the integral equation and solved it analytically by utilizing Laplace transforms. A comparison was made with existing analytical and numerical solutions given by other investigators. The results show excellent agreement between the one-node USEM and other solutions. An advantage of USEM is that only one node was needed in the interface and the results can be easily obtained without the need of a computer.

J. V. Beck and N. R. Keltner [2] discussed the problem of two semi-infinite bodies contacting over a circular area by using one-node USEM as shown in Figure 1.5. Both the temperature and heat-flux based USEM were employed. In this paper the perfect as well as imperfect contacting conditions were considered. The authors used the Laplace transform to simplify the integral equation derived from USEM.
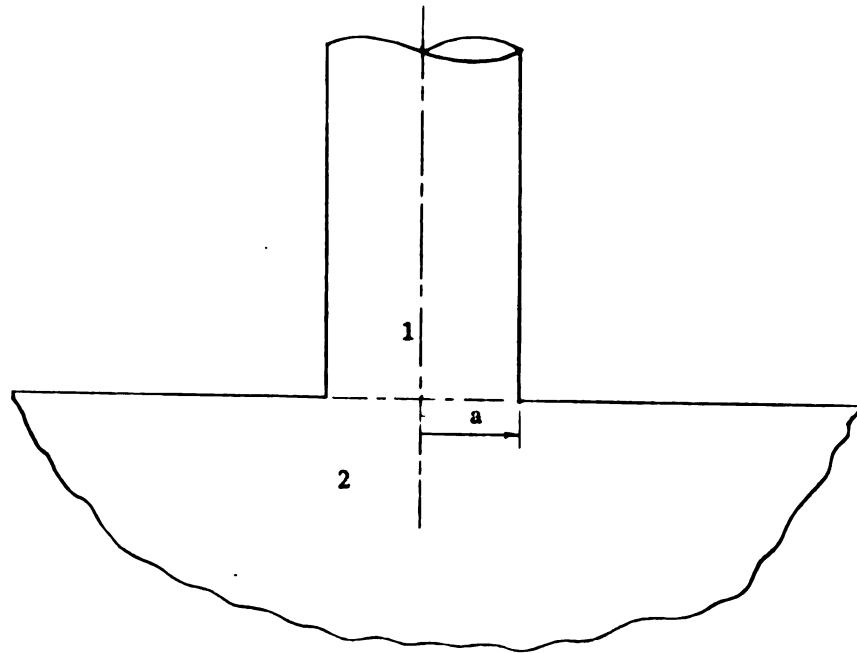
Figure 1.5 The geometry for the intrinsic thermocouple
problem
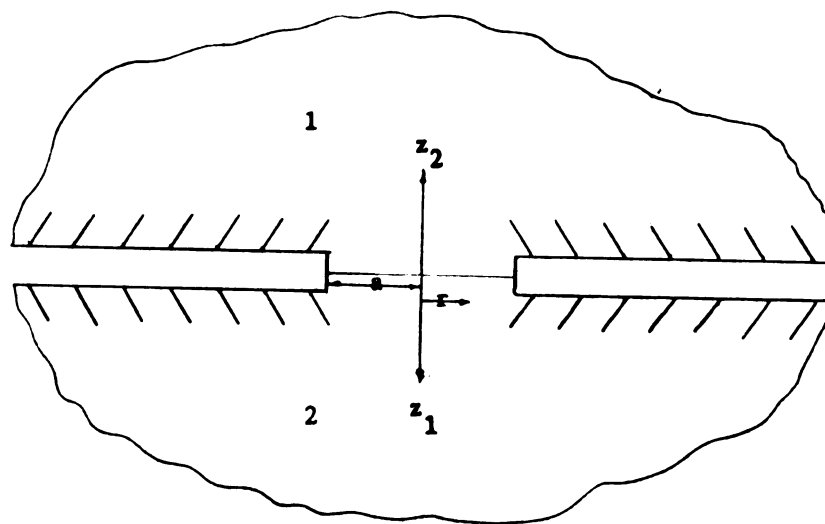
Figure 1.6 The geometry of thermal contact conductance
problem between two semi-infinite body.

B. Lithouhi and J. V. Beck [3] published the first paper discussing the mulitnode USEM for two arbitrary bodies contacting over part of their surface boundaries. To demonstrate the capability of this method, it was applied to the problem of two semi-infinite bodies initially at two different temperatures suddenly brought into perfect contact over a small circular region. The temperature at the interface was expressed in the form of an integral equation with space and time variables by utilizing Duhamel's theorem and the principle of superposition. In order to solve numerically the integral equation given by USEM, both the space and time domains was subdivided into small elements. Then, the integral equations were transformed into a set of algebraic equations by Stolz's method of constant heat flux in each time step. The heat flux and temperature for each element of the interface can be obtained step by step in time.

B. Lithouhi and J. V. Beck [4] discussed the same problem as [1] by using the multinode USEM. In multinode USEM the single numerical solution contains the whole time domain.

1.4 Outline of the Thesis

Chapter 2 describes the thermal cavity problem and gives the mathematical model and literature review. Both the integral equations derived by USEM and algebraic equations derived by the quasi-steady state method for the thermal cavity problem are given in Chapter 3. The procedure and results of the one-node USEM using Laplace transforms

is included in chapter 4. Chapter 5 gives the procedure and results of one-node USEM with Stolz's method. The influence of thermal properties of thermocouple on the temperature measurements is considered in this chapter. Chapter 6 describes the procedure and results of three-node USEM with Stolz's method. The five-node quasi-steady state solution is given in Chapter 7. Chapter 8 gives the conclusions from the results of thermal cavity problem by the USEM. Appendices include the derivation of influence functions needed in the thermal cavity problem.

CHAPTER 2

INTRODUCTION OF THE PROBLEM

2.1 Introduction

In many dynamic heat transfer situations, temperature measurements are used to determine surface heat flux. In this thesis the temperature is considered to be measured by a thermocouple which is located in a cylindrical hole normal to the heated surface as shown in Figure 1.1. The analysis is concerned with the case in which the thermocouple possesses much lower thermal properties than its surrounding material. Due to the existence of the thermocouple, the temperature distribution is disturbed. In turn the temperature measurements obtained from the thermocouple are different from those would exist if the thermocouple were not present. By modeling the heat transfer associated with the thermocouple, it is possible to develop corrections for the temperature measurements. One purpose of this thesis is to present an analysis for a thermocouple located as shown in Figure 1.1.

2.2 Motivation

One motivation is to improve and extend the transient solution given by the finite difference (FD) method [5]. Because the body is semi-infinite, the number of FD elements needed to analyze the problem becomes greater as time increases. The dimensionless time ($t^+=\alpha t/E^2$),

where α is the thermal diffusivity of the material and E is the distance between the top of thermocouple and the surface of material, was used only up to 30 for the FD method. Since in the USEL the time domain of the transient solution can be any value, this method can be used to contain a larger time domain for the transient temperature histories.

2.3 Objectives

1) The first objective is finding the transient temperature at the top of the thermocouple as well as at the hot spot, which is at the heated surface right above the thermocouple, of the thermal cavity problem as shown in Figure 1.1.

2) The second objective is to determine the "null point" [5]. In order to obtain an accurate surface temperature history, the thermocouple has to be placed at some distance below the surface. The temperature difference between the top of thermocouple and undisturbed heated surface (ie. without the thermocouple) is the function of dimensionless time ($t^+ = \alpha t / R^2$) and $g(=R/E)$. So, one objective of this thesis is to determine the value of g that makes the temperature difference between the top of thermocouple and undisturbed heated surface zero at time infinity. The location at which the temperature difference is zero at time infinity is call the "null point". It is the location at which the thermocouple should be placed in order to measure directly the surface temperature with the highest accuracy.

3) The third objective is to find the quasi-steady state tempera-

ture disturbance at the top of thermocouple and the hot spot directly by the quasi-steady state method, and then to compare with the results extrapolated from the transient solution by USEM. It is a unique contribution presented herein. The detailed description and procedure will be given in Chapter 3.

4) The fourth objective is to find the needed influence functions of USEM. These function are derived in the Appendices.

5) The fifth objective is to find the influence of the thermal properties of thermocouple on the temperature measurements. It will be discussed in Chapter 5.

2.4 Mathematical Model

A thermocouple embedded in the heat sink, which has a much higher thermal conductivity than the thermocouple, disturbs the surrounding temperature. The maximum temperature disturbance would be caused by replacing the thermocouple with an insulated cylindrical void with radius R and the distance E beneath the surface and perpendicular to the surface as shown in Figure 2.1.

The heat conduction equation in cylindrical coordinates is:

$$\partial^2 T/\partial z^2 + 1/r \partial(r \partial T/\partial r)/\partial r = 1/\alpha \partial T/\partial t \tag{2-1}$$

The boundary and initial conditions for the insulated cylindrical thermal cavity problem are:

$$k\partial T(0,r,t)/\partial z = -q_o(t) \tag{2-2}$$

$$\partial T(E,r,t)/\partial z = 0 \qquad r < R \tag{2-3}$$

$$\partial T(z,R,t)/\partial r = 0 \qquad z > E \tag{2-4}$$

$$T(z,r,0) = 0 \tag{2-5}$$

where k is the thermal conductivity of the material, α is the thermal diffusivity, and E is the distance between the top of thermocouple and the heated surface.
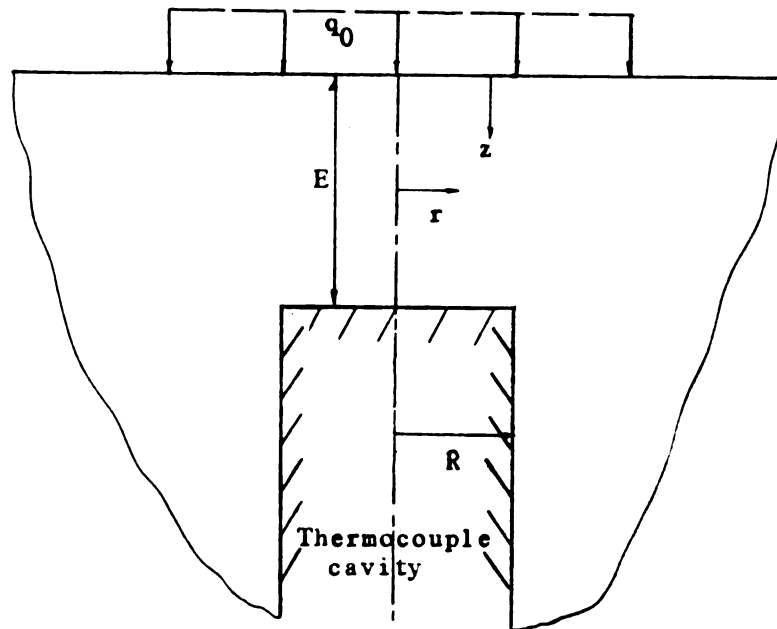
Figure 2.1 Geometry of the thermal cavity problem

with an insulated thermocouple.

For the surface element method, the assumption of an insulated

cylindrical void is not necessary.   It will be discussed in chapter 5.

2.5 Literature Review

The effect of thermocouple on the material   temperature distribution,   which has   a finite   depth   L   shown   in Figure 2.2, was first investigated by Masters and Stein [9] who effectively used the superposition principle.
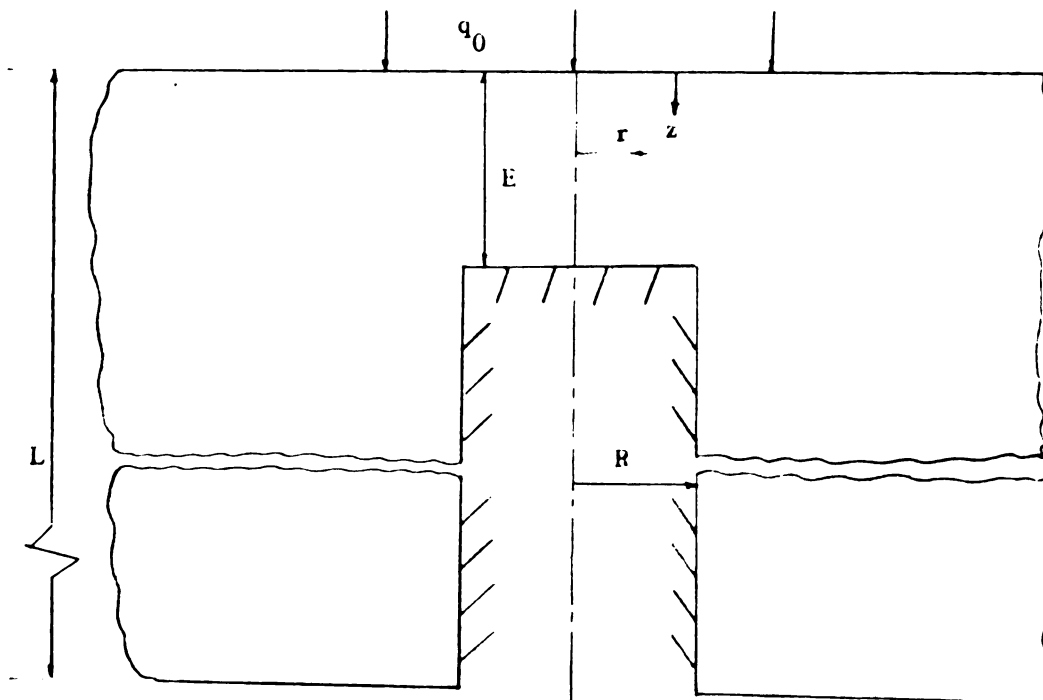
Figure 2.2 Boundary conditions and dimensions for the

thermal cavity problem [9]

The heat sink with a surface heat flux was   first   considered   with   an

F

imaginary void shown in Figure 2.3. The heat flux $q_e(t)$ passing through the imaginary void was determined. Consider now the heat flux $q_e(t)$ introduced into the negative z-direction from z=E circular plate into a finite body as shown in Figure 2-4. If the boundary conditions in Figure 2.3 and 2.4 are superimposed upon each other, the boundary conditions due to the thermocouple effect can be obtained. This change in boundary conditions still does not permit an analytical solution. Masters and Stein were able to find an analytical solution of the temperature response at the hot spot for a uniform heat flux for g(=R/E) of .25, .5 and 1 by assuming the heat rejected from the top of the void to diffuse only in the infinite plate (L=∞) of thickness E.

Figure 2.3 Boundary condition for one-dimension heat flow

Figure 2.4 Boundary condition for the thermocouple error

Bussell [10] also investigated and obtained the temperature at the hot spot for g=1.5 by using a passive element analog.

J. V. Beck and R. Hurwicz [5] employed the finite difference method for the thermal cavity problem with the assumption of an insulated thermocouple. Because the heat sink is a semi-infinite body, the number of elements needed to analyze the problem becomes greater as time increases. For this reason the duration of the transient solution was limited to a dimensionless time of $t^+ (=\alpha t/E^2)=30$.

J. V. Beck and R. Hurwicz employed a different method to determine both the quasi-steady state dimensionless temperature at the top of thermocouple and at the hot spot. The results are shown in Figure 2.5 and 2.6. As a result of the steady state disturbance, a "null point" is located at which location the thermocouple gives the undisturbed surface temperature with minimun error. The position suggested by the authors was at g=1.1.

C. J. Chen and Peter Li [11] also discussed the problem of temperature distortion in thermocouple cavity. The geometry is shown in Figure 2.7 in which a disk with thickness D is inserted a cavity of diameter d below the heated surface with distance e. The heat flux Q is assumed to be constant and the upper surface of the disk is considered to be insulated. A thermocouple with radius d_t is welded onto the cavity base. The portion of the cavity not filled by the thermocouple was filled with air or insulating meterial. The basic idea of eliminating or minimizing the temperature distortion by the finite

element method is based upon the proper choice of the thermocouple material and thermocouple size, which has a higher thermal conductivity than that of the disk.
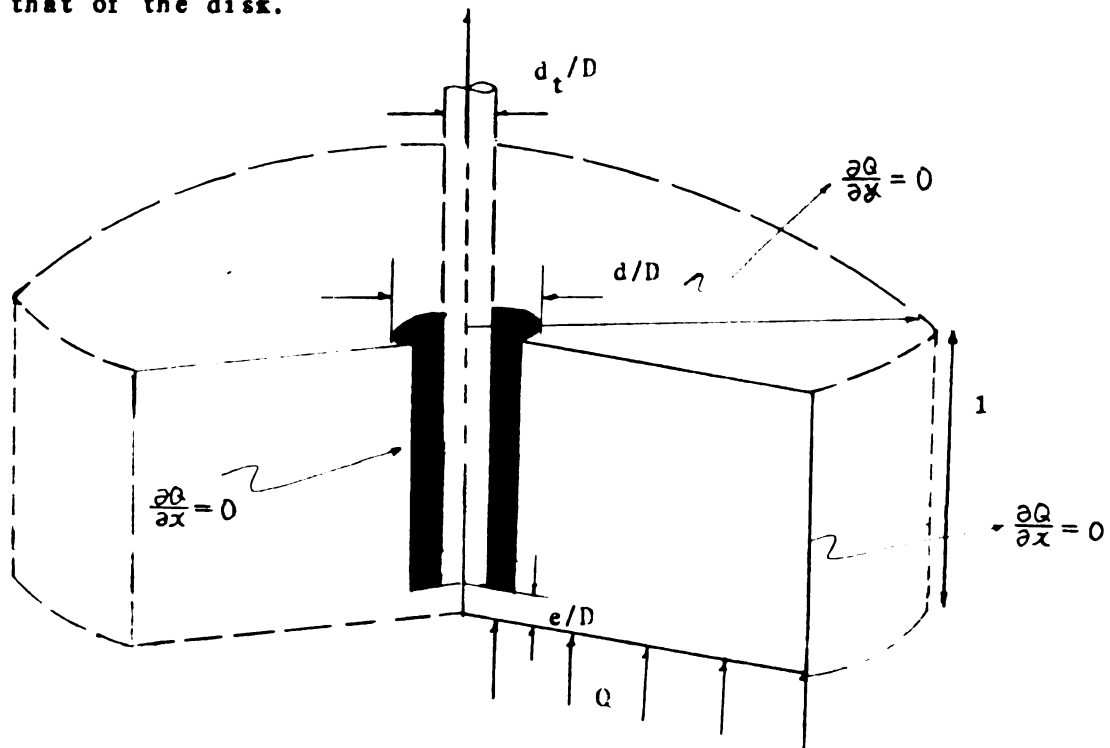
Figure 2.7 Geometry representation of problem [11]

Reference [12] gives 2 computer programs that can calculate the heat-transfer rates to the surface of a solid body using the recorded temperature response of a thermocouple. The thermocouple is located at the null-point of a transient calorimeter that is installed in the body and is configured to simulate a semi-infinite solid. The two programs and their acronyms are (1) Program for Analysis of Null Point Calorimeter Data (PANDA), and (2) Arnold Research Organization Thermal Heating Analysis (AROTHA). PANDA is a one-dimensional, implicit, finite difference solution of the inverse heat conduction problem. AROTHA is

a one-dimensional, closed form solution that uses the null point tem-
perature as the undisturbed surface temperature of a one-dimensional,
semi-infinite solid to calculate the surface heat-transfer rates.
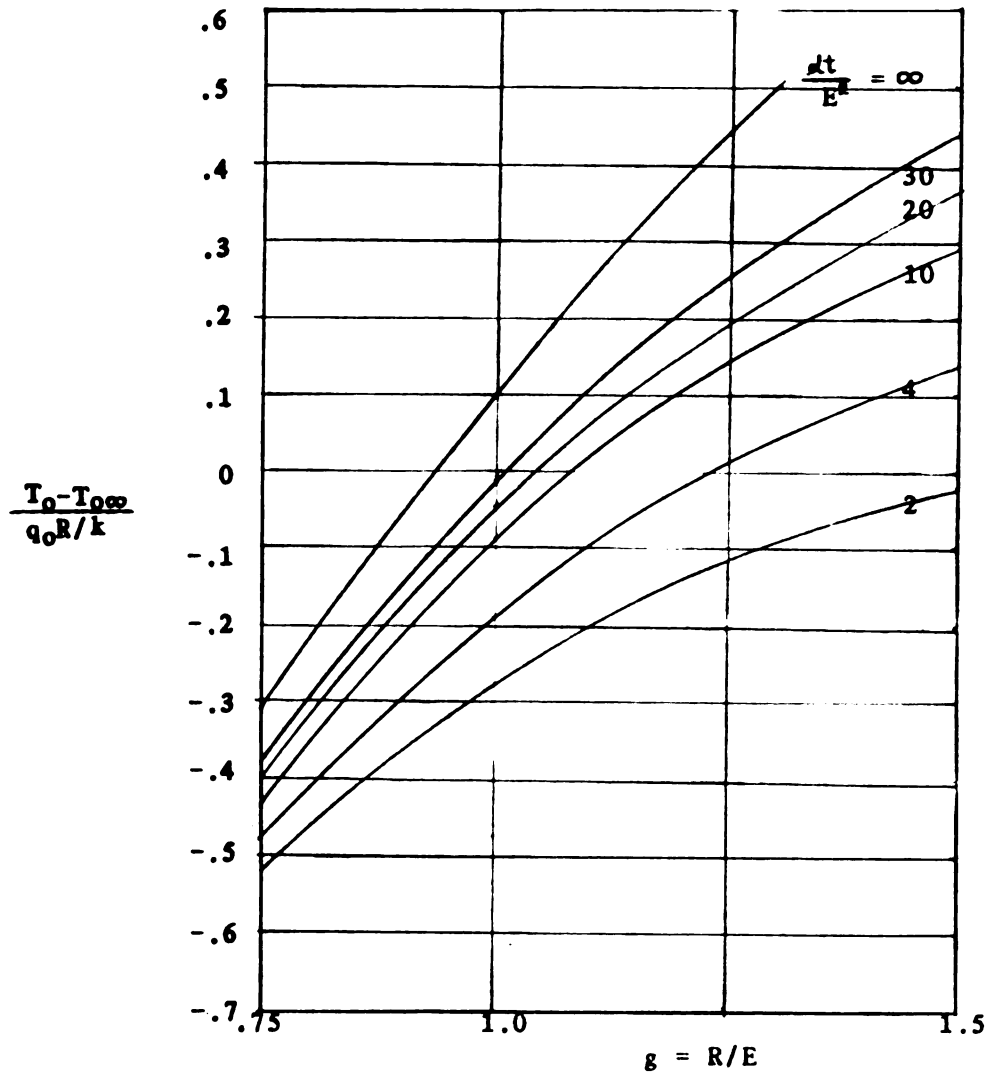
Figure 2.5 Transient thermocouple temperature

for a semi-infinite solid
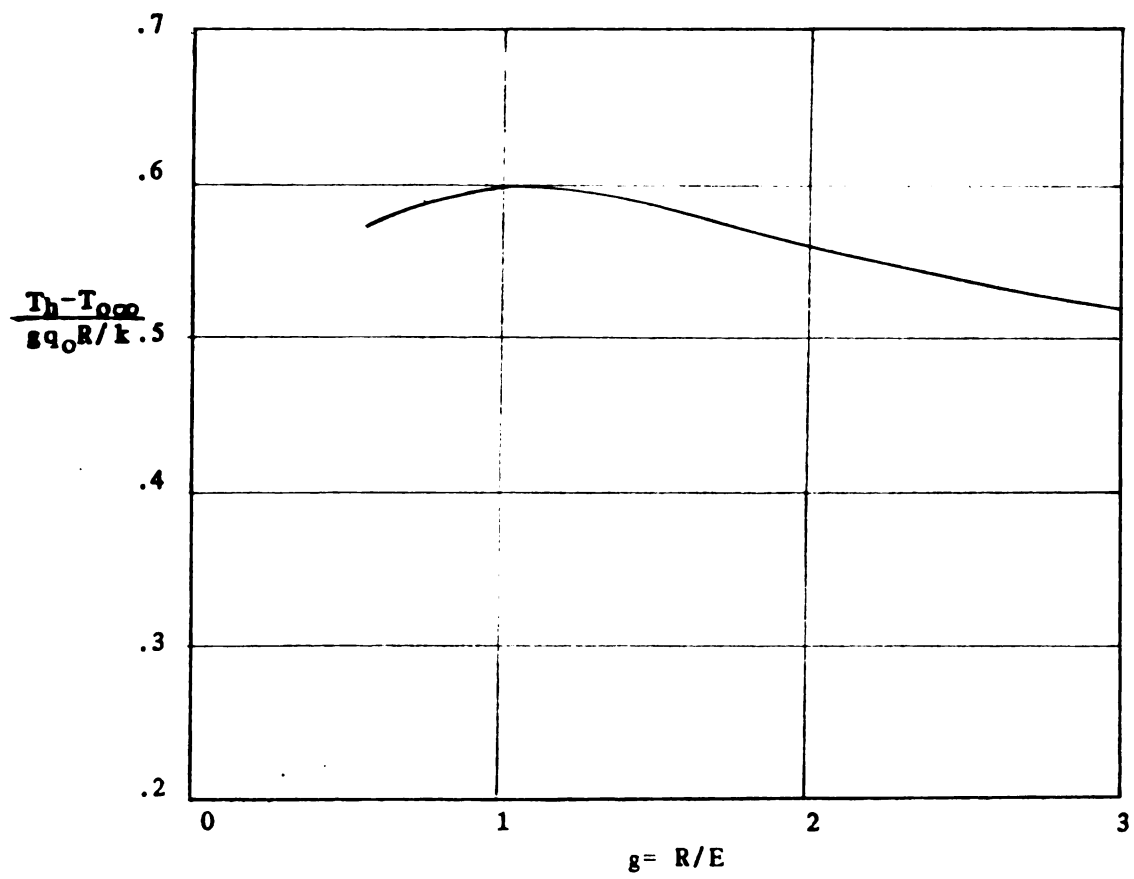
Figure 2.6 Steady state hot spot results

CHAPTER 3

TRANSIENT AND QUASI-STEADY STATE HEAT FLOW

FORMULATION DERIVATIONS

3.1 Introduction

The derivations of both the transient integral formulation and the quasi-steady state algebraic equations of heat flow for the thermal cavity problem with linear boundary conditions and perfect contact interface conditions are given in this chapter. These equations will be employed in subsequent chapters to find the transient and quasi-steady state thermal behavior for the thermal cavity problem.

Section 3.2 discusses the discretization of the interface as well as the interface conditions between connected geomtries. Section 3.3 starts with Duhamel's theorem and the principle of superposition to express the temperature integral equation at each element on the interface. The influence functions needed in the calculational procedure are also described in this section. Section 3.4 discusses the USEM by using the interface conditions to combine the temperature integral equations at the interface derived in Section 3.3. Section 3.5 derives the quasi-state state equations of thermal cavity problem; these equations have not previously been proposed.

3.2 Geometry Discretization and Interface Conditions

The outline of this section is as following: The space domain of

the thermal cavity problem is first subdivided into three basic geometries. Then interfaces between the geometries are discretized into several elements, and the number of elements is determined by the interface thermal behavior. The heat flux through each element is assumed to be constant in space. This is the basic assumption for the heat-flux based USEM. The thermal behavior of each element can be obtained either analytically or numerically. The information about the thermal behavior of each element will be used as the influence funtions in the temperature integral equations drived from Duhamel's theorem and the principle of superposition. The interface conditions are also considered in this section. Integral equations of heat flow for the thermal cavity problem will be established by these interface conditions.
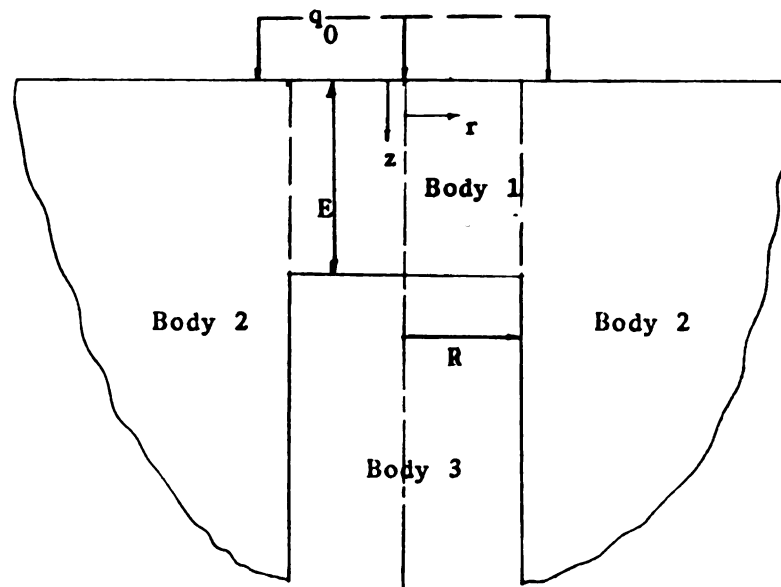
Figure 3.1 Geometries of the thermal cavity problem.

The whole domain shown in Figure 1.1 is first subdivided into three basic geometries and is shown in Figure 3.1. Body 1 is a solid cylinder with radius R and height E; Body 2 is a semi-infinite body outside a cylindrical void with radius R; Body 3 is a semi-infinite solid cylinder with radius R. Each of them contacts one another over part of the surface boundaries.

The imaginary boundary surface between body 1 and body 2, which is the radial surface of a circular cylinder with radius R and height E, is next subdivided into n finite, equally-spaced surface elements as shown in Figure 3.2. Each element has the radius R and height E/n.
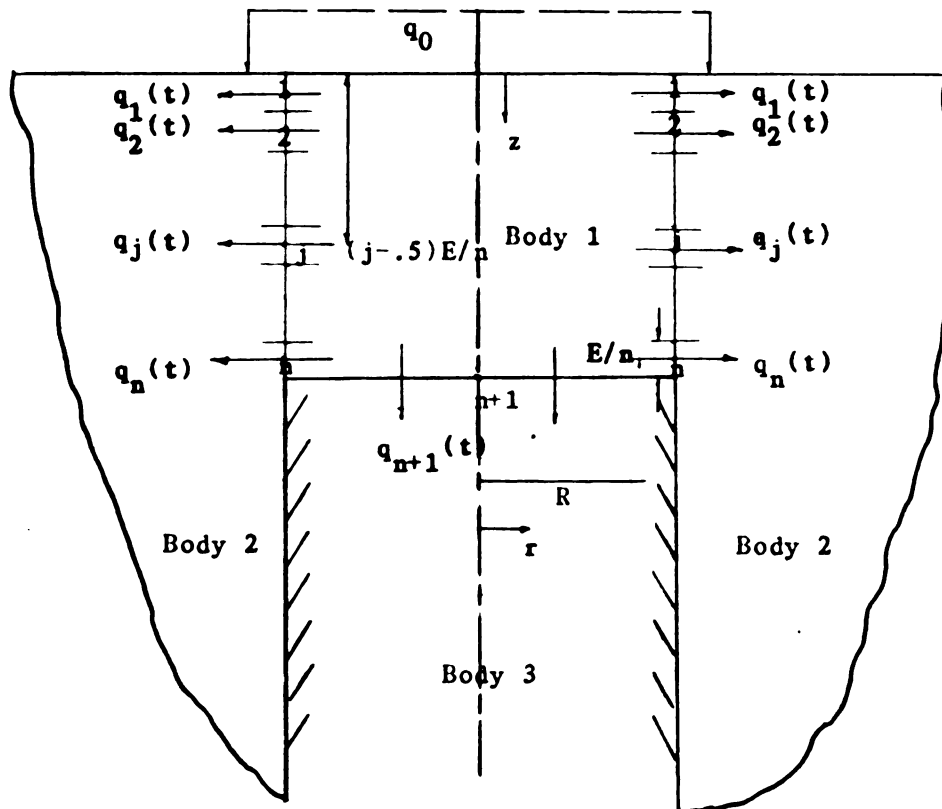
Figure 3.2 Possible distribution of surface element
for the thermal cavity problem.

By imaginary boundary means that there is no physical boundary between body 1 and body 2. The heat flux $q_j(t)$ which leaves body 1 is the same as that enters body 2 over the region from $z=z_{j-1}$ to $z=z_j$ as shown in Figure 3.2. It is assumed that there is no spatial variation of heat flux over each element. The heat fluxes $q_1(t)$, $q_2(t)$, ..., $q_n(t)$ over these n elements are arbitrary functions of time which are to be found. When this assumption of constant heat flux over element is used, the integral equations of heat flow constitute the heat-flux based USEM. The temperature based USEM [1,2] is derived using the assumption of uniform-in-space temperature over each element. Because of relatively low thermal conductivity of the thermocouple assembly compared with that of surrounding material, the heat flux passing through the interface between bodies 1 and 3, which is circular with radius R, is very small compared with that between bodies 1 and 2. For this reason there is only one element, which is the n+1th element, assigned to the interface between body 1 and body 3. One node means that the heat flux over the interface between body 1 and body 3 is uniform in space. To simplify the analysis, the radial surface of the thermocouple is assumed to be insulated. This means that the interface condition between body 2 and body 3 is insulated.

Since there is no physical boundary between body 1 and body 2, the temperature on both sides of interface are the same. Futhermore, if the thermal resistance between body 1 and body 3 is negligible, the temperature on both sides of the interface are also equal. In this thesis the case of perfect contact is considered. Note that the temperature at the center point of each element is used in the

calculational procedure. For example, the temperature at element j of body 1 means that the temperature at the location of $z=z_j-E/2n$ and $r=R$, which is shown in Figure 3.2. The center point of each element is called a node. So, node j means the center point of element j. The mathematical model for the perfect contact interface conditions can then be established as

$$T^1_j = T^2_j \qquad \text{for } j=1,2, \ldots, n \qquad (3-1)$$

$$T^1_{n+1} = T^3_{n+1} \qquad (3-2)$$

where T^k_j is the temperature at node j of body k. The next section will derive the integral expression of temperature at each node on the interface.

3.3 Temperature Expression for Each Node

The initial temperature distribution over the whole domain is considered to be zero. The temperature integral equations are derived from Duhamel's theorem and the principle of superposition.

The temperature at node j of body 1 is given by

$$T^1_j(t) = \int_0^t q_0(\lambda)[\partial\theta^1_{j0}(t-\lambda)/\partial t]d\lambda - \sum_{i=1}^n \int_0^t q_i(\lambda)[\partial\theta^1_{ji}(t-\lambda)/\partial t]d\lambda$$
$$-\int_0^t q_{n+1}(\lambda)[\partial\theta^1_{j,n+1}(t-\lambda)/\partial t]d\lambda \qquad (3-3)$$

where $j=1,2,\ldots,n$ and $T^1_j(t)=T^1(R,z_j-E/2n,t)$

Each term on the right hand side of (3-3) represents the contribution of heat flux q_i's, $i=0, 1, \ldots, n+1$, to the temperature history of $T_j^1(t)$. The direction of heat fluxes q_i's, $i=1, 2, \ldots, n+1$, in Figure 3.2 are assumed positive in the positive r and z directions. The following paragraphs explain the influence functions that influence the temperature history T_j^1.

The temperature rise at node j, $j=1, 2, \ldots, n$, of body 1 due to the unit heat flux on the top of solid cylinder and no heat flux over the rest of surface is denoted as $\Theta_{j0}^1(t)$ and is shown in Figure 3-3.
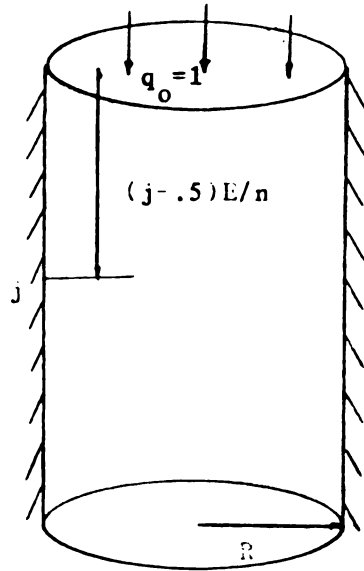
Figure 3.3 Geometry representation of $\Theta_{j0}^1(t)$.

From reference [7], page 112

$$\Theta_{j0}^{1+} = g t^+ + [\ z^{+2}/2 - 1/6 - (2/\pi^2) \sum_{n=1}^{\infty} [(-1)^n \exp[\ -(n\pi g)^2 t^+ \cos(n\pi z^+)/n^2\ ]]/g$$

$$\text{(3-4a)}$$

where

$\theta_{j0}^{1+} = \theta_{j0}^{1} k/Rq_0$, which is dimensionless; k is the thermal conductivity of material; R is the radius of the thermocouple assembly; q_0 is the unit step heat flux over the top surface of solid cylinder; and

$$z^+ = z/R \qquad (3-4b)$$

$$z = z_j - E/2n, \quad z_j = jE/n \qquad (3-4c)$$

$$t^+ = \alpha t/R^2 \qquad (3-4d)$$

The symbol t^+ is called the Fourier number which is the ratio between the rate of heat conduction and the rate of heat storage in a given volume element. A very important geometry parameter in this thesis is

$$g = R/E \qquad (3-4e)$$

For the given geometry and boundary conditions, the temperature histories at any point is function of g and t^+. Due to the disturbance caused by thermocouple, the temperature measured by the thermocouple is greater than that would exist if the thermocouple were not present. If g is very small (i.e., the depth E is very large compared to a given thermocouple radius R), the difference of temperature between that at the undisturbed heated surface and that measured by the thermocouple decreases a little compared with that existing if the thermocouple were not there. If g is very large (i.e., E is very small for a given thermocouple radius R), the temperature measured by the thermocouple can be greater than that at the undisturbed heated surface. So, the value of g can be changed to let the undisturbed heated surface temperature be equal to that measured by the thermocouple at large times. It should be noted that the temperature at the hot spot, which is at the heated surface right above the thermocouple, is always greater than that meas-

ured by the thermocouple as well as that at the undisturbed heated surface.

The symbol Θ^1_{ji} denotes the temperature rise at node j of body 1 due to the unit step heat flux q_i over the element i of body 1 and no heat flux over the rest of the area and is shown in Figure 3.4. The derivation of Θ^1_{ji} is in Appendix A, equation (A-9).
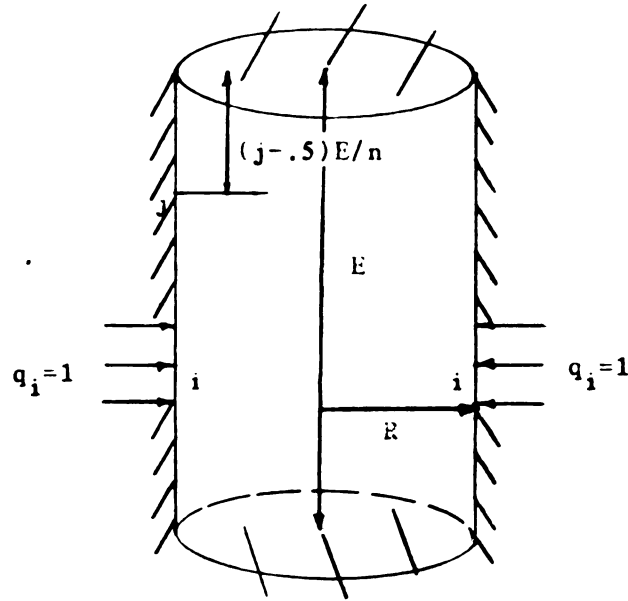
Figure 3.4 Geometry representation of Θ^1_{ji}.

If there are n elements on the radial surface of cylinder, only one half of the influence functions, Θ^1_{ji}, must be calculated from the expression given by (A-9). Others can be obtained from the following relationship,

$$\Theta^1_{ji} = \Theta^1_{n+1-j, n+1-i} \qquad (3-5)$$

which means that the temperature rise at node j due to unit step heat flux q_i is equal to the temperature rise at node $n+1-j$ due to unit step heat flux q_{n+1-i}. For example, $\Theta_{11}^1 = \Theta_{33}^1$ for n=3 as shown in Figure 3-5.
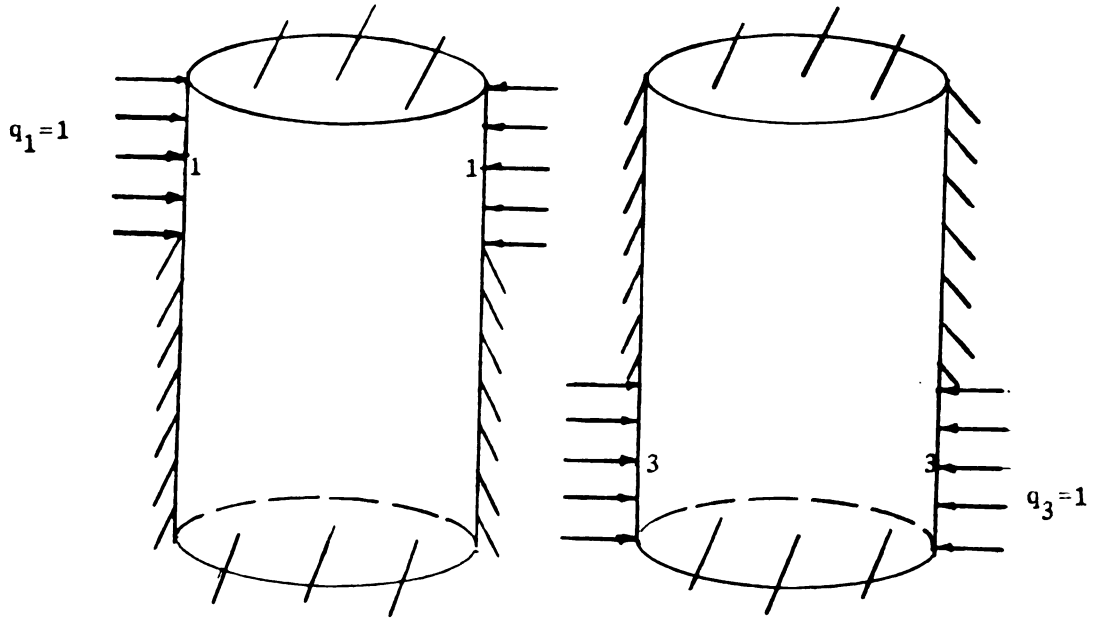
Figure 3.5 $\quad \Theta_{11}^1 = \Theta_{33}^1 \quad$ for n=3

The symbol $\Theta_{j,n+1}^1$ denotes the temperature rise at node j of body 1 due to the unit step heat flux on the bottom surface of soild cylinder (ie. the $n+1$th element) and no heat flux over the other surface. These influence functions, $\Theta_{j,n+1}^1$, can be obtained from the knowledge of Θ_{j0}^1 because q_{n+1} passes through the bottom surface of the cylinder while q_0 passes through the top surface of the cylinder. The following relationshop can be used in the calculation of $\Theta_{j,n+1}^1$.

$$\theta^1_{j,n+1} = \theta^1_{n-j+1,0} \tag{3-6}$$

For example $\theta^1_{10} = \theta^1_{34}$ for n=3 as shown in Figure 3.6.
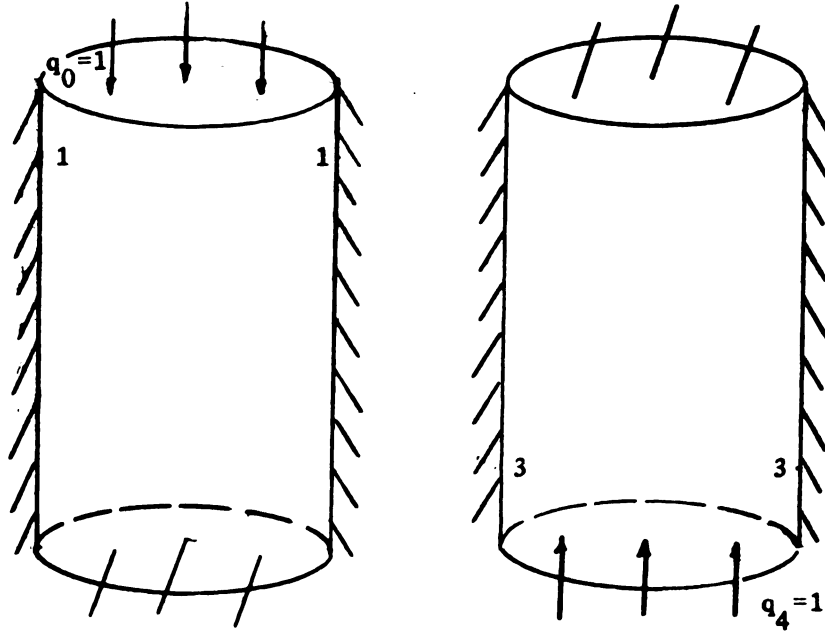
Figure 3.6 $\theta^1_{10} = \theta^1_{34}$ for n=3

The temperature at node j on the body 2 due to $q_i(t)$, i=0, 1, ...,n, can be expressed as

$$T^2_j(t) = \int_0^t q_0(\lambda)[\partial\theta^2_{j0}(t-\lambda)/\partial t]d\lambda + \sum_{i=1}^n \int_0^t q_i(\lambda)[\partial\theta^2_{ji}(t-\lambda)/\partial t]d\lambda \tag{3-7}$$

where j=1,2,...n and $T^2_j = T^2(R, z_j - E/2n, t)$. Since the radial surface of the thermocouple is assumed to be insulated, there is no heat flux passing through the interface between body 2 and body 3.

The temperature rise at node j of body 2 due to unit heat flux q_0 and insulated over the rest of the surface area is denoted as Θ^2_{j0}. It can be viewed as the temperature rise at the distance of $z_j - E/2n$ from the surface of semi-infinite body due to unit step heat flux on the surface as shown in Figure 3.7. It is a function of z and t only.
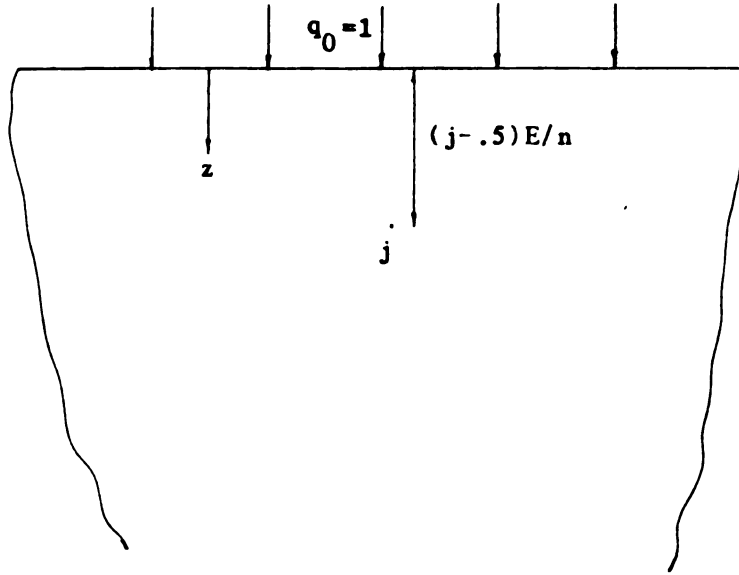
Figure 3.7 Geometry representation for Θ^2_{j0}

From reference [7], page 75

$$\Theta^{2+}_{j0} = 2[(t^+/\pi)^{1/2}\exp[-(z^+/2g)^2/t^+] - z^+\text{erfc}[z^+/(2gt^{1/2})]/2g] \quad (3-8)$$

The temperature rise at node j of body 2 due to the unit heat flux over the element i and insulated over the other surface area is denoted as Θ^2_{ji} and is shown in Figure 3.8.
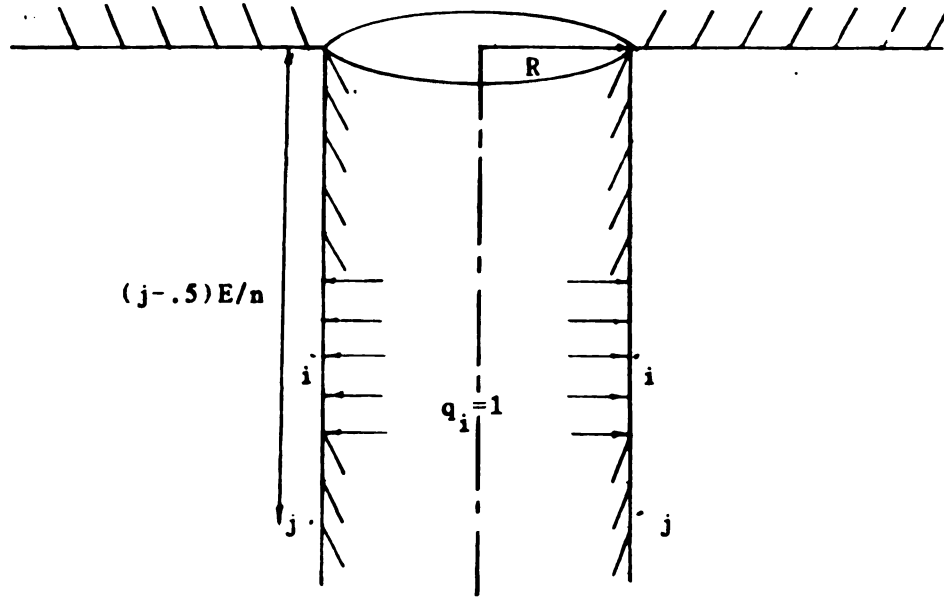
Figure 3.8 Geometry representation for θ^2_{ji}

The derivation of θ^2_{ji} is in the Appendix B, equations (B-10) and (B-14).

The temperature at node $n+1$ in body 1 is found using the equation,

$$T^1_{n+1}(t)=\int_0^t q_0(\lambda)[\partial\theta^1_{n+1,0}(t-\lambda)/\partial t]d\lambda-\sum_{i=1}^n\int_0^t q_i(\lambda)[\partial\theta^1_{n+1,i}(t-\lambda)/\partial t]d\lambda$$

$$-\int_0^t q_{n+1}(\lambda)[\partial\theta^1_{n+1,n+1}(t-\lambda)/\partial t]d\lambda \qquad (3-9)$$

where

$$T^1_{n+1} = T^1(0,E,t)$$

The temperature rise at node $n+1$ of body 1 due to unit step heat flux q_0 is denoted as $\theta^1_{n+1,0}$. The value of $\theta^1_{n+1,0}$ can be obtained from

(3-4a) by substituting z^+=0.

The temperature rise at the node n+1 of body 1 due to the unit step heat flux over the element i of body 1 and no heat flux over the rest area is denoted as $\Theta^1_{n+1,i}$ and is shown in Figure 3.9. The derivation is in Appendix C, equation (C-4).
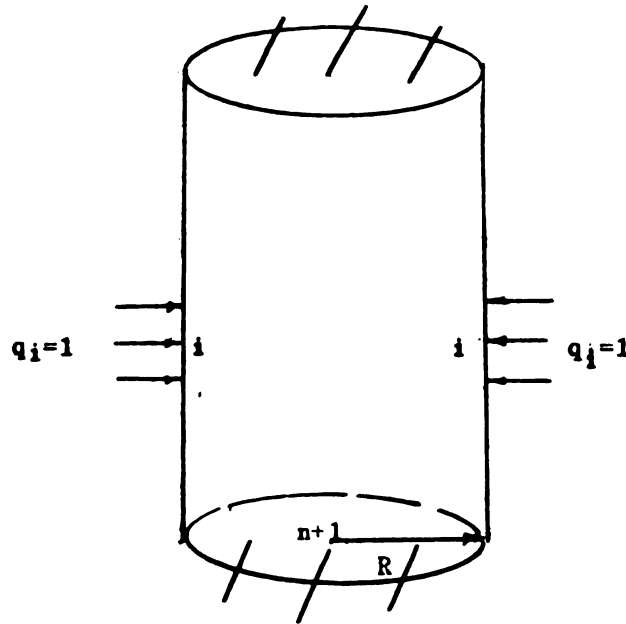
Figure 3.9 Geometry representation for $\Theta^1_{n+1,i}$

The temperature rise at node n+1 of body 1 due to the unit step heat flux on the bottom surface of cylinder is denoted as $\Theta^1_{n+1,n+1}$. The value can be obtained from (3-4) by substituting z^+=1.

The temperature at node n+1 on body 3 is only affected by the heat flux $q_{n+1}(t)$ since it is assumed that the radial surface of body 3 is insulated. Hence, it is given as,

$$T^3_{n+1} = \int_0^t q_{n+1}(\lambda)[\partial\theta^3_{n+1,n+1}(t-\lambda)/\partial t]d\lambda \qquad (3\text{-}10)$$

where $\theta^3_{n+1,n+1}$ can be viewed as the temperature rise at the heated surface of a semi-infinite body due to the unit step heat flux over the surface of body. From reference [7], page 75,

$$\theta^{3+}_{n+1,n+1} = 2k_T(t^+/\pi)^{1/2} \qquad (3\text{-}11)$$

where $k_T = (k_t\rho_t c_t/k\rho c)^{1/2}$; k is the thermal conductivity of material; ρ is the density; c is the thermal capability. subscript t denotes the property of a thermocouple.

The temperature at the hot spot, which is at the heated surface right above the top of thermocouple and is denoted as the $n+2$th node, can be expressed as

$$T^1_{n+2} = \int_0^t q_0(\lambda)[\partial\theta^1_{n+2,0}(t-\lambda)/\partial t]d\lambda - \sum_{i=1}^n\int_0^t q_i(\lambda)[\partial\theta^1_{n+2,i}(t-\lambda)/\partial t]d\lambda$$
$$-\int_0^t q_{n+1}(\lambda)[\partial\theta^1_{n+2,n+1}(t-\lambda)/\partial t]d\lambda \qquad (3\text{-}12)$$

where $T^1_{n+2} = T^1(0,0,t)$

Each term on the right hand side of (3-12) represents the contribution of heat flux q_j, $j=0, 1, \ldots, n+1$, on the temperature history T^1_{n+2}. Since node $n+2$ is on the top surface of solid cylinder and node $n+1$ is on the bottom surface, the influence functions for the node $n+1$ can be used in the procedure of calculating the influence functions for the node $n+2$.

The symbol $\theta^1_{n+2,i}$ is denoted as the temperature rise at node $n+2$ of body 1 due to unit step heat flux q_i, $i=0, 1, \ldots, n+1$, and insulated over the other surface. It can be obtained by the following relationship

$$\theta^1_{n+2,i} = \theta^1_{n+1,n-i+1} \quad i=0, 1, \ldots, n+1 \tag{3-13}$$

where (3-13) means the temperature rise at node $n+2$ due to unit step heat flux q_i, $i=0, 1, \ldots, n+1$, can be obtained from the temperature rise at node $n+1$ due to unit step heat flux q_{n-i+1}.

3.4 Derivation of Integral Equations from USEM

The purpose of this section is to derive the set of integral equations for the unsteady surface element method. The interface conditions, (3-1) and (3-2), are used to combine the integral expressions of temperature at each node of the interface derived in Section 3.3.

The temperatures at node j of body 1 and body 2 are the same. By introducing (3-3) and (3-7) into (3-1), a set of integral equations for $j=1, 2, \ldots, n$ can be obtained,

$$\sum_{i=1}^{n} \int_0^t q_i(\lambda)[\partial(\theta^1_{ji}+\theta^2_{ji})/\partial t]d\lambda + \int_0^t q_{n+1}(\lambda)[\partial\theta^1_{j,n+1}/\partial t]d\lambda$$
$$= \int_0^t q_0(\lambda)[\partial(\theta^1_{j0}-\theta^2_{j0})/\partial t]d\lambda \quad j=1, 2, \ldots, n \tag{3-14}$$

where (3-14) are called Volterra equations of the first kind because

the unknown functions, q_i's, are inside the integrals.

Since the interface between bodies 1 and 3 is considered perfect, the temperatures at node $n+1$ of bodies 1 and 3 are the same. A mathematical model in the form of an integral equation can be established by introducing (3-9) and (3-10) into (3-2),

$$\sum_{i=1}^{n}\int_0^t q_i(\lambda)[\partial\theta^1_{n+1,i}/\partial t]d\lambda + \int_0^t q_{n+1}(\lambda)[\partial(\theta^1_{n+1,n+1}+\theta^3_{n+1,n+1})/\partial t]d\lambda$$

$$= \int_0^t q_0(\lambda)[\partial\theta^1_{n+1,0}/\partial t]d\lambda \qquad (3-15)$$

Equations (3-14) and (3-15) represent a set of Volterra equations of the first kind, one for each element, which can be solved simultaneously for $n+1$ unknown heat flux histories $q_1(t)$, $q_2(t)$, ..., $q_{n+1}(t)$. The Volterra equations can be solved analytically by Laplace transform which will be discussed in chapter 4. These equations can also be approximated by a system of linear algebraic equations by replacing the integrals with suitable quadrature formulas which will be given in chapters 5 and 6. After these Volterra equations are solved, the heat fluxes $q_1(t)$, $q_2(t)$, ..., $q_{n+1}(t)$ can be substituted into (3-9) and (3-12) to find the temperature histories at the hot spot and the top of thermocouple.

3.5 Derivation of Quasi-steady State Equations

In this section the quasi-steady state method is derived. The basic idea is as follows: The system is said to be in a quasi-steady state if the rate of the temperature change approaches zero for large

time. If the temperature rise is proportional to the function of $t^{1/2}$, the system will be in quasi-steady at large time because the rate of temperature change is proportional to the function of $t^{-1/2}$. Since the rate of the temperature change approaches zero for quasi-steady state, the energy input is equal to the energy output near the heated surface. In this case the temperature distribution is indeterminate, but the shape of the temperature distribution can be determined from the quasi-steady state heat fluxes along the boundary. It means that the temperature at large time can not be determined from the quasi-steady state heat flux distribution only. It is also function of transient heat flux history. In the quasi-steady state method the transient heat flux is not needed. The temperature at large time still can be found from other information that has a relation with the transient heat flux. This information is obtained from the interface conditions and boundary conditions of connected bodies because the transient heat flux history is dependent on these conditions.

To simplify the analysis, the thermocouple is assumed to be insulated in this thesis. The interface between body 1 and body 2 is discretized into the same n equally-spaced surface element as the case of transient procedure in section 3.4 and the heat flux through each element is uniform in space, but a function of time.

For the quasi-steady state condition, the temperature at any point on body 1 is not only a function of the steady state heat fluxes along the boundaries but also the function of interface conditions and boundary conditions of connected bodies because the transient heat fluxes $q_1(t)$, $q_2(t)$, ..., $q_n(t)$ are also dependent on these conditions.

The mathematical model can be established as follows: From the principle of conservation of energy that the energy input to body 1 is found to be equal to the energy output from body 1 for quasi-steady state.

$$[q_1(t)+q_2(t)+\ldots+q_n(t)]2\pi RE/n = q_0\pi R^2 \tag{3-16}$$

$$\sum_{i=1}^{n}q_i(t) = nRq_0/2E \tag{3-17}$$

where (3-16) and (3-17) are suitable for large times when the rate of temperature rise is almost zero.

By using the principle of superposition the temperature at point j of body 1 at large time can be expressed as

$$T_j^1(t) = \sum_{i=0}^{n}q_i(t)\theta_{ji}^1(t) + B \tag{3-18}$$

where B is a constant for large times which is dependent on the boundary conditions of body 2 and the interface conditions between body 1 and body 2. Equation (3-18) means that the shape of the temperature distribution for the quasi-steady state is determined from the heat fluxes distribution at quasi-steady state, but the actual temperature distribution is dependent on the interface condition between bodies 1, 2 and the boundary condition of body 2. The symbol $\theta_{ji}^1(t)$ is the temperature rise at point j of body 1 for the large times due to the unit heat flux q_i.

The temperature at point j of body 2 at large time can be

expressed as

$$T_j^2(t) = \sum_{i=0}^{n} q_i(t)\theta_{ji}^2(t) \tag{3-19}$$

where θ_{ji}^2 is the temperature at point j of body 2 for large times due to a unit heat flux q_i. Because the domain of body 2 is infinite, the influence of the transient heat flux history on the quasi-steady temperature can be neglected. It is the effect of thermal diffusivity.

By substituting (3-18) and (3-19) into the interface condition (3-1), one obtains

$$B = \sum_{i=0}^{n} q_i(t)[\theta_{ji}^2(t) - \theta_{ji}^1(t)] \tag{3-20}$$

for $j=1,2,\ldots,n$

There are $n+1$ algebraic equations (i.e., n equations from (3-20) and 1 equation from (3-17)) and $n+1$ unknowns, which are B, $q_1(t)$, $q_2(t)$, ..., $q_n(t)$. These $n+1$ algebraic equations can be solved simultaneously without difficulty. The temperatures at the hot spot and the top of thermocouple for the large times can be obtained by using the following equations,

$$T_{n+1}^1 = \sum_{i=0}^{n} q_i(t)\theta_{n+1,i}^1(t) + B \tag{3-21}$$

$$T_{n+2}^1 = \sum_{i=0}^{n} q_i(t)\theta_{n+2,i}^1(t) + B \tag{3-22}$$

where $\theta^1_{n+1,i}(t)$ and $\theta^1_{n+2,i}(t)$ are the temperature rise at the top of thermocouple and hot spot, respectively, due to unit step heat flux q_j for the large time. Equations (3-21) and (3-22) represent the temperature at the hot spot and the top of thermocouple for the quasi-steady state. They can be derived directly without the need of the transient temperature distribution. The results derived from the quasi-steady state method will be used to check the large time solution extrapolated from the transient method derived in section 3.4. This method has not been previously proposed. It provides a powerful procedure for obtaining the quasi-steady errors associated with the thermocouple.

In this thesis the thermocouple is assumed to be insulated when the quasi-steady state method is derived. It is not necessary because the extra unknown q_{n+1} through the interface between body 1 and body 3 is accompanied with another algebraic equation from the interface condition between body 1 and body 3. There are n+2 unknowns, B, q_1, q_2, ..., q_{n+1}, with n+2 algebraic equations, n+1 from the interface conditions and one from the energy conservation principle. So, the system of algebraic equations can be solvable.

CHAPTER 4.

ONE-NODE LARGE TIME SOLUTION BY THE LAPLACE TRANSFORMATION

4.1 Introduction

The Laplace transform method has been widely used in the solution of time-dependent heat conduction problems [6,7]. The advantage of Laplace transform is that it simplifies the procedure of calculation because the partial derivative (or integral) with respect to the time variable can be removed from the differential (or integral) equation of heat conduction by application of the Laplace transform. In this chapter the Laplace transform is used to solve the thermal cavity problem.

The outline of this chapter is as follows: Section 4.2 includes the objectives of this chapter. Section 4.3 gives the description of the problem. Section 4.4 introduces the influence functions needed in the calculation for the large time solution. These influence functions are only suitable for large time. Section 4.5 discusses the Laplace transform method in the calculational procedure. Observations are given in section 4.6.

4.2 Objectives

1) The first objective is finding the transient temperature history at the top of the thermocouple as well as at the hot spot by the one

node USEM with the Laplace transform method.

2) The second objective is finding the null point for the thermal cavity problem.

4.3 Problem Description
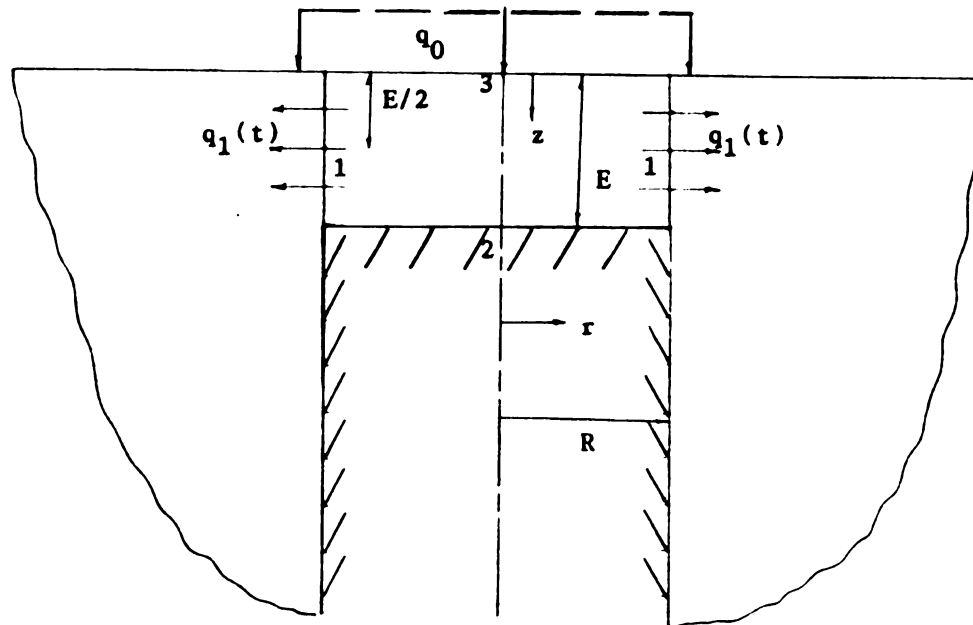
Figure 4.1 The geometry of thermal cavity problem

with one-node USEM

1) The initial temperature distribution is considered to be zero.

2) The thermocouple is assumed insulated.

3) The heat flux between body 1 and body 2, which is $q_1(t)$, is assumed uniform in space, but function of time. So, the one-node USEM is considered in this chapter.

4) Node 1 is at r=R and z=E/2; Point 2 is at r=0 and z=E ; Point 3 is at r=0 and z=0, which is the location of "hot spot".

5) The surface heat flux q_0 is assumed uniform in space and time.

6) The Laplace transform is used to remove the integral terms in the heat flow and temperature expressions to simplify the procedure of calculation.

7) The situation is shown in Figure 4.1.

4.4 The Influence Functions

The following influence functions that are needed in the procedure of calculation, equations (4-2,9), can be obtained in reference [7]. The last influence function, equation (4-10), is from reference [8]. θ^k_{ji}, except equation (4-10), means the temperature rise at node j of body k due to the unit step heat flux q_i.

$$\bar{\theta}^k_{ji}(s) = \mathcal{L}[\theta^k_{ji}] = \int_0^\infty \theta^k_{ji}\exp(-st)dt \qquad (4-1)$$

where $\bar{\theta}^k_{ji}(s)$ is the Laplace transform of θ^k_{ji}.

$$\theta^1_{10}(t) = R/k[\ g\alpha t/R^2 - 1/(24g)\ ] \qquad (4-2a)$$

$$\bar{\theta}^1_{10} = R/k[\ g\alpha/(Rs)^2 - 1/(24gs)\ ] \qquad (4-2b)$$

$$\theta^1_{11}(t) = R/k[\ 2\alpha t/R^2 + .25\ ] \qquad (4-3a)$$

$$\bar{\theta}^1_{11} = R/k[\ 2a/(Rs)^2 + 1/(4s)\ ] \tag{4-3b}$$

$$\theta^2_{10}(t) = 2(at)^{1/2} ierfc[R/4g(at)^{1/2}]/k \tag{4-4a}$$

$$\bar{\theta}^2_{10} = R/k[\ 1/R(a/s^3)^{1/2} - 1/(2gs) + R(1/sa)^{1/2}/(4g^2)\ ] \tag{4-4b}$$

$$\theta^1_{20}(t) = R/k[\ gat/R^2 - 1/(6g)\ ] \tag{4-5a}$$

$$\bar{\theta}^1_{20} = R/k[\ ga/(Rs)^2 - 1/(6gs)\ ] \tag{4-5b}$$

$$\theta^1_{21}(t) = R/k[\ 2at/R^2 - .25\ ] \tag{4-6a}$$

$$\bar{\theta}^1_{21} = R/k[\ 2a/(Rs)^2 - 1/(4s)\ ] \tag{4-6b}$$

$$\theta^1_{31}(t) = \theta^1_{21}(t) \tag{4-7}$$

$$\theta^1_{30}(t) = R/k[\ gat/R^2 + 1/(3g)\ ] \tag{4-8a}$$

$$\bar{\theta}^1_{30} = R/k[\ ga/(Rs)^2 + 1/(3gs)\ ] \tag{4-9b}$$

$$\theta^2_{11} = R/k[\ C - R/g(\pi at)^{1/2} + R^3/2g^2(\pi at)^{3/2}\ ] \tag{4-10a}$$

$$\bar{\theta}^2_{11} = R/k[\ C/s - R/g(as)^{1/2}\ ] \tag{4-10b}$$

There are no exponential terms in the influence functions (4-2,9), compared with those exact solutions in reference [7]. The exponential

terms in these exact solutions, with -t as parameter, decay very fast at large times compared with other terms such as a constant or a linear function of t. So, they are truncated to provide a simple analysis. The results of calculation obtained from these influence functions is only appropriate for large time.

Equation (4-10a) [8] is the average temperature over element 1 of body 2 due to unit step heat flux through element 1 for large time. The constant C in equation (4-10) can be found in [13] and is on the Table 4.1.

Table 4.1 The value of C versus the value of g

g	.1	.25	.50	1.0	1.333	4.0
C	2.7835	1.9936	1.4686	1.0300	.8674	.4423

4.4 Calculational Procedure

The Laplace transform is used in this section to remove the integral terms in the temperature and heat flow integral equations. In this section, the integral equation of heat flow derived from USEM, (3-14) with n=1 and no heat flus passing through the interface between body 1 and body 3 (i.e., $q_2=0$), is first transformed into an algebraic equation by the application of the Laplace transform. Then the transformed heat flux, $\bar{q}_1(s)$, can be expressed by an algebraic equation. The temperature integral equations (3-9), the temperature at the top of thermocouple, and (3-14), the temperature at hot spot, are next

simplified using the Laplace transform. The transformed heat flux, $\bar{q}_1(s)$, is then substituted into these two algebraic temperature equations. Finally, the inversion technique is applied to these algebraic temperature equations to recover the temperature expressions in the time domain.

The integral equation of heat flow is obtained by setting n=1 in equation (3-14) with no q_2 term,

$$\int_0^t q_0(\lambda)[\partial(\theta_{10}^1-\theta_{10}^2)/\partial t]d\lambda = \int_0^t q_1(\lambda)[\partial(\theta_{11}^1+\theta_{11}^2)/\partial t]d\lambda \qquad (4\text{-}10)$$

where the prescribed surface heat flux q_0 is considered to be constant in time as well as in space. Then (4-10) can be rewritten as,

$$[q_0[\theta_{10}^1(t)-\theta_{10}^2(t)] = \int_0^t q_1(\lambda)[\partial(\theta_{11}^1+\theta_{11}^2)/\partial t]d\lambda \qquad (4\text{-}11)$$

Taking the Laplace transform on the both sides of (4-11) gives

$$q_0[\bar{\theta}_{10}^1-\bar{\theta}_{10}^2] = s\bar{q}_1[\bar{\theta}_{11}^1+\bar{\theta}_{11}^2] \qquad (4\text{-}12)$$

where

$$\begin{aligned}
\mathcal{L}[\int_0^t q(\lambda)[\partial\theta_{ji}^k(t-\lambda)/\partial t]d\lambda] &= \mathcal{L}[\partial/\partial t[\int_0^t q(\lambda)\theta_{ji}^k(t-\lambda)d\lambda] \\
&= \mathcal{L}[\partial/\partial t(q*\theta_{ji}^k)] \\
&= s\bar{q}\bar{\theta}_{ji}^k \qquad (4\text{-}13)
\end{aligned}$$

where $q*\theta_{ji}^k$ is called convolution. Equation (4-12) can be rearranged as

$$\bar{q}_1 = q_0 [\bar{\theta}_{10}^1 - \bar{\theta}_{10}^2] / s [\bar{\theta}_{11}^1 + \bar{\theta}_{11}^2] \tag{4-14}$$

where equation (4-14) is an algebraic equation for $\bar{q}_1(s)$

The temperature at the top of thermocouple is obtained by setting $n=1$ in equation (3-9),

$$T_2^1 = q_0 \dot{\theta}_{20}^1(t) - \int_0^t q_1(\lambda) \partial \theta_{21}^1 / \partial t \, d\lambda \tag{4-15}$$

Taking the Laplace transform on both sides of equation (4-15) and using (4-13) to remove the integral term gives

$$T_2^1 = q_0 \bar{\theta}_{20}^1 - s\bar{q}_1 \bar{\theta}_{21}^1 \tag{4-16}$$

Substituting equation (4-14) into equation (4-16) yields

$$T_2^1 = q_0 [\bar{\theta}_{20}^1 - [\bar{\theta}_{21}^1 (\bar{\theta}_{10}^1 + \bar{\theta}_{10}^2) / (\bar{\theta}_{11}^1 + \bar{\theta}_{11}^2)]] \tag{4-17}$$

Taking the inverse Laplace transform of equation (4-17), one obtains

$$T_2^1(t) = q_0 [\theta_{20}^1 - D(t)] \tag{4-18}$$

where $D(t)$ is the inverse of Laplace transform of $\bar{D}(s)$

$$\bar{D}(s) = \bar{\theta}_{21}^1 (\bar{\theta}_{10}^1 - \bar{\theta}_{10}^2) / (\bar{\theta}_{11}^1 + \bar{\theta}_{11}^2) \tag{4-19}$$

Substituting influence equtions (4-1b), (4-2b), (4-3b), (4-4b), (4-6b)

into equation (4-19) gives

$$\overline{D}(s) = R^3/2k\alpha[2g\alpha^2/(R^4s^2)+(11-6g^2-12Cg^2)\alpha/(12gR^2s)+(3g^2+2g^2C-1)$$

$$(\alpha/s)^{1/2}/(2g^2R)-2(\alpha/s)^{3/2}/R^3] \tag{4-20}$$

Taking the inverse Laplace transform of (4-20) gives

$$D(t)=g\alpha t/kR+R(11-6g^2-12g^2C)/(24kg)+R^2(3g^2+2g^2C-1)/4kg^2(\alpha\pi t)^{1/2}$$

$$-2(\alpha t/\pi)^{1/2}/k \tag{4-21}$$

Substituting (4-21) and (4-5a) into (4-18) gives

$$T_2^1(t) = q_0[R(6g^2+12g^2C-15)/(24kg)+2(\alpha t/\pi)^{1/2}/k-R^2(3g^2+2g^2C-1)$$

$$(\alpha\pi t)^{-1/2}/(4kg^2)] \tag{4-22}$$

Define $T_{0\infty}=2q_0(\alpha t/\pi)^{1/2}/k$ which is the temperature rise at the heated surface of semi-infinite body due to constant heat flux q_0. Then one can write the temperature difference as

$$[T_2^1(t)-T_{0\infty}(t)]/(q_0R/k) = (6g^2+12g^2C-15)/(24g) - (3g^2+2g^2C-1)$$

$$(\pi t^+)^{-1/2}/(4g^2) \tag{4-23}$$

or

$$T_2^{+1}(t) = [T_2^1(t)-T_{0\infty}(t)]/(q_0R/k) = C_1 + C_2(t^+)^{-1/2} \tag{4-24}$$

where

$T_2^{+1}(t)$ is the dimensionless temperature difference between that at the top of thermocouple and that at undisturbed heated surface and

$$C_1 = (6g^2+12g^2C-15)/(24g) \qquad (4-25a)$$

$$C_2 = -(3g^2+2g^2C-1)/(4g^2\pi^{1/2}) \qquad (4-25b)$$

$$t^+ = \alpha t/R^2 \qquad (4-25c)$$

Equation (4-24) is an important equation which shows that the transient temperature disturbance caused by thermocouple is function of g and $(t+)^{-1/2}$ for large times and the steady state disturbance caused by the thermocouple is function of g only.

Figure 4.2 contains the temperature history, equation (4-24), at the top of thermocouple versus the value of g. Table 4.2 contains the value of C_1 and C_2 versus the value of g. C_1 is the quasi-steady state temperature difference between that at the top of thermal cavity and that at the heated surface far away from the thermocouple. If C_1 is greater than zero, it means that the temperature measured by the thermocouple is greater than that at the undisturbed heated surface for large time. If C_1 is less than zero, it means that the temperature measured by the thermocouple is less than that at the undistured surface for large time. If C_1 is equal zero, then the temperature measured by the thermocouple is tha same as that at the undisturbed heated surface for large time. The value of g corresponding to a zero

value of C_1 can be obtained by drawing the value of C_1 versus the value of g. The location corresponding to this value of g is called the "null point", which is the location that the thermocouple can measure the undisturbed heated surface temperature with minimum error. C_2 represents the transient disturbance due to the existence of thermocouple. From (4-24) transient disturbance decays as the function of $(t^+)^{-1/2}$.
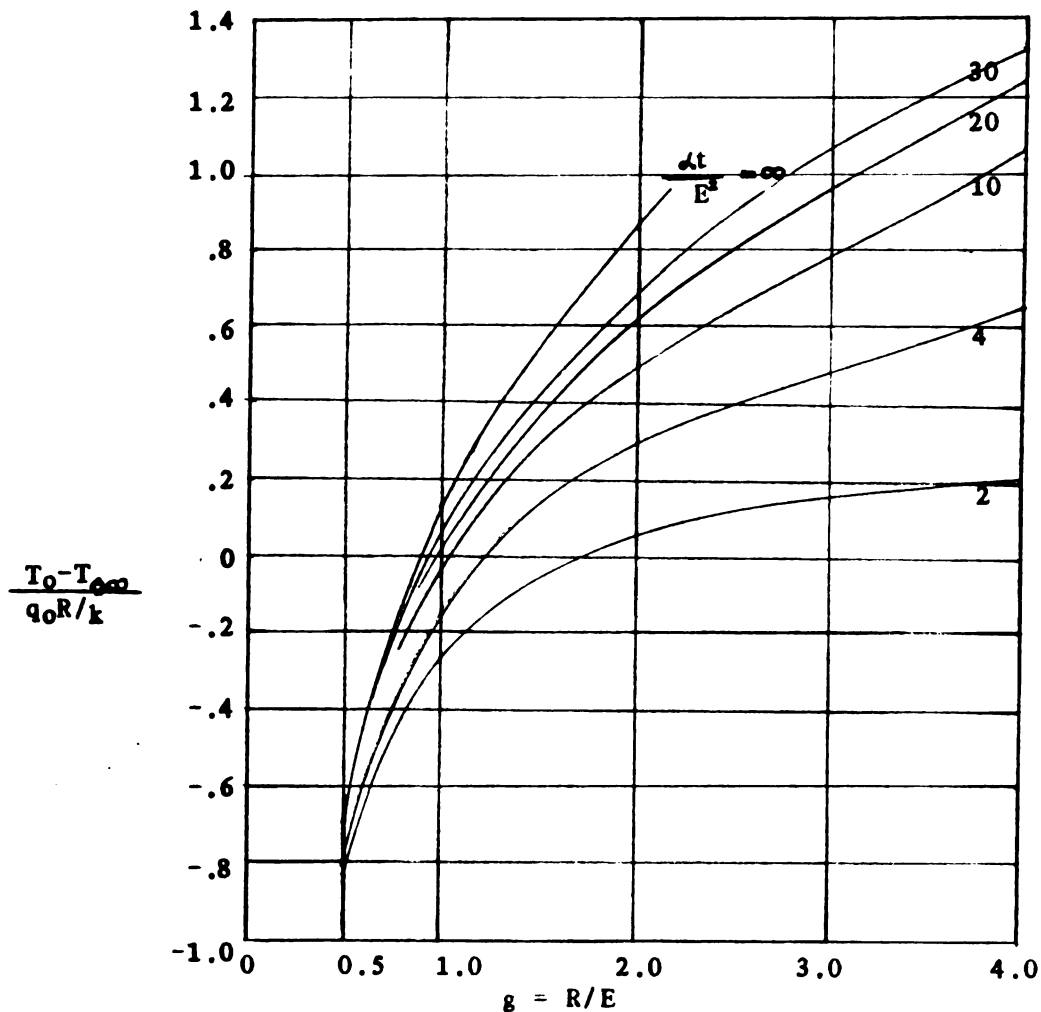
Figure 4.2 The transient temperature histories at

the top of the thermocouple.

Table 4.2 The steady and transient disturbance coefficient

(i.e., C_1 and C_2) at the top of thermocouple.

g	.1	.25	.5	1.0	1.333	4.0
C_1	-6.086	-2.251	-.7579	.14	.3714	1.7283
C_2	18.890	1.2712	-.2732	-.5727	-.5910	-.5391

The temperature at the "hot spot" is obtained by setting n=1 in equation (3-12),

$$T_3^1 = q_0 \theta_{30}^1 - \int_0^t q_1(\lambda) \partial \theta_{31}^1(t-\lambda)/\partial t \, d\lambda \qquad (4-26)$$

Taking the Laplace transform on both sides of equation (4-26) and using (4-13) gives

$$T_3^1 = q_0 \bar{\theta}_{30}^1 - s \bar{q}_1 \bar{\theta}_{31}^1 \qquad (4-27)$$

Substituting equations (4-14) and (4-19) into (4-27) yields

$$T_3^1 = q_0 [\bar{\theta}_{30}^1 - \bar{D}] \qquad (4-28)$$

Taking the inverse Laplace transform of (4-28) and substituting (4-21) into (4-28) gives

$$T_3^{1+} = (T_3^1 - T_{0\infty})/(q_0 R/k) = (6g^2 + 12Cg^2 - 3)/24g - (3g^2 + 2g^2 C - 1)/4g^2 (\pi t^+)^{1/2}$$

$$=D_1+D_2(t^+)^{-1/2} \tag{4-29}$$

where

$T_3^{1+}(t)$ is the dimensionless temperature difference between that at the hot spot and that at the undisturbed heated surface and

$$D_1 = (6g^2 + 12g^2C - 3)/24g \tag{4-30a}$$

$$D_2 = -(3g^2 + 2g^2C - 1)/4g^2\pi^{1/2} \tag{4-30b}$$

Both the value of D_1 and D_2 are in Table 4.3. The symbol D_1 represents the quasi-steady state temperature difference between that at "hot spot" and that at heated surface far away from the thermocouple. Due to the disturbance of the thermocouple, the value of D_1 should always be greater than zero for any value of g. This characteristic can be used to check the results of one node USEM by using the Laplace transform method. The symbol D_2 represents the transient disturbance due to the thermocouple. The transient disturbance also decays as a function of $(t^+)^{-1/2}$.

Table 4.3 The steady and tranient disturbance coeficient

(i.e., D_1 and D_2) at the hot spot.

g	.1	.25	.5	1.0	1.333	4.0
D_1	-1.0858	-.1883	.2422	.6400	.8238	1.8533
D_2	12.8964	1.2712	-.2732	-.5727	-.5910	-.5391

4.6 Observations

1) From the above calculations, it is shown that the one-node USEM with the Laplace transform method is a very easy and quick procedure for the solution of the thermal cavity problem compared with the procedure needed in the finite difference method [5].

2) From Figure 4.2 the transient temperature histories by the one-node USEM are greater than those obtained by the finite difference method from $at/E^2 = 0$ to 30. But the difference decreases with the increment of g. It means that the one-node assumption is suitable for large values of g.

3) From the inspection of Figure 4-2, the temperature histories at the top of the thermocouple from one-node USEM with the Laplace transform, the best location for the thermocouple is at g=.925, which is the location of "null point". At this location the temperature measurements have the minimun error with respect to the undisturbed surface temperature. From reference [5] the calculated value of g is equal to 1.

4) From (4-25b) and (4-30b), the expressions for C_2 and D_2 are the

same. It means the temperature difference between that at the hot spot and that at the top of thermocouple is a function of the value of g only. This phenomenon is true only for large times.

5) From equation (4-24) and (4-29), the transient disturbance caused by the thermocouple is function of $t^{-1/2}$. This characteristic will be used in the following chapters to extrapolate the quasi-steady state temperature from the transient solution by USEM. Then these values can be compared with those given from quasi-steady state method to show the accuracy of these two methods.

6) From Table 4-3, the value of D_1 for g=.1 and .25 is negative. It shows that the quasi-steady state temperature at the hot spot is less than that at the heated surface far away from the thermocouple. This situation can not happen in the physical world. So, it means that the one-node assumption is not sufficient to analyze the problem if the value of g is smaller than .5. For the same thermocouple assembly (R=constant), a small value of g means that the distance between the top of the thermocouple and heated surface increases. The assumption of uniform heat flux in space over the interface between body 1 and body 2 is not correct. Three and five nodes on the interface between body 1 and body 2 will be considered in analyzing the situation of small values of g in Chapters 6 and 7.

CHAPTER 5

ONE-NODE TRANSIENT SOLUTION BY THE STOLZ'S METHOD

5.1 Introduction

Equations (3-14) and (3-15), integral equations of heat flow derived from the USEM, represent a set of n+1 Volterra equations of the first kind with the unknown heat fluxes, $q_i(t)$'s, appearing inside the integrals. These integral equations can be approximated by a system of linear algebraic equations by replacing the integral with suitable quadrature formulas. The first step is to divide the time region 0 to t into m finite equally small time intervals, Δt, so that t_m represents the value of t at the end point of the mth interval,

$$t = t_m = m\Delta t \qquad (5-1)$$

where Δt^+ (ie. $\alpha \Delta t/R^2$) in this thesis is taken to be 1, 2 and 3 in the calculational procedure. Then equations (3-17) and (3-18) can be rewritten as,

$$\sum_{i=1}^{n}\sum_{k=1}^{m}\int_{t_{k-1}}^{t_k}q_i(\lambda)\partial[\theta^1_{j,i}+\theta^2_{j,i}]/\partial t d\lambda + \sum_{k=1}^{m}\int_{t_{k-1}}^{t_k}q_{n+1}(\lambda)\partial\theta^1_{j,n+1}/\partial t d\lambda$$
$$=\sum_{k=1}^{m}\int_{t_{k-1}}^{t_k}q_0(\lambda)\partial[\theta^1_{j,0}-\theta^2_{j,0}]/\partial t d\lambda \qquad j=1,2,\ldots,n \qquad (5-2)$$

$$\sum_{i=1}^{n}\sum_{k=1}^{m}\int_{t_{k-1}}^{t_k}q_i(\lambda)\partial\theta^1_{n+1,i}/\partial t d\lambda + \sum_{k=1}^{m}\int_{t_{k-1}}^{t_k}q_{n+1}(\lambda)\partial[\theta^1_{n+1,n+1} +$$
$$\theta^3_{n+1,n+1}]/\partial t d\lambda = \sum_{k=1}^{m}\int_{t_{k-1}}^{t_k}q_0(\lambda)\partial\theta^1_{n+1,0}/\partial t d\lambda \qquad (5-3)$$

57

where $\qquad$ $t_0 = 0$ $\qquad$ (5-4)

In the simplest form of approximation the heat flux histories $q_j(t)$ are assumed to be constant values in each time interval, which is Stolz's method, and is shown in Figure 5.1.

$$q_m = q[(m-.5)\Delta t]$$
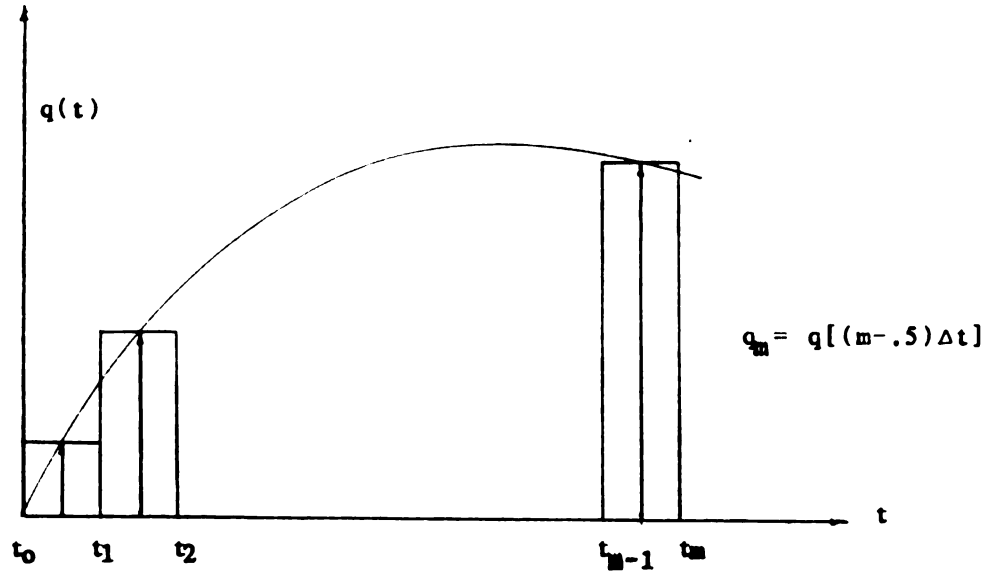
Figure 5.1 Geometry illustrating uniform heat
assumption over each time interval.

Then

$$\int_{t_{k-1}}^{t_k} q_i(\lambda)[\partial\theta^r_{j,i}(t-\lambda)/\partial t]d\lambda = q_i(k)\int_{t_{k-1}}^{t_k}[\partial\theta^r_{j,i}(t-\lambda)/\partial t]d\lambda$$

$$= q_i(k)[\theta^r_{j,i}(t_m-t_{k-1})-\theta^r_{j,i}(t_m-t_k)]$$

$$= q_{ik}\Delta\theta^r_{ji,m-k} \qquad (5-5)$$

where

$$q_{ik} = q_i(k) = q_i[(k-1/2)\Delta t] \qquad (5\text{-}6)$$

$$\Delta\theta^r_{ji,m-k} = \theta^r_{ji,m-k+1} - \theta^r_{ji,m-k} \qquad (5\text{-}7)$$

and $\theta^r_{ji,k}$ is the temperature rise at node j of body r due to unit step heat flux q_i at time $t_k = k\Delta t$. The initial temperature, $\theta^r_{ij,0}$, is 0.

So, equations (5-2) and (5-3) can be simplified by using the assumption of constant heat flux over each time interval to obtain

$$\sum_{i=1}^n \sum_{k=1}^m q_{i,k}[\Delta\theta^1_{j,i,m-k} + \Delta\theta^2_{j,i,m-k}] + \sum_{k=1}^m q_{n+1,k}\Delta\theta^1_{j,n+1,m-k}$$

$$= \sum_{k=1}^m q_{0k}[\Delta\theta^1_{j,0,m-k} - \Delta\theta^2_{j,0,m-k}] \qquad j=1, 2, \ldots, n \qquad (5\text{-}8)$$

$$\sum_{i=1}^n \sum_{k=1}^m q_{ik}\Delta\theta^1_{n+1,i,m-k} + \sum_{k=1}^m q_{n+1,k}[\Delta\theta^1_{n+1,n+1,m-k} + \Delta\theta^3_{n+1,n+1,m-k}]$$

$$= \sum_{k=1}^m q_{0k}\Delta\theta^1_{n+1,0,m-k} \qquad (5\text{-}9)$$

From equations (5-8) and (5-9), the heat fluxes q_{im}'s (for i=1,2, ..., n+1) can be determined at different time intervals one after another by marching forward in time for,

m=1, 2, 3, ...

Thus for each time step, equations (5-8) and (5-9) represent a system of n+1 linear algebraic equations with n+1 unknowns, $q_{1,m}$, $q_{2,m}$, ..., $q_{n+1,m}$, and the heat fluxes at previous times, $q_{i,k}$ for k=1, 2,

..., m-1, are all known.

By using the same assumption of constant heat flux over each time interval the temperature integral equations (3-9) and (3-12) can be simplified as,

$$T^1_{n+1}(m) = \sum_{k=1}^{m} q_{0k} \Delta\theta^1_{n+1,0,m-k} - \sum_{i=1}^{n+1}\sum_{k=1}^{m} q_{ik} \Delta\theta^1_{n+1,i,m-k} \qquad (5-10)$$

$$T^1_{n+2}(m) = \sum_{k=1}^{m} q_{0k} \Delta\theta^1_{n+1,0,m-k} - \sum_{k=1}^{n+1}\sum_{k=1}^{m} q_{ik} \Delta\theta^1_{n+2,i,m-k} \qquad (5-11)$$

where (5-10) and (5-11) are the temperature histories at the top of thermocouple and the hot spot, respectively, for time $t=t_m$. $T(m)$ means that the temperature at time $t=t_m$.

Thus for each time step, equations (5-8) and (5-9) represent $n+1$ linear algebraic equations with $n+1$ unknowns q_{1m}, q_{2m}, ..., $q_{n+1,m}$. After these $n+1$ equations are solved, these $n+1$ quantities, q_{im}'s, are then substituted into equations (5-10) and (5-11) to get the temperature at time t_m (for m=1, 2, 3, ...).

The outline of this chapter is as follows: Section 5.2 includes the objectives of this chapter. Section 5.3 gives the problem description. Section 5.4 lists the influence functions needed in the calculational procedure. Section 5.5 includes the procedure of transient solution by Stolz's method. The quasi-steady state method will be presented in section 5.6. Section 5.7 gives the observations.

5.2 Objectives

1) The first objective is finding the influence of the thermal properties of thermocouple on the transient temperature history at the top of thermocouple by the one node USEM with Stolz's method of constant heat flux in each time step.

2) The second objective is finding the influence of the thermal properties of thermocouple on the location of null point.

3) The third objective is finding the quasi-steady state temperature at the top of thermocouple as well as at the hot spot directly by the quasi-steady state method with the assumption of insulated thermocouple.

5.3 The Problem Description

1) The initial temperature distribution of the whole domain is assumed to be 0.

2) The combination of thermal properties of thermocouple, $k\rho c$, is assumed to be much lower than that of surrounding material, k is the thermal conductivity, ρ is the material density, and c is the thermal capacity.

3) The contact between the top of the thermocouple and the material is perfect.

4) There is no heat flux passing through the radial surface of thermocouple.

5) The heat fluxes between bodies 1, 2 (ie. $q_1(t)$) and 1, 3 (ie. $q_2(t)$) are uniform in space, but function of time. So, the one node

USEM is considered in this Chapter.

6) Point 1 is at r=R and z=E/2; Point 2 is at r=0 and z=E; Point 3 is at r=0 and z=0.

7) The situation is shown in Figure 5.2.
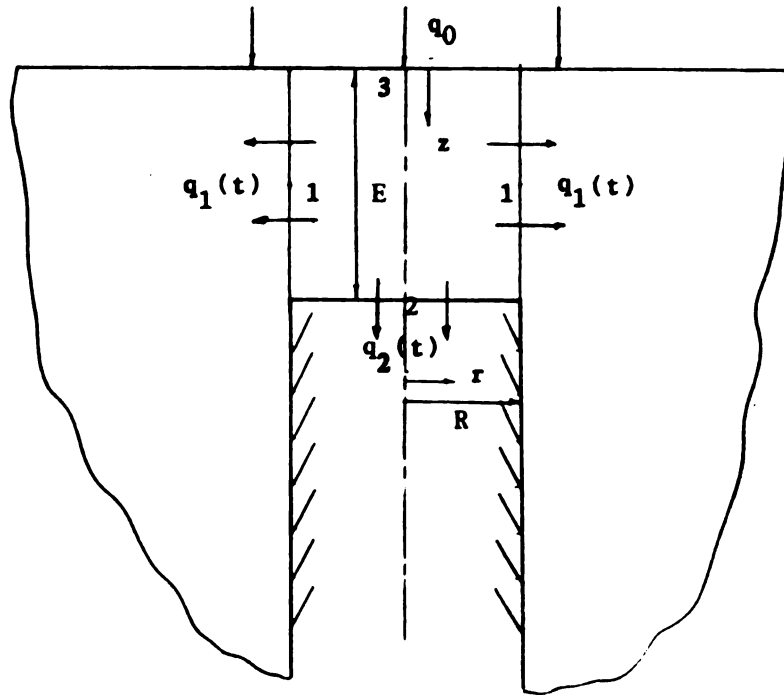
Figure 5.2   One-node USEM with the consideration

of the thermal properties of thermocouple.

5.4 The Influence Functions

The following are the influence functions needed in the procedure of one node USEM and quasi-steady state method. These influence function, except (5-23) can be obtained from reference [7]. The symbol Θ^i_{jk} means the temperature rise at node j of body i due to unit heat flux

q_k.

$$\theta^1_{10}(t^+) = R/k[gt^+ - 1/24g - 2/g\pi^2 \sum_{n=1}^{\infty}(-1)^n \exp(-4n^2\pi^2g^2t^+)/4n^2] \quad (5\text{-}12)$$

$$\theta^1_{11}(t^+) = R/k[\; 2t^+ + .25 - 2\sum_{n=0}^{\infty}\exp(-a_n^2 t^+)/a_n^2 \;] \quad (5\text{-}13)$$

$$\theta^1_{12}(t^+) = \theta^1_{10}(t^+) \quad (5\text{-}14)$$

$$\theta^1_{20}(t^+) = R/k[gt^+ - 1/6g - 2/g\pi^2 \sum_{n=1}^{\infty}(-1)^n \exp(-4n^2\pi^2g^2t^+)/n^2] \quad (5\text{-}15)$$

$$\theta^1_{21}(t^+) = R/K[\; 2t^+ - .25 - 2\sum_{n=1}^{\infty}\exp(-a_n^2 t^+)/a_n^2 J_0(a_n) \;] \quad (5\text{-}16)$$

$$\theta^1_{22}(t^+) = R/k[gt^+ + 1/3g + 2/g\pi^2 \sum_{n=1}^{\infty}(-1)^n \exp(-4n^2\pi^2g^2t^+)/n^2] \quad (5\text{-}17)$$

$$\theta^1_{30}(t^+) = \theta^1_{22}(t^+) \quad (5\text{-}18)$$

$$\theta^1_{31}(t^+) = \theta^1_{21}(t^+) \quad (5\text{-}19)$$

$$\theta^1_{32}(t^+) = \theta^1_{20}(t^+) \quad (5\text{-}20)$$

$$\theta^3_{22}(t^+) = \theta_{0\infty}(t^+) = (2R/k)(t^+/\pi)^{1/2}k_T \quad (5\text{-}21)$$

$$\theta^2_{10}(t^+) = R/k[2(t^+/\pi)^{1/2}\exp(-1/16g^2t^+) - \text{erfc}(1/4gt^{+1/2})/2g] \quad (5\text{-}22)$$

$$\theta^2_{11} = a/k\int_0^t d\tau \int_s G_{R20}G_{X20}dS' \quad (5\text{-}23)$$

where

$t^+ (= at/R^2)$ is called the Fourier number and is a measure of the rate of heat conduction in comparison with the rate of heat storage in a given volume element.

In equations (5-13) and (5-16) α_n is satisfied by the relation of $J_1(\alpha_n)=0$ where J_1 is the Bessel function of the first kind with order 1. J_0 is the Bessel function of the first kind with order 0.

An important ratio of thermal properties is $k_T=(k_t\rho_t c_t/k\rho c)^{1/2}$, c and ρ are the thermal capacity and density of the material. The subscript t means the property of the thermocouple. In this chapter the values of k_T are taken to be 0, 0.01, 0.05 and .10.

In equation (5-23) the influence function is derived from Green's functions, which is discussed in the Appendix A. In general, G_{Rij} means that the Green's function in cylindrical form with the ith kind inner boundary condition and jth kind outer boundary condition. The 1st kind of boundary condition is that the temperature is prescribed along the boundary. The 2nd kind of boundary condition is that the normal derivative of temperature along the boundary is precribed. The 3rd kind of boundary condition is that the combination of temperature and its normal derivative is prescribed along the boundary. The symbol 0 means that there is no boundary. In this thermal cavity problem i=2 and j=0. The Green's function in rectangular coordinate is G_{Xij} with the ith kind of boundary condition on the left (or top) boundary and jth kind of boundary condition on the right (or bottom) boundary. In this thermal cavity problem i=2 and j=0.

In equation (5-23) ds'=$2\pi R dz'$ and z' is from 0 to E. The value of

Θ^2_{11} cab be obtained from Appendix B, equation (B-10) and (B-14) by setting n=1.

In equations (5-13) and (5-16) α_n is satisfied by the relation of $J_1(\alpha_n)=0$ where J_1 is the Bessel function of the first kind with order 1. J_0 is the Bessel function of the first kind with order 0.

An important ratio of thermal properties is $k_T=(k_t\rho_t c_t/k\rho c)^{1/2}$, c and ρ are the thermal capacity and density of the material. The subscript t means the property of the thermocouple. In this chapter the values of k_T are taken to be 0, 0.01, 0.05, and 0.1

In equation (5-23) the influence function is derived from Green's functions, which is discussed in the Appendix A. In general, G_{Rij} means that the Green's function in cylindrical form with the ith kind inner boundary condition and jth kind outer boundary condition. The 1st kind of boundary condition is that the temperature is prescribed along the boundary. The 2nd kind of boundary condition is that the normal derivative of temperature along the boundary is precribed. The 3rd kind of boundary condition is that the combination of temperature and its normal derivative is prescribed along the boundary. The symbol 0 means that there is no boundary. In this thermal cavity problem i=2 and j=0. The Green's function in rectangular coordinate is G_{Xij} with the ith kind of boundary condition on the left (or top) boundary and jth kind of boundary condition on the right (or bottom) boundary. In this thermal cavity problem i=2 and j=0.

In equation (5-23) ds'=2πRdz' and z' is from 0 to E. The value of Θ^2_{11} can be obtained from Appendix B, equations (B-10) and (B-14), by setting n=1.

5.5 Calculational Procedure

In this chapter only one node is assumed in the interface between body 1 and body 2. So, n=1 in the heat flow algebraic equations, (5-8) and (5-9). Now there are two equations with two unknowns, $q_1(k)$ and $q_2(k)$, for each time step. These calculated heat fluxes then are substituted into (5-10) and (5-11) to find the temperature histories at the top of the thermocouple and the hot spot.

The algebraic equation of heat flow from the interface condition between body 1 and body 2 is found by seeting n=1 in equation (5-8)

$$\sum_{k=1}^{m} q_{1k}[\ [\Delta\theta_{11,m-k}^1 + \Delta\theta_{11,m-k}^2] + q_{2k}\Delta\theta_{12,m-k}^1 - q_{0k}[\Delta\theta_{10,m-k}^1 - \Delta\theta_{10,m-k}^2]\ ] = 0 \qquad (5\text{-}24)$$

The algebraic equation of heat flow from the interface condition between body 1 and body 3 is obtained by setting n=1 in equation (5-9)

$$\sum_{k=1}^{m} [\ q_{1k}\Delta\theta_{21,m-k}^1 + q_{2k}(\Delta\theta_{22,m-k}^1 + \Delta\theta_{22,m-k}^3) - q_{0k}\Delta\theta_{20,m-k}^1] = 0 \qquad (5\text{-}25)$$

Now there are two equations (5-24) and (5-25) with two unknowns, q_{1k} and q_{2k}.

$$q_{1k} = q_1[(k-1/2)\Delta t] \qquad (5\text{-}26a)$$

$$q_{2k} = q_2[(k-1/2)\Delta t] \qquad (5\text{-}26b)$$

Define

$$A_1 = \theta_{10}^1 - \theta_{10}^2 \qquad (5\text{-}27a)$$

$$A_2 = \theta_{11}^1 + \theta_{11}^2 \qquad (5\text{-}27b)$$

$$A_3 = \theta_{12}^1 \qquad (5\text{-}27c)$$

$$B_1 = \theta_{20}^1 \qquad (5\text{-}28a)$$

$$B_2 = \theta_{21}^1 \qquad (5\text{-}28b)$$

$$B_3 = \theta_{22}^1 + \theta_{22}^3 \qquad (5\text{-}28c)$$

Substituting the above expressions, (5-27) and (5-28), into equations (5-24) and (5-25) and assuming that q_0 is constant in time as well as in space gives,

$$q_0 A_1(m) = \sum_{k=1}^{m} [\ q_1(k)\Delta A_2(m\text{-}k) + q_2(k)\Delta A_3(m\text{-}k)\ ] \qquad (5\text{-}29)$$

$$q_0 B_1(m) = \sum_{k=1}^{m} [\ q_1(k)\Delta B_2(m\text{-}k) + q_2(k)\Delta B_3(m\text{-}k)\ ] \qquad (5\text{-}30)$$

where

$m=1,2,3,\ldots\infty$

$$\Delta A(m\text{-}k) = A(m\text{-}k+1) - A(m\text{-}k) \qquad (5\text{-}31a)$$

$$\Delta B(m\text{-}k) = B(m\text{-}k+1) - B(m\text{-}k) \qquad (5\text{-}31b)$$

$$q_1(k) = q_{1k} \qquad\qquad q_2(k) = q_{2k} \qquad (5\text{-}31c)$$

$$\sum_{k=1}^{m}\Delta A(m\text{-}k) = \Delta A(m\text{-}1) + \Delta A(m\text{-}2) +\ldots+ \Delta A(0)$$

$$= [A(m)\text{-}A(m\text{-}1)] + [A(m\text{-}1)\text{-}A(m\text{-}2)] +\ldots+ [A(1)\text{-}A(0)]$$

$$= A(m)\text{-}A(0)$$

$$= A(m) \qquad (5\text{-}32)$$

Define

$$q_0 A_1(m) - \sum_{k=1}^{m-1} [\ q_1(k)\Delta A_2(m-k) + q_2(k)\Delta A_3(m-k) \ ] = C(m) \qquad (5\text{-}33)$$

$$q_0 B_1(m) - \sum_{k=1}^{m-1} [\ q_1(k)\Delta B_2(m-k) + q_2(k)\Delta B_3(m-k) \ ] = D(m) \qquad (5\text{-}34)$$

where $C(m)$ and $D(m)$ are known values at $t=t_m$.

Substituting (5-33) and (5-34) into equations (5-29) and (5-30) gives

$$C(m) = q_1(m)A_2(1) + qC_2(m)A_3(1) \qquad (5\text{-}35)$$

$$D(m) = q_1(m)B_2(1) + q_2(m)B_3(1) \qquad (5\text{-}36)$$

The left hand side of equations (5-35) and (5-36) are known. $q_1(m)$ and $q_2(m)$ are the unknowns to be calculated. They can be obtained step by step by marching forward in time for,

$$m=1,2,3,..$$

These two unknowns, $q_1(m)$ and $q_2(m)$, can be obtained by the following formulas,

$$q_1(m) = \Delta_1/\Delta \qquad (5\text{-}37a)$$

$$q_2(m) = \Delta_2/\Delta \qquad (5\text{-}37b)$$

where

$$\Delta = \begin{vmatrix} A_2(1) & A_3(1) \\ B_2(1) & B_3(1) \end{vmatrix} \qquad \Delta_1 = \begin{vmatrix} C(m) & A_3(1) \\ D(m) & B_3(1) \end{vmatrix} \qquad \Delta_2 = \begin{vmatrix} A_2(1) & C(m) \\ B_2(1) & D(m) \end{vmatrix}$$

The temperature at the top of thermocouple and the hot spot at t_m can be obtained by substituting n=1 and j=1 in equations (5-10) and (5-11) to get

$$T_2^1(m) = \sum_{k=1}^{m} [q_{0k}\Delta\theta_{20,m-k}^1 - q_{1k}\Delta\theta_{21,m-k}^1 - q_{2k}\Delta\theta_{22,m-k}^1] \qquad (5-38)$$

$$T_3^1(m) = \sum_{k=1}^{m} [q_{0k}\Delta\theta_{30,m-k}^1 - q_{1k}\Delta\theta_{31,m-k}^1 - q_{2k}\Delta\theta_{32,m-k}^1] \qquad (5-39)$$

where $T_2^1(m)$ and $T_3^1(m)$ are the temperature at the top of thermocouple and the hot spot, respectively, at $t=t_m$. The procedure of calculation is as follows:

1) Set m=1.

2) Substitute the value of m into equations (5-33) and (5-34) and calculate $C(m)$ and $D(m)$.

3) Substitute $C(m)$ and $D(m)$ into equations (5-35) and (5-36) to calculate the value of $q_1(m)$ and $q_2(m)$ by using equations (5-37a) and (5-37b).

4) Substitute $q_1(m)$ and $q_2(m)$ into equations (5-38) and (5-39) to calculate the temperature at the top of thermocouple and at the hot spot.

5) Increase m by 1, then go to step 2.

From the results of calculations, the transient temperature at the top of thermocouple for large times can be expressed as $T_2^{1+}(t) =$

$(T_2^1 - T_{0\infty})/(q_0 R/k) = C_1 + C_2 t^{+-1/2}$. Tables 5.1 to 5.4 contain the values of C_1 and C_2 versus the values of g for $k_T^2 = 0$, 0.01, 0.05, and 0.1, respectively. Figures 5.3 to 5.6 are the transient temperature histories at the top of thermocouple versus the values of g for $k_T^2 = 0$, 0.01, 0.05, and 0.1, respctively. Figure 5.7 contain the value of g corresponding to the location of null point versus the values of k_T^2.

Table 5.1 C_1 and C_2 versus g for $k_T^2 = 0$.

g	.50	.75	1.0
C_1	−.7474	−.1830	.1536
C_2	−.5475	−.6360	−.6440

Table 5.2 C_1 and C_2 versus g for $k_T^2 = .01$

g	.50	.75	1.0
C_1	−.8735	−.2982	.0384
C_2	−.4470	−.5860	−.6180

Table 5.3 C_1 and C_2 versus g for $k_T^2 = .05$

g	.75	1.0	1.5
C_1	−.4480	−.1048	.3063
C_2	−.5040	−.5600	−.6050

Table 5.4 C_1 and C_2 versus g for $k_T^2 = .1$

g	.75	1.0	1.0
C_1	−.5471	−.2112	.3063
C_2	−.4290	−.5080	−.5830
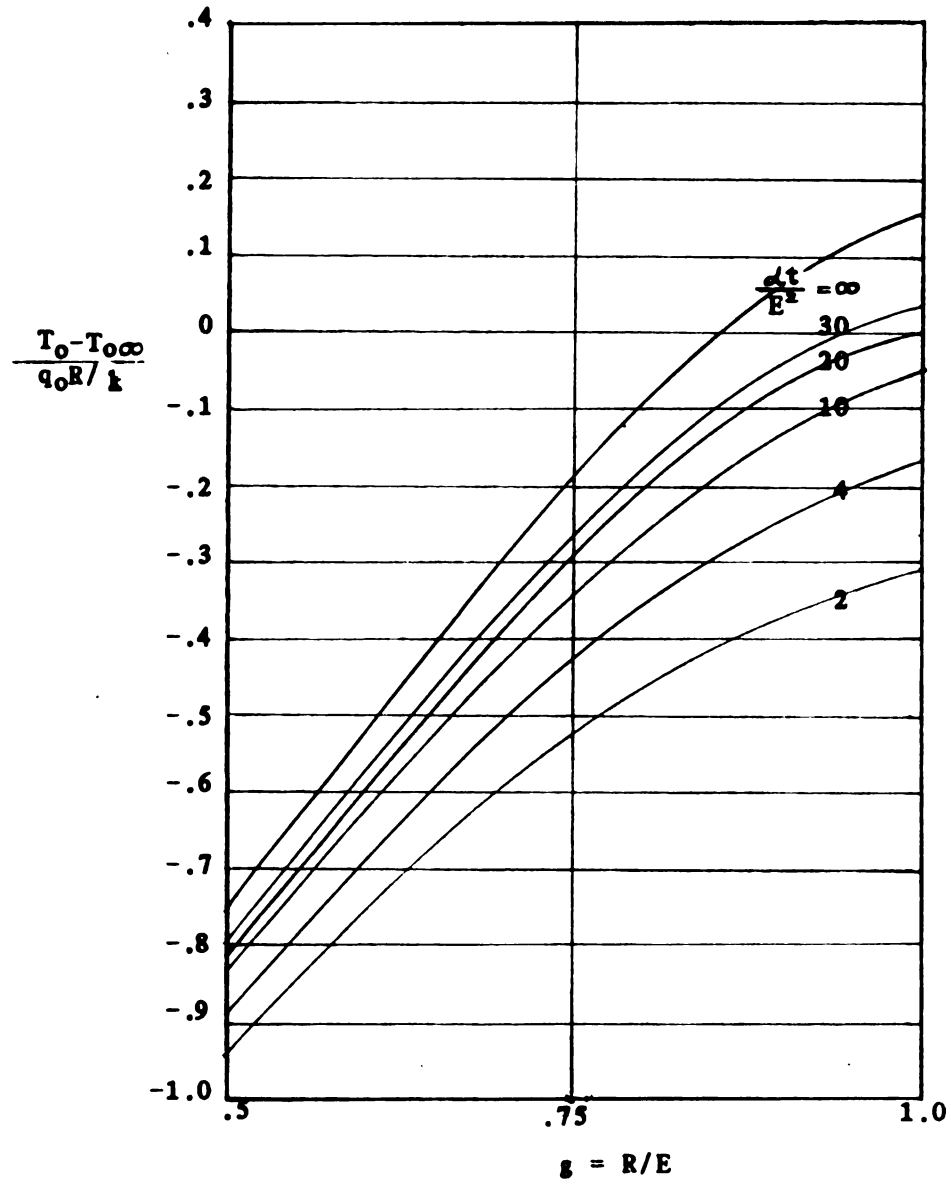
Figure 5.3 Transient temperature at the top of thermocouple for $k\frac{z}{T}=0$.
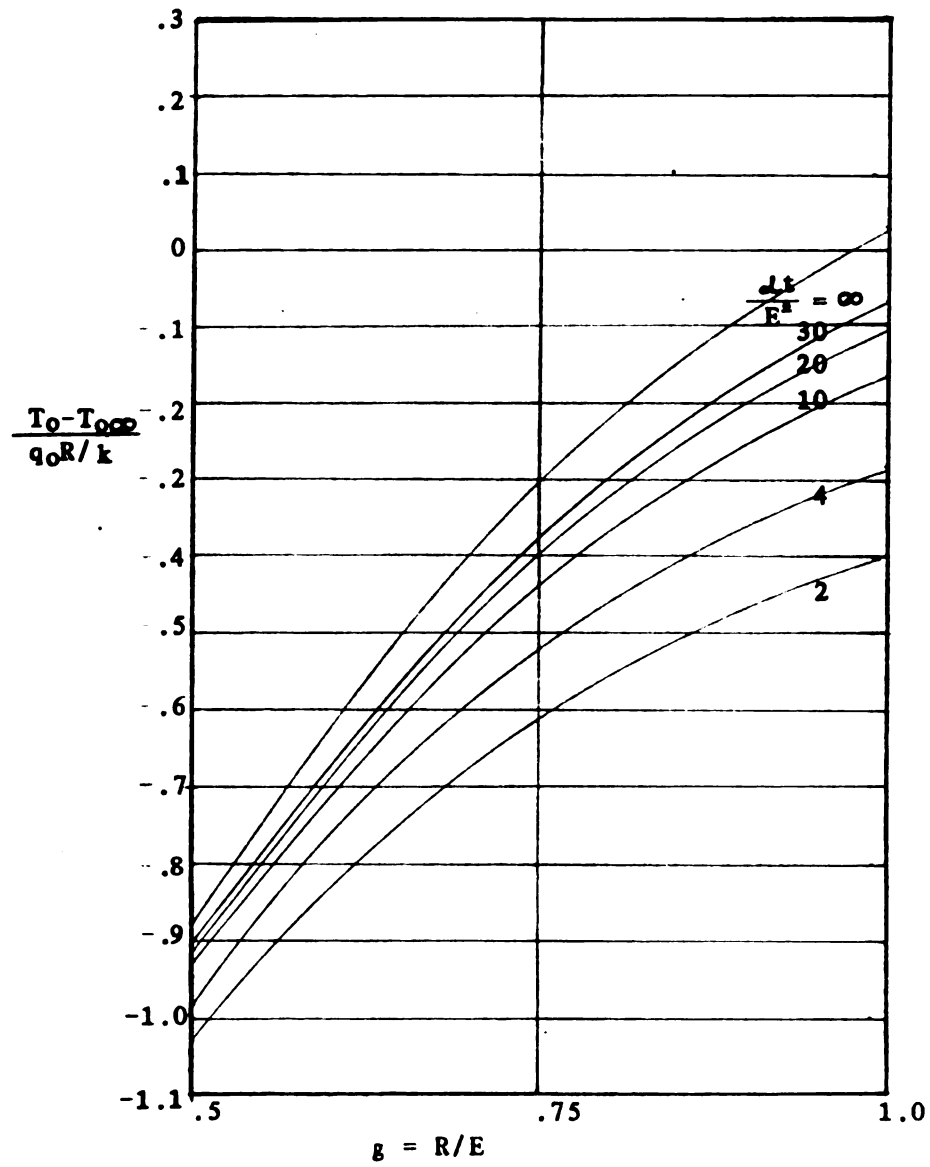
Figure 5.4 Transient temperature at the top of thermocouple for $k\frac{Z}{I}=0.01$
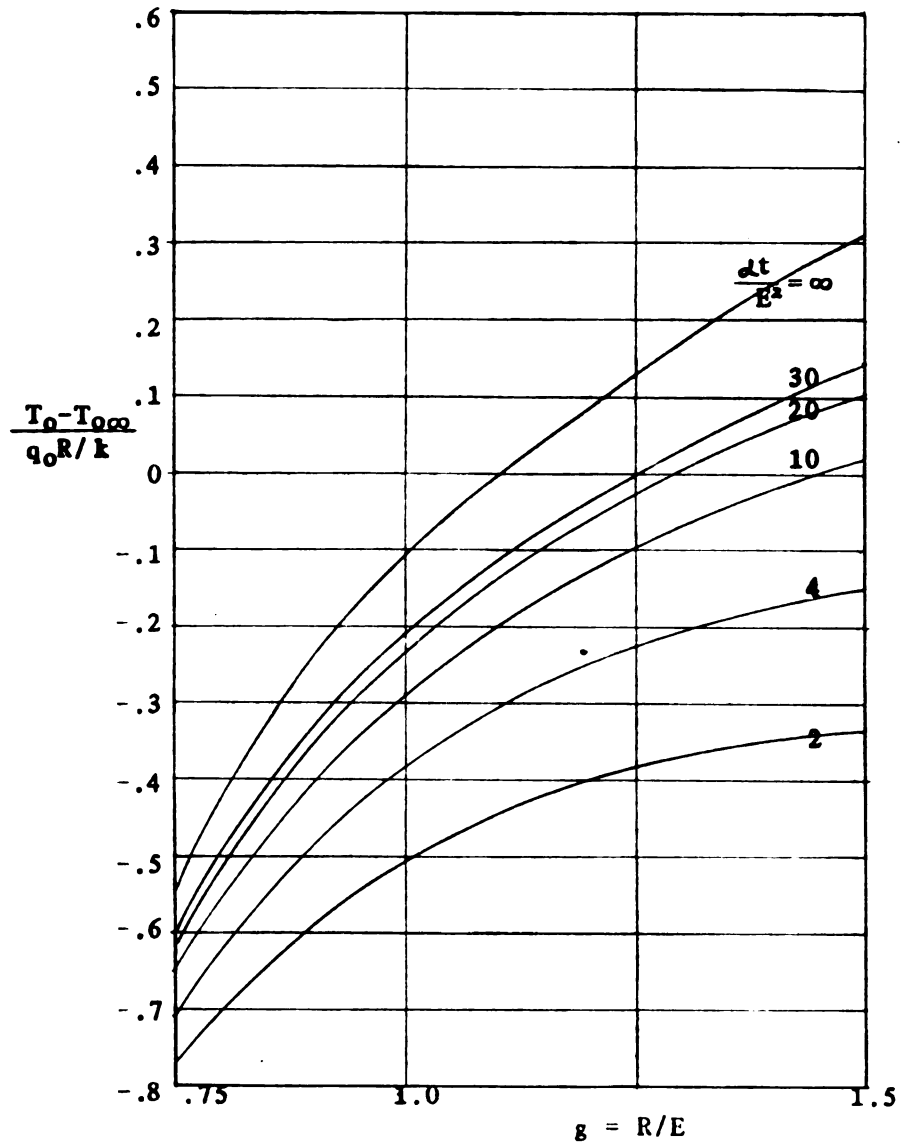
Figure 5.5 Transient temperature at the top of thermocouple for $\frac{z}{k_T} = .05$

$$\frac{T_0 - T_{O\infty}}{q_0 R/k}$$

.5
.4
.3
.2
.1
0
-.1
-.2
-.3
-.4
-.5
-.6
-.7
-.8

.75 1.0 1.5

$\frac{\alpha t}{E^2} = \infty$

30

20

10

4

2

g = R/E
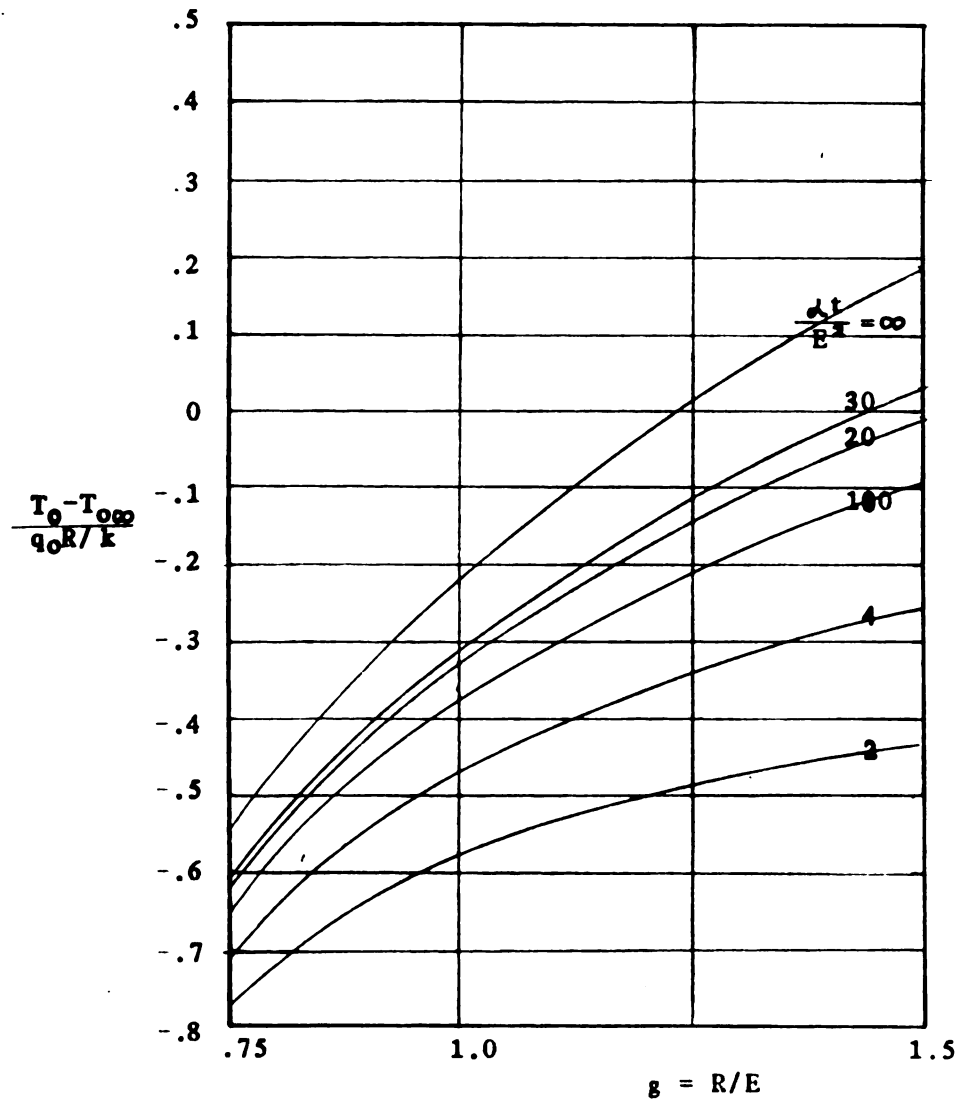
Figure 5.6 Transient temperature at the top of thermocouple for $k\frac{Z}{T} = .10$
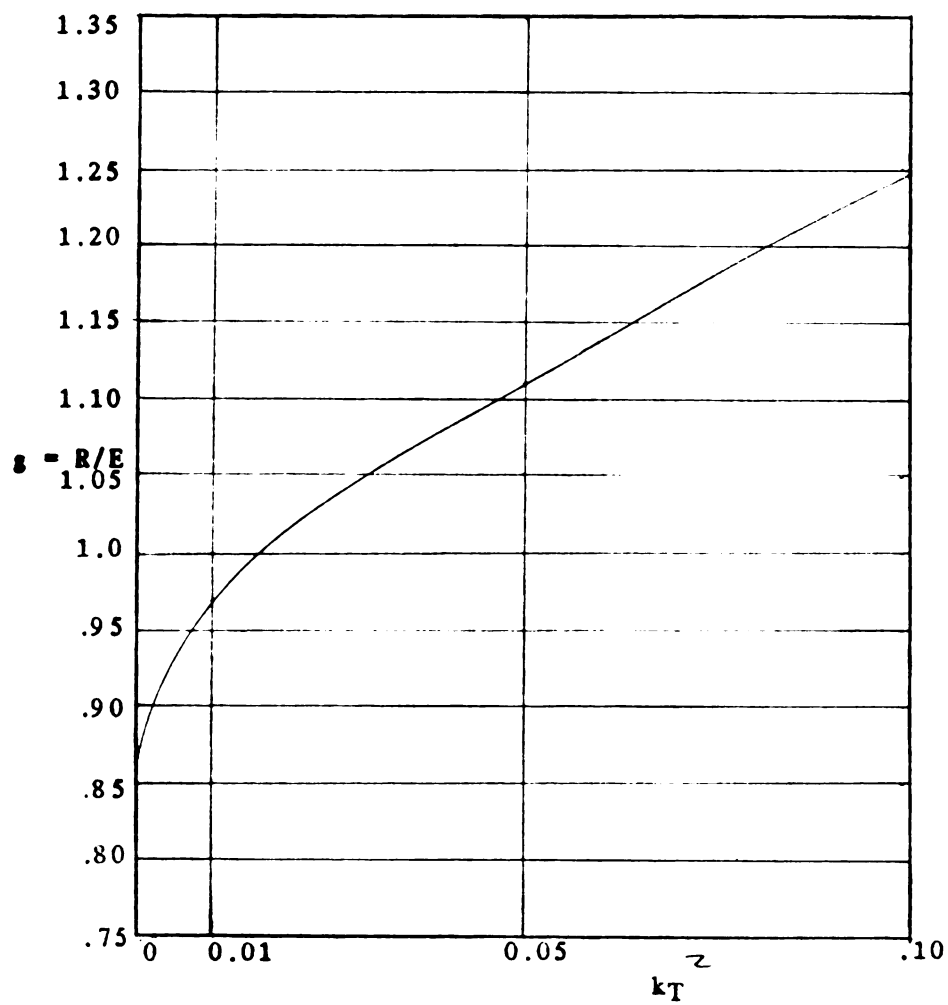
Figure 5.7 The null point location versus k_T^2

5.6 Quasi-steady State Solution

In this section the quasi-steady state method derived in Chapter 3 is used to calculate some thermal behavior of interest at quasi-steady state. They are the temperatures at the hot spot and the top of the thermocouple. For simple analysis the thermocouple is assumed to be insulated.

The energy conservation equation is obtained by setting $n=1$ in equation (3-17)

$$q_1 = Rq_0/2E = gq_0/2 \tag{5-40}$$

The large time temperature at node 1 of body 1 can be expressed by setting $n=1$ and $j=1$ in equation (3-18)

$$T_1^1 = q_0\theta_{10}^1(t) - q_1\theta_{11}^1(t) + B \tag{5-41}$$

where the constant B is dependent on the boundary condition of body 2 and the interface condition between body 1 and body 2.

The exponential terms in the influence functions θ_{10}^1 and θ_{11}^1 in (5-12) and (5-13) are dropped because they are negligible for large times compared with other terms in the equations. Then substitute these modified functions into (5-41) to obtain

$$T_1^1 = -q_1R(2t^+ + .25)/k + q_0R(gt - 1/24g)/k + B \tag{5-42}$$

Substituting (5-40), the energy conservation equation, into (5-42),

then gives

$$T_1^1 = q_0 R(-g/8 - 1/24g)/k + B \qquad (5\text{-}43)$$

For $\quad$ g=.5 $\qquad$ $T_1^1 = q_0 R(-7/48)/k + B$ $\qquad$ (5-44a)

For $\quad$ g=1.0 $\qquad$ $T_1^1 = q_0 R(-1/6)/k + B$ $\qquad$ (5-44b)

For $\quad$ g=2.0 $\qquad$ $T_1^1 = q_0 R(-13/48)/k + B$ $\qquad$ (5-44c)

where equations (5-44) are meant that the temperature at node 1 of body 1 for large time is a function of g, the interface condition between body 1 and body 2 and boundary condition of body 2.

The large time temperature at node 1 of body 2, can be expressed by setting n=1 and j=1 in equation (3-19)

$$T_1^2 = q_0 \theta_{10}^2(t) + q_1 \theta_{11}^2(t) \qquad (5\text{-}45)$$

Substituting (5-22), the influence function θ_{10}^2, and the steady state value of θ_{11}^2, which is from [13], into (5-45) and replacing $q_1(t)$ by $q_0(t)$ by the energy conservation equation gives

For $\quad$ g=.5 $\qquad$ $T_1^2 = q_1 R(1.515174)/k - q_0 R/2gk + T_{0\infty}$

$$= q_0 R(-.6212065)/k + T_{0\infty} \qquad (5\text{-}46a)$$

For $\quad$ g=1.0 $\quad$ $T_1^2 = q_1R(1.05779)/k - q_0R/2gk + T_{0\infty}$

$$= q_0R(.028596)/k + T_{0\infty} \qquad (5-46b)$$

For $\quad$ g=2.0 $\quad$ $T_1^2 = q_0R(.703691)/k - q_0R/2gk + T_{0\infty}$

$$= q_0R(.453691)/K + T_{0\infty} \qquad (5-46c)$$

where equations (5-46) is meant that the temperature at node 1 of body 2 is determined by the value of g. The values of 1.515174, 1.05779 and .703691 are from [13] and $T_{0\infty}$ is the temeprature at the surface of semi-infinite body due tò unit step heat flux over the surface.

The interface condition between body 1 and body 2 is considered perfect, $T_1^1 = T_1^2$.

For $\quad$ g=.5 $\quad$ $B = -q_0R(.475373)/k + T_{0\infty} \qquad (5-47a)$

For $\quad$ g=1.0 $\quad$ $B = q_0R(.195562)/k + T_{0\infty} \qquad (5-47b)$

For $\quad$ g=2.0 $\quad$ $B = q_0R(.724524)/k + T_{0\infty} \qquad (5-47c)$

The temperature at the top of thermocouple, T_2^1, for large times is

$$T_2^1 = q_0R(gt - 1/6g)/k - q_1R(2t - .25)/k + B \qquad (5-48)$$

For $\quad$ g=.5 $\quad$ $T_2^1 = q_0R(-.746206)/k + T_{0\infty} \qquad (5-49a)$

$$\text{For} \quad g=1. \quad T_2^1 = q_0 R(.153894)/k + T_{0\infty} \quad\quad (5\text{-}49b)$$

$$\text{For} \quad g=2. \quad T_2^1 = q_0 R(.891191)/k + T_{0\infty} \quad\quad (5\text{-}49c)$$

The temperature at hot spot, T_3^1, for large times is

$$T_3^1 = q_0 R(gt + 1/3g)/K - q_1 R(2t - .25)/K + B \quad\quad (5\text{-}50)$$

$$\text{For} \quad g=.5 \quad T_3^1 = q_0 R(.25379)/K + T_{0\infty} \quad\quad (5\text{-}51a)$$

$$\text{For} \quad g=1.0 \quad T_3^1 = q_0 R(.653895)/K + T_{0\infty} \quad\quad (5\text{-}51b)$$

$$\text{For} \quad g=2.0 \quad T_3^1 = q_0 R(1.141191)/K + T_{0\infty} \quad\quad (5\text{-}51c)$$

5.7 Observations

1) The difference between temperature histories at the top of the thermocouple by the one-node USEM, Figure 5.3, and the finite difference method, Figure 2.5, with the assumption of insulated thermocouple decreases with increment of the value of g. The difference increases with the increment of t^+, but the rate of difference approaches zero at large time.

2) Compareing the results by the finite difference method and one-node USEM with the assumption of insulated thermocouple, the value of g corresponding to the null point location is 1 by the finite difference method but it is only .85 by the one-node USEM. This is due

to the assumption of uniform heat flux in space passing through the interface between body 1 and body 2. Since this assumption increases the disturbance caused by the thermocouple, the thermocouple has to be placed a little far away from the heated surface.

3) From the Tables 5.1 to 5.4, the transient disturbance caused by the thermocouple (ie. the absolute value of C_2) for the same value of g decreases with the increment of k_T. The steady state disturbace caused by the thermocouple (ie. C_1) also decreases with increment of k_T for the same value of g. It means that the distubance caused by the thermocouple decreases with the increment of thermal proproties of the thermocouple.

4) From Figure 5.7, the value of g corresponding to the location of null point is increasing with the increment of k_T. It means that the thermocouple should be placed near the heated surface with a larger value of k_T because the disturbance caused by the thermocouple decreases. Though one-node assumption is not accurate for the insulated thermocouple case, the error decreases as the k_T value increases because more energy passes through the interface between body 1 and body 3. In this case one node in enough to model the interface thermal behavior between body 1 and body 2.

5) Comparing the dimensionless temperature at the top of thermocouple, $\theta_2^{1+} = (T_2^1 - T_{0\infty})/(q_0 R/k)$, the results from the quasi-steady state method and the transient solution of USEM are almost the same. It means that the both method are acceptible.

CHAPTER 6

THREE-NODE TRANSIENT SOLUTIONS OF USEM

6.1 Introduction

In this chapter the interface between body 1 and body 2 is divided into 3 equally-spaced surface elements and the thermocouple is assumed to be insulated. Stolz's method of constant heat flux assumption in each time interval is used to simplify the integral equation of heat flow derived from USEM. Due to the use of 3 elements on the interface between body 1 and body 2, the results of the calculated thermal behavior is more accurate compared with those by the one-node USEM, especially for the small value of g.

The outline of this chapter is as follows: Section 6.2 gives the objectives of this chapter. Section 6.3 describes the problem. Section 6.4 includes the influence functions needed in the calculational procedure. Section 6.5 includes the calculational procedure. Section 6.6 discusses the quasi-steady state method. Section 6.7 includes the observations.

6.2 Objectives

1) The first objective is finding the transient temperature at the top of thermocouple by the three-node USEM with Stolz's assumption of constant heat flux over each time interval.

81

2) The second objective is to make an accurate prediction of null point location.

3) The third objective is to illustrate the quasi-steady state method with three nodes on the interface between body 1 and body 2.

6.3 The Problem Description
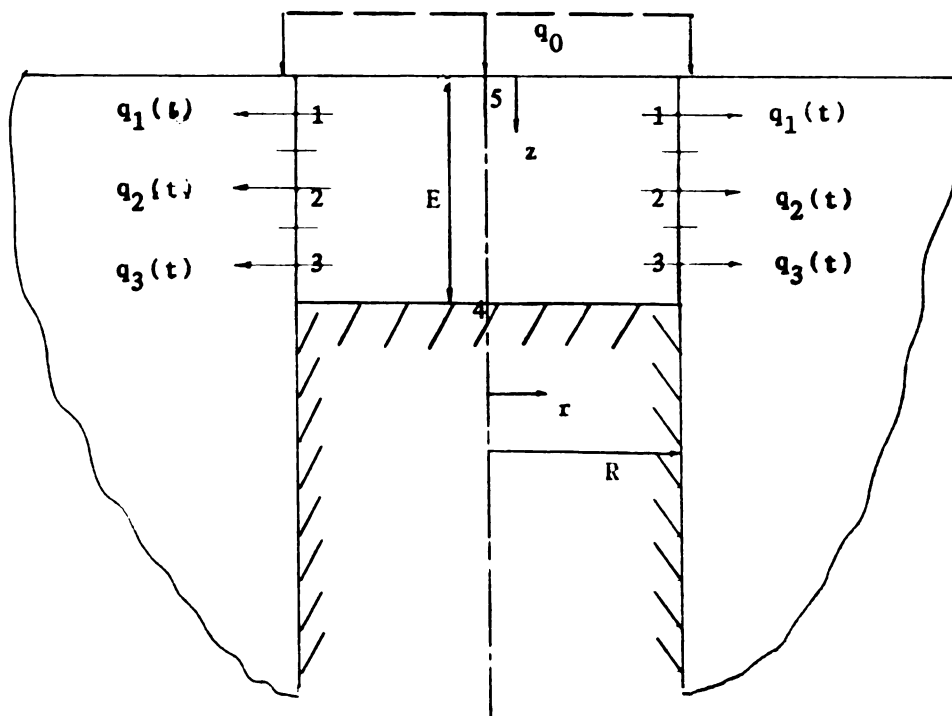
Figure 6.1 Geometry representation of 3-node USEM

The following is a description of the problem. See figure 6.1

1) The thermocouple is assumed insulated.

2) The boundary between body 1 and body 2 is discretized into 3

equally-spaced surface elements. Each of which has radius R and height E/3.

3) Node 1 is at r=R and z=E/6. Node 2 is at r=R and z=E/2. Node 3 is at r=R and z=5E/6. Point 4, which is at the top of the thermocouple, is at r=0 and z=E. Point 5, which is the location of the hot spot, is at r=0 and z=0.

4) The transient temperature histories at the top of thermocouple is calculated by the three-node USEM. The quasi-steady state method will be used to find the quasi-steady state disturbance at the top of thermocouple as well as at the hot spot.

5) The heat fluxes $q_1(t)$, $q_2(t)$ and $q_3(t)$ are assumed uniform over each element in space and functions of time only. Stolz's method of constant heat flux over each time interval is used to simplify the calculational procedure.

6.3 The Influence Functions

The following influence functions are needed in the calculational procedure. The temperature at node (or point) j of body m due to unit step heat flux q_i is denoted as θ_{ji}^m.

$$\theta_{ji}^{m+} = \theta_{ji}^m / (q_i R/k) \tag{6-1}$$

The temperature at node j of body 1 due to a unit step heat flux q_i which is over the radial region from a to b, can be obtained from Appendix A, equation (A-9) with n=3, and is denoted as θ_{ji}^{1+}.

$$\Theta_{ji}^{1+} = 2t^{+}/3 + C_{ji}^{1} - A_1 - A_2 - A_3 \qquad (6\text{-}2)$$

where

$i, j = 1, 2,$ and 3

$$t^{+} = \alpha t/R^{2} \qquad (6\text{-}3)$$

$$A_1 = \sum_{m=1}^{\infty} 2\exp(-\beta_m^2)/3\beta_m^2 \qquad (6\text{-}4a)$$

$$A_2 = \sum_{n=1}^{\infty} 8\cos(n\pi z^{+})\sin(n\pi(a^{+}+b^{+})/2)\sin(n\pi(b^{+}-a^{+})/2)$$
$$\exp(-n^2\pi^2 g^2 t^{+})/(n^3\pi^3 g^2) \qquad (6\text{-}4b)$$

$$A_3 = \sum_{n=1}^{\infty}\sum_{m=1}^{\infty} 8\cos(n\pi z^{+})\sin(n\pi(b^{+}+a^{+})/2)\sin(n\pi(b^{+}-a^{+})/2)$$
$$\exp(-(\beta_m^2+n^2\pi^2 g^2)t^{+})/n\pi(\beta_m^2+n^2\pi^2 g^2) \qquad (6\text{-}4c)$$

$$z^{+} = z/E \qquad z = (j-1/2)E/3 \qquad (6\text{-}5a)$$

$$a^{+} = a/E \qquad a = z_{i-1} \qquad (6\text{-}5b)$$

$$b^{+} = b/E \qquad b = z_{i} \qquad (6\text{-}5c)$$

β_m is satisfied by $J_1(\beta_m)=0$, J_1 is the Bessel function of first kind with order zero. Tables 6.1, 6.2 and 6.3 contain the constant C_{ji}^{1}'s for g=.5, 1.0, and 1.5.

Table 6.1 Values of C^1_{ji} for $g=.5$

C^1_{11}	C^1_{12}	C^1_{13}	C^1_{21}	C^1_{22}
0.646841	−0.040476	−0.356447	−0.040469	0.330934

Table 6.2 Values of C^1_{ji} for $g=1.0$

C^1_{11}	C^1_{12}	C^1_{13}	C^1_{21}	C^1_{22}
0.299399	0.027527	−0.076945	0.027534	0.194940

Table 6.3 Values of C^1_{ji} for $g=1.5$

C^1_{11}	C^1_{12}	C^1_{13}	C^1_{21}	C^1_{22}
0.217573	0.047193	−0.014773	0.047197	0.155609

The principle of superposition can be used to check the accuracy of C^1_{ji}'s. For example, the temperature at node 2, $z^+=.5$, due to unit step heat flux over the whole radial surface of body 1, θ^{1+}_2, can be obtained from equation (6-2) as,

$$\theta^{1+}_2 = \theta^{1+}_{21} + \theta^{1+}_{22} + \theta^{1+}_{23} \tag{6-6}$$

For the case of $g=.50$, the constant terms on the right hand side

of equation (6-6) can be obtained from Table 6.1 and the sum of these constants is .646841 − .040469 − .356447 = .249925. The theoretical value of constant term on the left hand side [7], page 203, is .25. Other constant C_{ji}^1's can be checked by using a similiar procedure.

The temperature at point 4 due to a unit step heat flux q_i can be found in Appendix C, equation (C-4) with n=3, and is denoted as θ_{4i}^{1+},

$$\theta_{4i}^{1+} = 2t^+/3 + C_{4i}^1 + B_1 + B_2 + B_3 \qquad (6-7)$$

where

$$B_1 = \sum_{m=1}^{\infty} 2\exp(-\beta_m^2 t^+)/3\beta_m^2 J_0(\beta_m) \qquad (6-8a)$$

$$B_2 = 4\sum_{n=1}^{\infty} [\ \sin(n\pi b^+)-\sin(n\pi a^+)\ ]\exp(-n^2\pi^2 g^2 t^+)/(n^3\pi^3 g^2) \qquad (6-8b)$$

$$B_3 = 4\sum_{m=1}^{\infty}\sum_{n=1}^{\infty} [\ \sin(n\pi b^+)-\sin(n\pi a^+)\ ]\exp[-(\beta_m^2+n^2\pi^2 g^2)t^+]$$
$$/n\pi(\beta_m^2+n^2\pi^2 g^2)J_0(\beta_m) \qquad (6-8c)$$

where β_m is satisfied by $J_1(\beta_m)=0$. The value of C_{4i}^1 is in Tables 6.4, 6.5 and 6.6.

Table 6.4 Values of C_{4i}^1 for $g=.5$

C_{41}^1	C_{42}^1	C_{43}^1
$-.089575$	$-.083372$	$-.077055$

Table 6.5 Values of C_{4i}^1 for $g=1.0$

C_{41}^1	C_{42}^1	C_{43}^1
$-.121857$	$-.084432$	$-.043712$

Table 6.6 Values of C_{4i}^1 for $g=1.5$

C_{41}^1	C_{42}^1	C_{43}^1
$-.397066$	$-.121797$	$-.268917$

The principle of superposition can be used to test the accuracy of C_{4i}^1's. For example, the temperature at point 4 due to a unit step heat flux over the whole radial surface of body 1, θ_4^{1+}; can be expressed as,

$$\theta_4^{1+} = \theta_{41}^{1+} + \theta_{42}^{1+} + \theta_{43}^{1+} \tag{6-9}$$

The constant terms on the right hand side of equation (6-9) for the case of $g=.50$ can be found in Table 6.4 and the sum is .268917 -

.121797 - .397066 = -.249946. The theoretical value of the constant term [7], page 112, on the left hand side of equation is -.25.

The temperature rise at node j of body 2 due to unit heat flux q_i, i=1, 2, 3, can be obtained from Appendix B, equation (B-10), and is denoted as θ_{ji}^{2+}.

The steady state part of θ_{ji}^{2+} is denoted as C_{ji}^2. Tables 6.7, 6.8 and 6.9 contain the value of C_{ji}^2 for g=.5, 1.0 and 1.5, respectively. From these Table $C_{21}^2 = C_{21}^2$, $C_{13}^2 = C_{31}^2$ and $C_{23}^2 = C_{32}^2$.

Table 6.7		Table 6.8		Table 6.9	
The value of C_{ji}^2		The value of C_{ji}^2		The value of C_{ji}^2	
for g=.5		for g=1.0		for g=1.5	
C_{11}^2	.841121	C_{11}^2	.543134	C_{11}^2	.413439
C_{12}^2	.445051	C_{12}^2	.324921	C_{12}^2	.261967
C_{13}^2	.301813	C_{13}^2	.236434	C_{13}^2	.197672
C_{21}^2	.444946	C_{21}^2	.324873	C_{21}^2	.261976
C_{22}^2	.694849	C_{22}^2	.454707	C_{22}^2	.349355
C_{23}^2	.374903	C_{23}^2	.278038	C_{23}^2	.226652
C_{31}^2	.301815	C_{31}^2	.236435	C_{31}^2	.197672
C_{32}^2	.374967	C_{32}^2	.278038	C_{32}^2	.226679
C_{33}^1	.651746	C_{33}^2	.424298	C_{33}^2	.325793

The steady state dimensionless temperature at node 2, $z^+=1.5$, due to a unit step heat flux over the boundary etween body 1 and body 2 for $g=0.5$ and 1.0 are [8]

$$at \ g = 0.5 \qquad C_2^2 = 1.515174 \qquad (6-10a)$$

$$at \ g = 1.0 \qquad C_2^2 = 1.05779 \qquad (6-10b)$$

From the principle of superposition the temperature at node 2 due to a unit step heat flux can be expressed as,

$$C_2^2 = C_{21}^2 + C_{22}^2 + C_{23}^2 \qquad (6-11)$$

where C_{2i}^2's can be found in Tables 6.7 and 6.8 for the case of $g=0.5$ and 1.0,

$$at \ g=0.5 \quad C_2^2 = .444946 + .694849 + .374903 = 1.514698 \qquad (6-12a)$$

$$at \ g=1.0 \quad C_2^2 = .324873 + .454707 + .278038 = 1.057618 \qquad (6-12b)$$

The difference between (6-10) and (6-12) are very small. So, this means that values in Tables 6.7, 6.8, and 6.9 are very accuracy.

The temperature at node j of body 2 due to a unit step heat flux q_0 can be found in reference [7], page 75,

$$\theta_{j0}^{2+} = 2(t^+/\pi)^{1/2}\exp(-z^2/4g^2t^+) - z^+\text{erfc}(z^+/2gt^{1/2}) \qquad (6\text{-}13)$$

The temperature at node (point) j of body 1 due to a unit step heat flux q_0 can be found in reference [7], page 112,

$$\theta_{j0}^{1+} = gt^+ - (z^+/2 - 1/6) - 2/\pi^2 \sum (-1)^n\cos(n\pi z^+)\exp(n^2\pi^2g^2t^+)/n^2$$

$$(6\text{-}14)$$

6.4 Calculational Procedure

In this section the 3-node USEM is used to calculate the transient temperature history at the top of the thermocouple. Stolz's method of constant heat flux over each time interval is used to simplify the integral eqautions of heat flow derived from the USEM. The resulted algebraic equations are (5-8), with n=3 and no q_{n+1} term, because of the assumption of insulated thermocouple. The procedure of calculation is similiar as that in section 5.4.

The algebraic equation of heat flow is

$$\sum_{i=1}^{3}\sum_{k=1}^{m}q_{ik}[\ \Delta\theta_{ji,m-k}^1 + \Delta\theta_{ji,m-k}^2\ ] = \sum_{k=1}^{m}q_{0k}[\ \Delta\theta_{j0,m-k}^1 - \Delta\theta_{ji,m-k}^2\ ]$$

$$j=1,2,3 \qquad (6\text{-}15)$$

Now there are three equations with three unknowns, q_{1k}, q_{2k} and q_{3k}.

$$q_{ik} = q_i[(k-1/2)\Delta t] \qquad (6\text{-}16a)$$

$$\Delta\theta_{ji,m-k}^k = \theta_{ji,m-k+1}^k - \theta_{ji,m-k}^k \qquad (6\text{-}16b)$$

Set

$$A_j(k) = \Theta_{j0}^1(k) - \Theta_{j0}^2(k) \tag{6-17a}$$

$$B_j(k) = \Theta_{j1}^1(k) + \Theta_{j1}^2(k) \tag{6-17b}$$

$$C_j(k) = \Theta_{j2}^1(k) + \Theta_{j2}^2(k) \tag{6-17c}$$

$$D_j(k) = \Theta_{j3}^1(k) + \Theta_{j3}^2(k) \tag{6-17d}$$

for $j=1$, 2, and 3

Substituting (6-17) into (6-15) and assuming that q_0 is constant in time as well as in space gives

$$q_0 A_j(m) = \sum_{k=1}^{m} q_1(k)\Delta B_j(m-k+1) + q_2(k)\Delta C_j(m-k+1) + q_3(k)\Delta D_j(m-k+1) \tag{6-18}$$

where

$$\Delta B_j(m-k+1) = B_j(m-k+1) - B_j(m-k) \tag{6-19a}$$

$$\Delta C_j(m-k+1) = C_j(m-k+1) - C_j(m-k) \tag{6-19b}$$

$$\Delta D_j(m-k+1) = D_j(m-k+1) - D_j(m-k) \tag{6-19c}$$

Define

$$L_j(m) = q_0 A_j(m) - \sum_{k=1}^{m-1} [\, q_1(k)\Delta B_j(m-k+1) + q_2(k)\Delta C_j(m-k+1)$$
$$+ q_3(k)\Delta D_j(m-k+1) \tag{6-20}$$

Substituing (6-20) into (6-18) gives

$$L_j(m) = q_1(m)B_j(1) + q_2(m)C_j(1) + q_3(m)D_j(1) \qquad (6\text{-}21)$$

where at each time step the left hand side of (6-17), $L_j(m)$'s, are known. The heat flux $q_1(m)$, $q_2(m)$ and $q_3(m)$ can be obtained by the following algorithm

$$q_1(m) = \Delta_1/\Delta \qquad (6\text{-}22a)$$

$$q_2(m) = \Delta_2/\Delta \qquad (6\text{-}22b)$$

$$q_3(m) = \Delta_3/\Delta \qquad (6\text{-}22c)$$

where

$$\Delta = \begin{vmatrix} B_1(1) & C_1(1) & D_1(1) \\ B_2(1) & C_2(1) & D_2(1) \\ B_3(1) & C_3(1) & D_3(1) \end{vmatrix} \qquad \Delta_1 = \begin{vmatrix} L_1(m) & C_1(1) & D_1(1) \\ L_2(m) & C_2(1) & D_2(1) \\ L_3(m) & C_3(m) & D_3(m) \end{vmatrix}$$

$$\Delta_2 = \begin{vmatrix} B_1(1) & L_1(m) & D_1(1) \\ B_2(1) & L_2(m) & D_2(1) \\ B_3(1) & L_3(m) & D_3(1) \end{vmatrix} \qquad \Delta_3 = \begin{vmatrix} B_1(1) & C_1(1) & L_1(m) \\ B_2(1) & C_2(1) & L_2(m) \\ B_3(1) & C_3(m) & L_3(m) \end{vmatrix}$$

The temperature at node 4, the top of the thermocouple, can be obtained from (5-10) by setting n=3

$$T_4^1(m) = \sum_{k=1}^{m} q_{0k}\Delta\theta_{40,m-k}^1 - \sum_{i=1}^{3}\sum_{k=1}^{m} q_{ik}\Delta\theta_{4i,m-k}^1 \qquad (6\text{-}23)$$

["

6.5 Quasi-steady State Solution

From the principle of energy conservation, (3-17), the quasi-steady state equation is given by

$$q_1(t) + q_2(t) + q_3(t) = 3gq_0(t)/2 \qquad (6-24)$$

where (6-24) is suitable only when the rate of the temperature change within body 1 is almost zero.

The temperature at node j of body 1 due to q_0, q_1, q_2 and q_3 for large times can be expressed as

$$T_j^1 = q_0(t)\theta_{j0}^1(t) + \sum_{i=1}^{3} q_i(t)\theta_{ji}^1(t) + B \qquad (6-25)$$

where B is a constant which is dependent on the boundary condition of body 2 and the interface condition between body 1 and body 2.

Substituting the related influence functions into (6-25) and deleting the exponential terms with -t as parameter gives

$$T_1^1 = [\ 13q_0/72g - \sum_{i=1}^{3} C_{1i}^1 q_i(t)\ ]R/k + B \qquad (6-26a)$$

$$T_2^1 = [\ -q_0/24g - \sum_{i=1}^{3} C_{2i}^1 q_i(t)\ ]R/k + B \qquad (6-26b)$$

$$T_3^1 = [\ -11q_0/72g - \sum_{i=1}^{3} C_{3i}^1 q_i(t)\ ]R/k + B \qquad (6-26c)$$

where C_{ji}^1's are in Talbes 6.1, 6.2 and 6.3.

The temperature at node j, $j=1$, 2, and 3, of body 2 due to unit heat flux q_i's, $i=0$, 1, 2 and 3, for large times can be expressed as

$$T^2_j = q_0(t)\theta^1_{j0} + \sum_{i=1}^{3}\theta^2_{ji}q_i(t) \tag{6-27}$$

Substituting the related influence functions into (6-18) and deleting the smaller terms gives

$$T^2_1 = [-q_0/6g + \sum_{i=1}^{3}C^2_{1i}q_i(t)]R/k + T_{0\infty} \tag{6-28a}$$

$$T^2_2 = [-q_0/2g + \sum_{i=1}^{3}C^2_{2i}q_i(t)]R/k + T_{0\infty} \tag{6-28b}$$

$$T^2_3 = [-5q_0/6g + \sum_{i=1}^{3}C^2_{3i}q_i(t)]R/k + T_{0\infty} \tag{6-28c}$$

where the value of C^2_{ji} are in Tables 6.7, 6.8 and 6.9 and $T_{0\infty}$ is the temperature rise at the heated surface of semi-infinite body due to unit heat flux over its surface.

From the perfect interface conditions between body 1 and body 2 one obtains

$$T^1_j = T^2_j \qquad j=1,2,3 \tag{6-29}$$

Now, there are four equations; one is from energy conservation equation, (6-24) and the other three are from the interface conditions, (6-29). There aslo are four unkowns, which are q_1, q_2, q_3 and B. After solving these algebraic equations one obtains

If g=.5 $\quad\quad\quad\quad$ B = -.583536$q_0 R/k$ + $T_{0\infty}$ $\quad\quad\quad\quad$ (6-30a)

If g=1. $\quad\quad\quad\quad$ B = .125900$q_0 R/k$ + $T_{0\infty}$ $\quad\quad\quad\quad$ (6-30b)

If g=1.5 $\quad\quad\quad\quad$ B = .454823$q_0 R/k$ + $T_{0\infty}$ $\quad\quad\quad\quad$ (6-30c)

The dimensionless quasi-steady state temperature at the top of thermocouple, $T_4^+ = (T_4 - T_{0\infty})/(q_0 R/k)$, is

If g=.5, $\quad\quad$ T_4^+ = -1.031338 $\quad\quad\quad\quad$ (6-31a)

If g=1.0, $\quad\quad$ T_4^+ = .057749 $\quad\quad\quad\quad$ (6-31b)

If g=1.5, $\quad\quad$ T_4^+ = .526313 $\quad\quad\quad\quad$ (6-31c)

The dimensionless quasi-steady state temperature at hot spot, $T_5^+ = (T_5 - T_{0\infty})/(q_0 R/k)$, is

If g=.5, $\quad\quad$ T_5^+ = .306696 $\quad\quad\quad\quad$ (6-31a)

If g=1.0, $\quad\quad$ T_5^+ = .610165 $\quad\quad\quad\quad$ (6-31b)

If g=1.5, $\quad\quad$ T_5^+ = .869435 $\quad\quad\quad\quad$ (6-31c)

6.7 Observations

a) Comparing the transient temperature histories at the top of the thermocouple, the difference between the USEM and finite difference method decreases with the increment of the value of g.

b) Comparing the quasi-steady state temperature at the top of thermocouple, the difference between the quasi-steady state method and that extrapolated from the transient temperature derived from USEM increases with the increment of the value of g. The relative error at g = 0.5 is about 0.1% and 1% at g = 1.5.

c) The null point location is found to be at g=.95.

CHAPTER 7

FIVE-NODE QUASI-STEADY STATE SOLUTION

7.1 Introduction

In this chapter the interface between body 1 and body 2 is subdi-
vided into 5 surface elements, each of which has radius R and height
E/5. For simple analysis the thermocouple is assumed to be insulated.
The quasi-steady state method will be used to obtained the temperature
at the top of thermocouple as well as at the hot spot.

The outline of this chapter is as follows: Section 7.2 gives the
objectives of this chapter. Section 7.3 describes the influence func-
tions needed in the calculations. Section 7.4 includes the procedure
of calculation of the quasi-steady state method. Section 7.5 gives
observations.

7.2 Objectives

1) The first objective is checking the results from the three-node
USEM for the case of g=0.5.

2) The second objective is to find an accurate quasi-steady state
disturbance at the top of thermocouple and at the hot spot for small
value of g.

7.3 Problem description
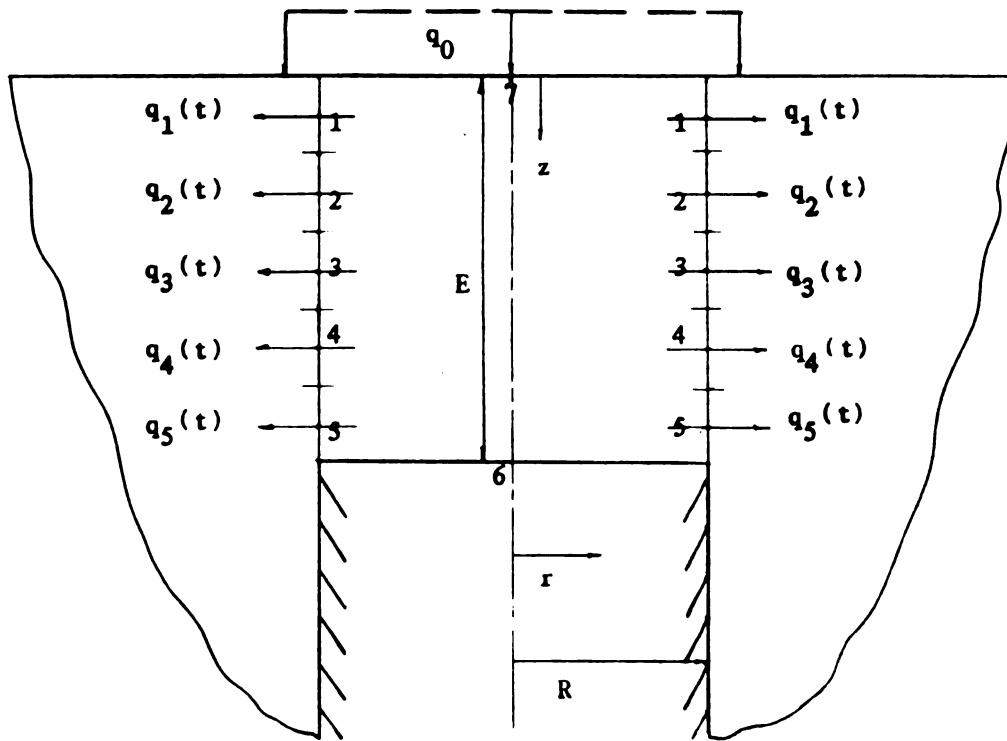
Figure 7.1 Geometry representation of

5-node assumption

The following is a description of the problem. See figure 7.1.

1) The thermocouple is assumed to be insulated.

2) The boundary between body 1 and body 2 is subdivided into 5 equally-spaced surface elements, each of which has height $E/5$ and radius R.

3) The heat flux $q_i(t)$ passing through element i is uniform in space, but function of time.

4) The quasi-steady state method for the thermal cavity problem

derived in chapter 3 is used to obtain the steady state error caused by the thermocouple at the top of thermocouple and the hot spot.

7.4 Influence functions

The influence function θ_{ji}^m means the temperature rise at node j of body m due to a unit step heat flux q_i,

$$\theta_{ji}^{m+} = \theta_{ji}^m / (Rq_i/k) \tag{7-1}$$

The temperature at node j of body 1 due to a unit step heat flux q_i can be obtained from Appendix A, equation (A-9) with n=5, as

$$\theta_{ji}^{1+} = 2t^+/5 + C_{ji}^1 - A_1 - A_2 - A_3 \tag{7-2}$$

where

i,j=1, 2, 3, 4 and 5

$$A_1 = \sum_{m=1}^{\infty} 2\exp(-\beta_m^2)/5\beta_m^2 \tag{7-3a}$$

$$A_2 = \sum_{n=1}^{\infty} 8\cos(n\pi z^+)\sin[n\pi(a^+ + b^+)]\sin[n\pi(b^+ - a^+)] \\ \exp(-(\beta_m^2 + n^2\pi^2 g^2)/(n^3\pi^3 g^2) \tag{7-3b}$$

$$A_3 = \sum_{n=1}^{\infty}\sum_{m=1}^{\infty} 8\cos(n\pi z^+)\sin[n\pi(a^++b^+)/2]\sin[n\pi(b^+-a^+)/2] \\ \exp[-(\beta_m^2 + n^2\pi^2 g^2)t^+]/n\pi(\beta_m^2 + n^2\pi^2 g^2) \tag{7-3c}$$

$$z^+ = (j-1/2)/5$$

$$a^+ = z_{i-1}/E$$

$$b^+ = z_i/E; \qquad z_i = iE/5$$

The value of C^1_{ji}'s are given in Tables 7.1 and 7.2 for $g=0.5$ and .25.

Table 7.1		Table 7.2	
The value od C^1_{ji} for g=.50		The value of C^1_{ji} for g=0.5	
C^1_{11}	.556266	C^1_{11}	1.641059
C^1_{12}	.173018	C^1_{12}	.560032
C^1_{13}	-.049160	C^1_{13}	-.223333
C^1_{14}	-.182574	C^1_{14}	-.736041
C^1_{15}	-.247643	C^1_{15}	-.992068
C^1_{21}	.173018	C^1_{21}	.560032
C^1_{22}	.334102	C^1_{22}	.857702
C^1_{23}	.039623	C^1_{23}	.047440
C^1_{24}	-.114232	C^1_{24}	-.479377
C^1_{25}	-.182574	C^1_{25}	-.746044
C^1_{31}	-.049159	C^1_{31}	-.223228
C^1_{32}	.039624	C^1_{32}	.047440
C^1_{33}	.269042	C^1_{33}	.601691

The temperature at node 6 of body 1 due to a unit step heat flux q_i can be obtained from Appendix C, equation (C-4) with n=5, as

$$\theta_{6i}^{1+} = 2t^{+}/5 + C_{6i}^{1} - B_1 - B_2 - B_3 \qquad (7-4)$$

where

i=1, 2, 3, 4, and 5

$$B_1 = \sum_{m=1}^{\infty} 2\exp(-\beta_m^2 t^{+})/5\beta_m^2 J_0(\beta_m) \qquad (7-5a)$$

$$B_2 = 4\sum_{n=1}^{\infty} [\sin(n\pi b^{+})-\sin(n\pi a^{+})]\exp(n^2\pi^2 g^2 t^{+})/(n^3\pi^3 g^2) \qquad (7-5b)$$

$$B_3 = 4\sum_{m=1}^{\infty}\sum_{n=1}^{\infty} [\sin(n\pi b^{+})-\sin(n\pi a^{+})]\exp[-(\beta_m^2+n^2\pi^2 g^2)t^{+}]$$
$$/[(\beta_m^2+n^2\pi^2 g^2)n\pi J_0(\beta_m)] \qquad (7-5c)$$

The value of C_{6i}^{1}'s are given in Tables 7.3, 7.4, 7.5 and 7.6 for g=.5, .25, .20 and .10, respectively.

Table 7.3 The value of C_{6i}^{1} for g=0.5

C_{61}^{1}	C_{62}^{1}	C_{63}^{1}	C_{64}^{1}	C_{65}^{1}
-.256705	-.194673	-.075931	.077325	.199970

Table 7.4 The value of C^1_{6i} for $g=0.25$

C^1_{61}	C^1_{62}	C^1_{63}	C^1_{64}	C^1_{65}
-1.02405	-.768057	-.256710	.497422	1.301256

Table 7.5 The value of C^1_{6i} for $g=0.2$

C^1_{61}	C^1_{62}	C^1_{63}	C^1_{64}	C^1_{65}
-1.60006	-1.20006	-.400167	.792921	2.157107

Table 7.6 The value of C^1_{6i} for $g=0.1$

C^1_{61}	C^1_{62}	C^1_{63}	C^1_{64}	C^1_{65}
-6.40025	-4.80026	-1.60006	3.199722	9.349653

The temperature at node j of body 2 due to unit heat flux q_i, i is from 1 to 5, can be derived from Appendix B, equation (B-10) with n=5 and is denoted as θ^{2+}_{ji}.

The steady state part of θ^{2+}_{ji} is denoted as C^2_{ji}. Tables 7.7 and 7.8 contain the values of C^2_{ji} for the cases of g=.5 and .25. From the inspection of these Tables $C^2_{ji} = C^2_{5-j,5-i}$ except the case of i=j.

Table 7.7 C_{ji}^2 for $g=.5$		Table 7.8 C_{ji}^2 for $g=.25$	
C_{11}^2	.610843	C_{11}^2	.932319
C_{12}^2	.355317	C_{12}^2	.477489
C_{13}^2	.254073	C_{13}^2	.317559
C_{14}^2	.201475	C_{14}^2	.241121
C_{15}^2	.167780	C_{15}^2	.194762
C_{22}^2	.510005	C_{22}^2	.772400
C_{23}^2	.302710	C_{23}^2	.401047
C_{24}^2	.220387	C_{24}^2	.271203
C_{25}^2	.177719	C_{25}^2	.209681
C_{33}^2	.476346	C_{33}^2	.710120
C_{34}^2	.278954	C_{34}^2	.369598
C_{35}^2	.202627	C_{35}^2	.248360
C_{44}^2	.458577	C_{44}^2	.703188
C_{45}^2	.265111	C_{45}^2	.352185
C_{55}^2	.447461	C_{55}^2	.689275

The temperature at node j of body 2 due to unit heat flux q_0 can be found in [7], page 75,

$$\theta_{j0}^2 = 2(t/\pi)^{1/2} \exp(-z^{+2}/4g^2 t^+) - z^+ \mathrm{erfc}(z^+/2gt^{+1/2}) \qquad (7\text{-}6)$$

The temperature at point j of body 1 due to unit heat flux q_0 is [7], page 112,

$$\theta_{j0}^1 = gt^+ - (z^+/2-1/6)2/\pi^2 \sum_{n=1}^{\infty} (-1)^n \cos(n\pi z^+)\exp(-n^2\pi^2 g^2 t^+)/n^2$$

(7-7)

7.5 Quasi-steady State Solution

From the principle of energy conservation for the quasi-steady state

$$2\pi RE[q_1(t)+q_2(t)+q_3(t)+q_4(t)+q_5(t)]/5 = q_0 \pi R^2$$ (7-8a)

$$q_1(t) + q_2(t) + q_3(t) + q_4(t) + q_5(t) = 5gq_0/2$$ (7-8b)

The temperature at node j, j is from 1 to 5, of body 1 and body 2 due to heat flux $q_i(t)$'s can be expressed as

$$T_j^1(t) = q_0\theta_{j0}^1 + \sum_{i=1}^{5} \theta_{ji}^1 q_i(t) + B$$ (7-9)

$$T_j^2(t) = q_0\theta_{j0}^1 + \sum_{i=1}^{5} \theta_{ji}^1 q_i(t)$$ (7-10)

where B is a constant at large times and is dependent on the boundary condition of body 2 and the interface condition between body 1 and body 2.

Substituting the related influence functions into (7-9), (7-10) and neglecting the exponential terms. Then the quasi-steady state tem-

perature at the top of the thermocouple and at the hot spot can be expressed as

$$T^1_j = [q_0 E_j - \sum_{i=1}^{5} C^1_{ji} q_i(t)]R/K + B \qquad (7-11)$$

$$T^2_j = [q_0 F_j + \sum_{i=1}^{5} C^2_{ji} q_i(t)]R/k + T_{0\infty} \qquad (7-12)$$

where C^1_{ji}'s are given in the Tables 7.1, 7.2 and C^2_{ji}'s are given in the Table 7.7, 7.8. The temperature at the heated surface of semi-infinite body due to unit heat flux over the surface is denoted as $T_{0\infty}$, and

$$E_j = -(z^+/2-1/6)$$

$$F_j = -z^+$$

The perfect interface condition between body 1 and body 2 is used. Then there are 6 equations; one is from the energy conservation equation and others are from the interface conditions. the unknowns are B and the $q_i(t)$'s. After solving these linear algebraic equations, one obtains

For g=.5 $B = -.5968787R/k + T_{0\infty}$ $\qquad$ (7-15)

$$T^+_6 = (T_6-T_{0\infty})/(R/k) = -1.02976 \qquad (7-16a)$$

$$T^+_7 = (T_7-T_{0\infty})/(R/K) = .300941 \qquad (7-16b)$$

For g=.25   B = -1.7421645 + $T_{0\infty}$ (7-17)

T_6^+ = -3.063315   (7-18a)

T_7^+ = .143894   (7-18b)

where T_6^+ and T_7^+ are the quasi-steady error at the top of the thermocouple and the hot spot, respectively. Figure 7.2 shows the quasi-steady state dimensionless temperature at the top of the thermocouple, $(=(T_0 -T_{0\infty})/(Rq_0/k))$, from the 3-node, 5 node-quasi-steady state method and finite difference method. Figure 7.3 shows the quasi-steady state temperature at the hot spot, $(=(T_h - T_{0\infty})/(gRq_0/k))$, form the 3-node and 5-node quasi-steady state method. Figure 7.4 shows the dimensionless error at the hot spot, $(=(T_h - T_{0\infty})/(Rq_0/k))$, from the quasi-steady method and the finite defference method.

7.6 Observations

1) From Figure 7.3 the difference between the quasi-steady state temperature at g=.5 from the 3-node and 5-node quasi-steady state methods are very small. It can be concluded that the 3-node USEM is accurate enough to analyze the thermal cavity problem for the case of g > 0.5.

2) From Figure 7.3, dimensionless quasi-steady error at the hot spot $(=(T_h-T_{0\infty})/(Rgq_0/k))$, the results between the 3-node USEM and finite difference method are very close for the case of g > 1. But the

difference becomes greater as g is smaller than 0.5. So, the results obtained from the finite difference are accurate only when g is greater than 1. Furthermore the number of elements used in this problem is greater than 200 by the finite difference method. Finite difference needs more elements to analyze the problem for g < 0.5. It can be concluded that the USEM is superior to the finite difference in this problem.

3) From Figure 7.2, dimensionless quasi-steady state error at the top of thermocouple (=(T_0 - $T_{0\infty}$)/(Rq_0/k)), the difference between quasi-steady state method and the finite difference method are negligible. It proves the superiority of quasi-steady state method to the finite difference method.
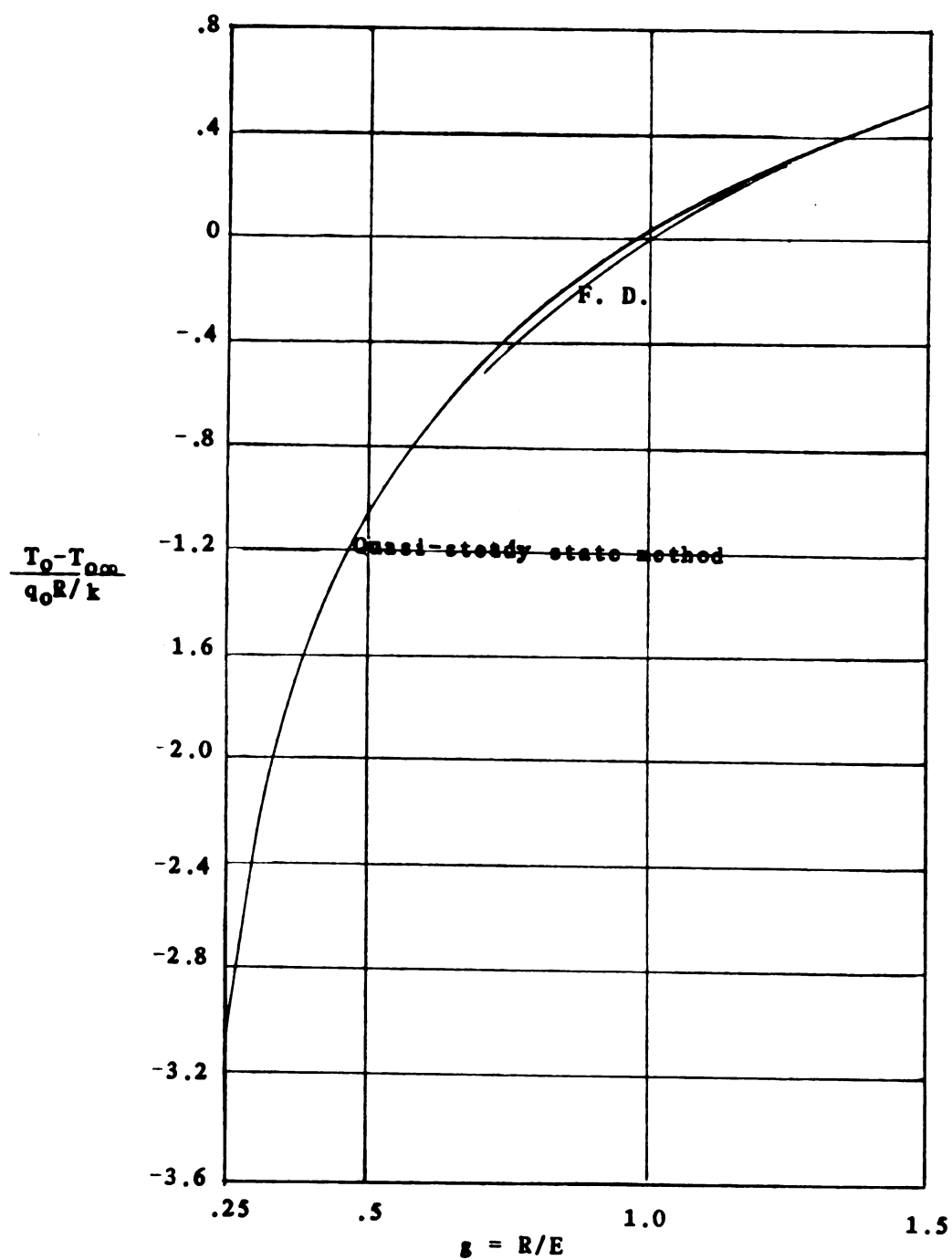
Figure 7.2 Quasi-steady state temperature at the
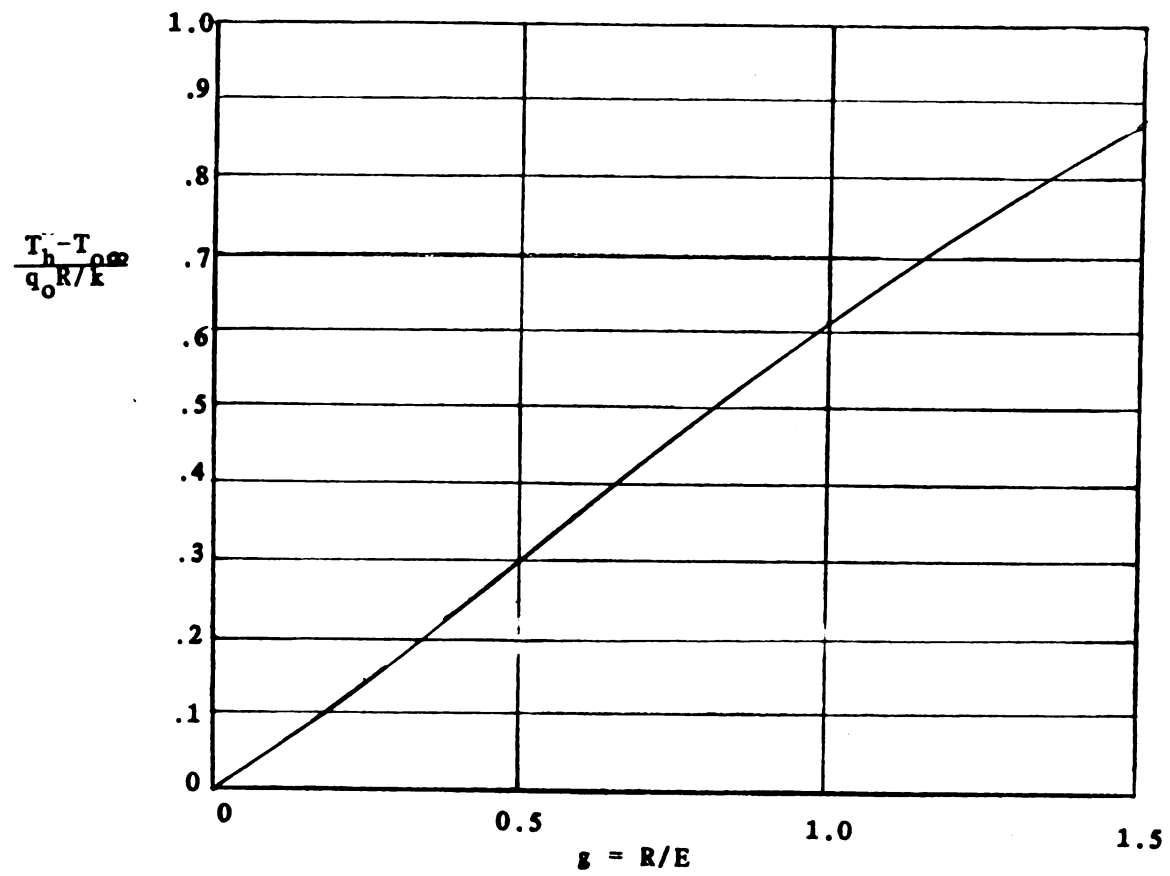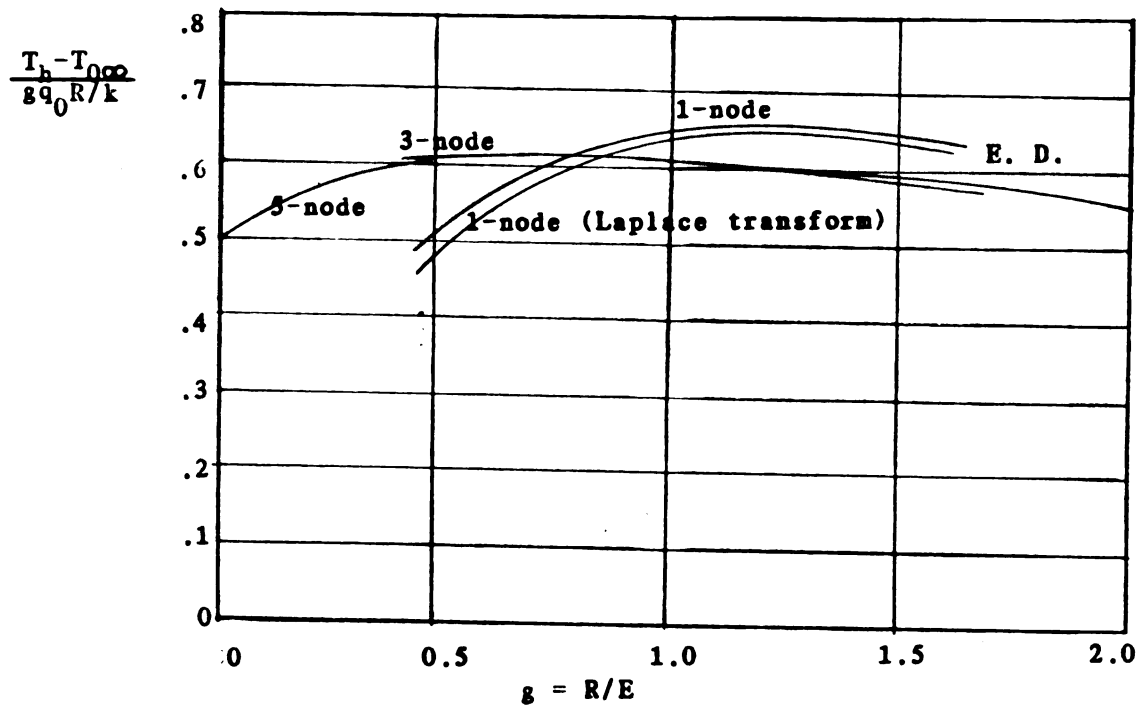
top of thermocouple

Figure 7.3 Quasi-steady state temperature at the

hot spot

Figutr 7.4 Quasi-steady state temperature at the

hot spot

CHAPTER 8

CONCLUSIONS

The multinode unsteady surface element method (MUSEM) and the quasi-steady state method for solution of the thermal cavity problem with linear boundary conditions and perfect contacting interface conditions have been presented. Both methods are developed from Duhamel's integral theroem and the principle of superposition. MUSEM involves a set of Volterra integral equation, one for each surface element. The quasi-steady state method involves a set of linear algebraic equations, one from the energy conservation principle and others from the interface conditions. In this thesis the radial surface of the thermocouple is assumed insulated and the thermal properties of the thermocouple are very small compared with those of surrounding material. The numbers of elements taken in this thesis are 1, 3 and 5 instead of several hundred that are required by the finite difference method.

From the results of calculations, the USEM and quasi-steady state methods can be concluded to have the following advantages compared with finite difference, finite element and boundary integral method.

1) They are more suitable for problems having infinite or semi-infinite space domain.

2) They are appororiate for problems having a finite contacting area between connected geometries. The number of elements needed to analyze the problem is fixed for USEM but must increase with time for

other related methods if the space domain of problem is infinite or semi-infinite and very large time periods are needed

3) They are suitable for problems if the number of location of interest is not large. The number of influence functions needed in the calculational procedure is proportional to the numbers of location of interest. In FD and FE methods the solution at all internal nodes is unavoidable generated, whether or not this information is needed.

4) They are suitable for problems having a small but important region, such as body 2 in the thermal cavity problem.

5) Extremely accurate solution can be obtained with very few elements compared with other related methods.

6) Simple analytical results can be obtained by using small number of nodes with the Laplace transform method.

The disadvantages of USEM are as follows:

1) A difficult part in the USEM is determining the influence functions in the integral equations of heat flow. If the derivation of the influence functions is restricted to use of Green's functions, it is not suitable for problems having irregular boundaries. But if the same problem is needed to be analyzed again and again, finite difference and finite element methods can be used to find the influence functions. Then this information can be used later to analyze the same or related problems.

2) It is not suitable for problems having temperature dependent thermal properties.

3) Since USEM is developed form Duhamel's integral, it is suitable for linear heat conduction equation. But the boundary conditions can

be linear or nonlinear. In particular, the radiative boundary condition can be investigated.

APPENDIX A

GENERAL EXPRESSION FOR θ^1_{ji}

The radial surface of solid cylinder with radius R and height E is divided into n equally-spaced surface element, each of which has height E/n and radius R, and is shown in Figure A.1. The center point in each element is called a node. θ^1_{ji} means the temperature rise at node j due to a unit step heat flux over surface element i and insulated over the rest of the area. It will be derived by using the Green's function.
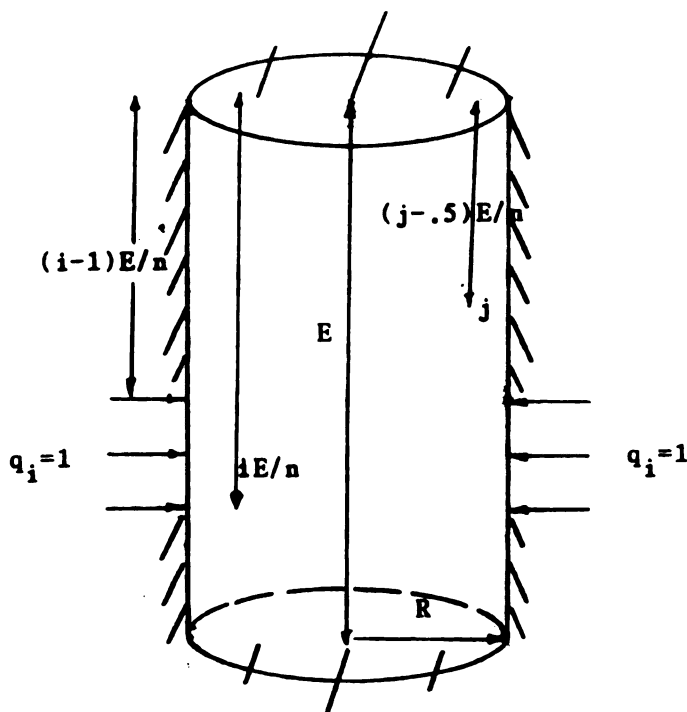

Figure A-1 Geometry representation of θ^1_{ji}

For the linear, transient heat conduction problems the Green's function method [6], [7], [14] and [15] is a simplified, systematic procedure for obtaining the solution.

Consider the following three-dimensional, nonhomogeneous boundary value problem of heat conduction.

$$\nabla^2 T(r,t) + g(r,t)/k = (1/a)\partial T(r,t)/\partial t \quad \text{in region R} \quad t > 0 \quad \text{(A-1a)}$$

$$k_i \partial T/\partial n_i + h_i T = f_i(r,t) \quad \text{on boundary } S_i \quad t > 0 \quad \text{(A-1b)}$$

$$T(r,t) = F(r) \quad \text{in region R} \quad t = 0 \quad \text{(A-1c)}$$

where k is the thermal conductivity, a is thermal diffusivity, $g(r,t)$ is the internal heat generation, $F(r)$ is the initial temperature distribution and $f_i(r,t)$ is the non-homogeneous term in the boundary conditions.

The solution of heat conduction problem (A-1) in terms of the Green's function $G(r,t|r',\tau)$ is given [6] as

$$T(r,t) = \int_R G(r,t|r',\tau)\big|_{\tau=0} F(r')dv'$$
$$+(a/k)\int_0^t [\int_R G(r,t|r',\tau)g(r',\tau)dv']d\tau$$
$$+a\int_0^t [\sum_{i=1}^m \int_{S_i} G(r,t|r,\tau)\big|_{r'=r_i} f_i(r,t)/k_i dS_i]d\tau \quad \text{(A-2)}$$

where the first term of (A-2) is due to the initial temperature distribution, the second term of (A-2) is from the internal heat generation and the third term comes from the nonhomogeneous boundary conditions.

The Green's function in (A-2) is satisfied by the following equations with the corrseponding homogeneous boundary conditions.

$$v^2 G(r,t|r',\tau) + (1/a)\delta(r-r')\delta(t-\tau) = (1/a)\partial G/\partial t \qquad t>\tau \qquad \text{(A-3a)}$$

$$k_i \partial G/\partial n_i + h_i G = 0 \qquad\qquad\qquad\qquad \text{on } S_i \; t>\tau \qquad \text{(A-3b)}$$

$$G(r,t|r',\tau) = 0 \qquad\qquad\qquad\qquad\qquad\qquad \text{if } t<\tau \qquad \text{(A-3c)}$$

where $\delta(r-r')$ is the three dimensional delta function for the space variable, that is, $\delta(x-x')\delta(y-y')\delta(z-z')$ for (x, y, z) coordinate, and so forth, and $\delta(t-\tau)$ is the delta function for the time variable. $\delta(r-r')\delta(t-\tau)/a$ represents an impulsive point heat source of strength unity located at r' and releasing its heat spontaneously at time τ. For the 1st kind boudary condition, which means that temperature is prescribed along the boundary surface, $k_i=0$; For the 2nd kind boudary condition, which means that normal derivative of temperature is prescribed along the boundary, $h_i=0$; For the 3rd kind boundary condition, which means that a linear combination of the temperature and its normal derivative is prescribed along the boundary, both k_i and h_i are not zero. More complex boundary conditions are included in [14].

The auxiliary problem (A-3) satisfied by the Green's function has homogeneous boundary conditions that are the homogeneous version of those for the original problem (A-1) and has an impusle point heat source and zero initial condition (i.e., medium at zero temperature for time $t<\tau$)

If there is no internal heat generator and initial temperature distribution is zero. The solution in terms of Green's function can be rewritten as

$$T(r,t) = \alpha \int_0^t d\tau \sum_{i=1}^m \int_{S_i} G(r,t|r',\tau)\Big|_{r'=r_i} f_i(r,t)/k_i dS_i \qquad (A-4)$$

Then θ_{ji}, the temperature rise at node j due to unit heat flux q_i with no heat generation and zero initial temperature distribution, can be expressed as

$$\theta_{ji}^1 = \alpha/k \int_0^t d\tau \int_{S'} G(r,t|r',\tau) \cdot_{r'=R} ds' \qquad (A-5)$$

where the unit heat flux q_i is over the radial surface of the solid cylinder from $a=z_{i-1}$ to $b=z_i$ and $r=R$ and

$$ds' = 2\pi R dz'$$

Two- and three- dimensional Green's functions can be found for many cases by simple multiplication of one-dimensional Green's function [14]. This is true for almost all of the boundary condition of rectangular system, provided the problem is linear, the body is homogeneous and the geometry is "simple". By simple geometry is meant that any boundary must be located only by one coordinate such as $x=0$ or $x=L$, but not at $x+y=0$,for example. For the cylindrical coordinate system one can use the multiplication method for the two-dimensional problem only for r, z coordinate and θ, z coordinate with the restrction of almost

constant value of r. For the spherical coordinate system no multiplication relation is possible for the one-dimensional Green's function to get two- or three-dimensional Green's function.

The one-dimensional Green's function of rectangular, cylindrical and spherical coordinate system can be found in [16], [17] and [18].

By the multiplication method, Θ_{ji} can be written as

$$\Theta_{ji}^1 = \alpha/k \int_0^t d\tau \int_a^b G_{R02} G_{X22} (2\pi R dz') \tag{A-6}$$

where

$$G_{R02} = [\ 1 + \sum_{m=1}^{\infty} \exp(-\alpha\beta_m^2(t-\tau)/R^2)\ ]/\pi R^2 \tag{A-7}$$

$$G_{X22} = [\ 1 + 2\sum_{m=1}^{\infty} \cos(n\pi z/E)\cos(n\pi z'/E)\exp(-n^2\pi^2\alpha(t-\tau)/E^2)\ ]/E \tag{A-8}$$

G_{R02} and G_{X22} are from [16] and [17], respectively. β_m is satisfied by the relation of $J_1(\beta_m)=0$, J_1 is the Bessel function of the first kind with order one. In general, G_{Rij} means the Green function in cylindrical coordinate with the ith kind of inner boundary condition and jth kind of outer boundary condition. G_{Xij} means the Green's function in rectangular coordinate with the ith kind of boundary condition on its left (or top) boundary and jth kind of boundary condition on its right (or bottom) boundary.

Substituting (A-7) and (A-8) into (A-6) gives

$$\theta_{ji}^{1+} = \theta_{ji}^1/(q_iR/K) = C_{ji} + 2t^+/n - A_1 - A_2 - A_3 \qquad (A-9)$$

where

$$A_1 = \sum_{m=1}^{\infty} 2\exp(-\beta_m^2 t^+)/\beta_m^2 \qquad (A-10)$$

$$A_2 = \sum_{n=1}^{\infty} 8\cos(n\pi z^+) \sin[n\pi(b^+-a^+)/2] \sin[n\pi(b^++a^+)/2]$$
$$\exp(-n^2\pi^2 g^2 t^+)/(n^3\pi^3 g^2) \qquad (A-11)$$

$$A_3 = \sum_{m=1}^{\infty}\sum_{n=1}^{\infty} 8\cos(n\pi z^+) \sin[n\pi(b^+-a^+)/2] \sin[n\pi(b^++a^+)/2]$$
$$\exp[-(\beta_m^2+n^2\pi^2 g^2)t^+]/[n\pi(\beta_m^2+n^2\pi^2 g^2)] \qquad (A-12)$$

$$t^+ = \alpha t/R^2$$

$$g = K/E$$

$$z_{j-1} = (j-1)E/n$$

$$z^+ = z/E; \qquad z = z_{j-1}+E/2n$$

$$b^+ = b/E; \qquad b = z_i; \qquad z_i = iE/n$$

$$a^+ = a/E; \qquad a = z_{i-1}$$

n is the number of equally-spaced surface elements

C^1_{ji} is the constant to be found

If $\alpha(t-\tau)/R^2 < .07$, G_{RO2} can be approximated [16] by

$$G_{RO2} = [\ (\pi\lambda)^{-1/2} + .5 + .75(\lambda/\pi)^{1/2} + 3\lambda/8 + 21\lambda^{3/2}/(32\pi^{1/2})\ ]$$
$$/(2\pi R^2) \tag{A-13}$$

where $\lambda = \alpha(t-\tau)/R^2$ \hfill (A-14)

An alternate form for G_{X22} [17] is given by

$$G_{X22} = \sum_{n=1}^{\infty} [\exp(-(2nE+x-x')^2/4\alpha(t-\tau))+\exp(-(2nE+x+x')^2/4\alpha(t-\tau))]$$
$$/(4\pi\alpha(t-\tau)^{1/2}) \tag{A-15}$$

Comparing (A-15) and (A-8), different expressions for G_{X22}, the t variable in the exponential terms is at the numerator for (A-8) while is the denominator for (A-15). So, (A-15) is suitable for the small time domain while (A-8) is appropriate for the large time domain. In the procedure of calculating the influence function, Θ_{ji}, if λ (i.e., $\alpha(t-\tau)/R^2$) is smaller than 0.07, (A-13) and (A-15) are used for G_{RO2} and G_{X22}, respectively. If λ is greater than 0.07, (A-7) and (A-8) are used for G_{RO2} and G_{X22}, respectively. Θ^1_{ji} can be rewritten as

$$\Theta^1_{ji} = 2\pi R\alpha/k \int_{\tau=0}^{t} d\tau G_{R20} \int_{a}^{b} G_{X22} dz' \tag{A-16}$$

where G_{R20}, equation (A-7) or (A-13), is not function of z.

For the case of $\alpha(t-\tau)/R^2 < .07$, $\int G_{X22}$ can be calculated by substituing equation (A-15) and using the following formulas,

$$\int_a^b G_{X22} dz' = [\ erf((z^++b^+)/2gt^{+1/2}) - erf((z^++a^+)/2gt^{+1/2}) +$$
$$erf((z^+-a^+)/2gt^{+1/2}) - erf((z^+-b^+)/2gt^{+1/2})\ ]/2$$

$$\text{for} \quad z^+ > b^+ \qquad \text{(A-17a)}$$

$$\int_a^b G_{X22} dz' = [\ erf((z^++b^+)/2gt^{+1/2}) - erf((z^++a^+)/2gt^{+1/2}) +$$
$$erf((b^+-z^+)/2gt^{+1/2}) - erf((a^+-z^+)/2gt^{+1/2})\ ]/2$$

$$\text{for} \quad z^+ < a^+ \qquad \text{(A-17b)}$$

$$\int_a^b G_{X22} dz' = [\ erf((z^++b^+)/2gt^{+1/2}) - erf((z^++a^+)/2gt^{+1/2}) +$$
$$2erf((b^+-z^+)/2gt^{+1/2}\ ]/2$$

$$\text{for} \quad z^+=(b^+-a^+)/2 \qquad \text{(A-17c)}$$

where $n=0$ is assumed in equation (A-15) in order to simplify the calculation of $\int_a^b G_{X22} dz'$.

In oder to calculate the constant C_{ji} in equation (A-9), the procedure of calculation are as follows:

Change the time variable in (A-6) and rearrange it

$$\theta_{ji}^1 = \alpha/k \int_{\lambda=0}^{t^+} [\ (R^2/\alpha) \int_a^b G_{R02} G_{X22} 2\pi R dz'\ ] d\lambda$$
$$= 2\pi R^3/k \int_{\lambda=0}^{t^+} d\lambda \int_a^b G_{R02} G_{X22} dz' \qquad \text{(A-18)}$$

Then divide the dimensionless time domain, λ, into two subregions. One is from 0 to 0.07; The other is from 0.07 to t^+. Then (A-18) can be rewritten as

$$\theta^1_{ji} = 2\pi R^3/k \int_{\lambda=0}^{.07} d\lambda \int_a^b G_{R20} G_{X22} dz' + 2\pi R^3/k \int_{.07}^{t^+} d\lambda \int_a^b G_{R02} G_{X22} dz'$$

$$(A-19)$$

The first term on the right hand side of (A-19) can be obtained by substituting equations (A-13) and (A-15) and using equation (A-17). The second term on the right hand side can be derived from (A-7) and (A-8) directly. After above calculations, (A-19) can be expressed as

$$\theta^{1+}_{ji} = C^1_{ji} + f(t^+)$$

$$(A-20)$$

Note that the expression (A-20) is a general one for the temperature rise at any point on the radial surface of solid cylinder due to unit step heat flux over the radial surface region from b to a. But (A-9) is a special one for the temperature rise at element j due to unit step heat flux over element i where the radial surface of solid cylinder is divided into n equally-spaced surface elements. exit

APPENDIX B

GENERAL EXPRESSION FOR Θ^2_{ji}

The symbol Θ^2_{ji} means that the temperature rise at node j of body 2 due to unit heat flux q_i over element i. Body 2 is a semi-infinite body outside a cylindrical void with radius R. The situation is shown in Figure B.1.

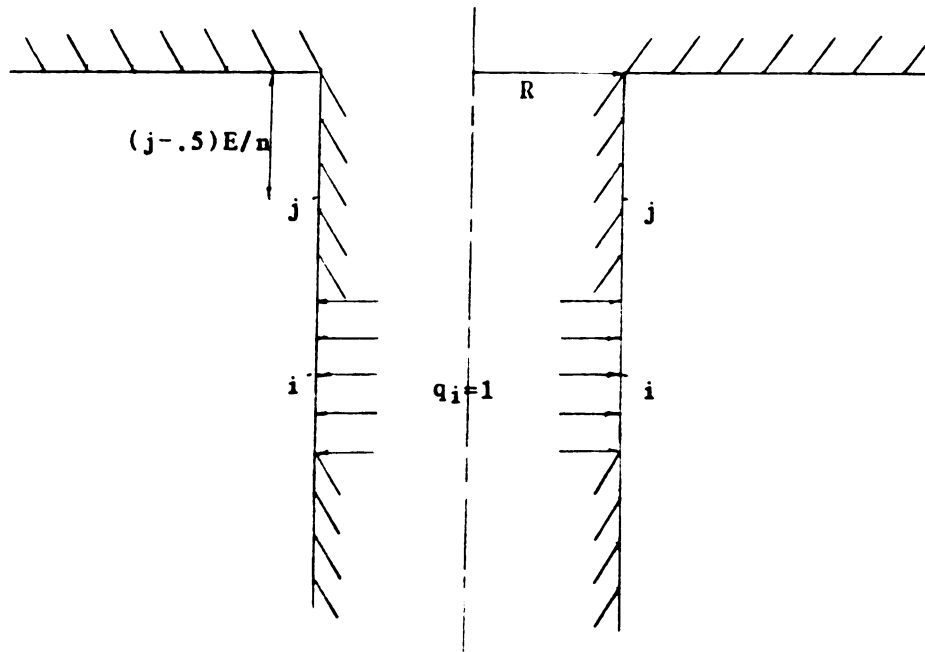Figure B-1 Geometry representation of Θ^2_{ji}

From the multiplication method of Green's function Θ^2_{ji} can be expressed as

$$\Theta^2_{ji} = \alpha/k \int_{\tau=0}^{t} d\tau \int_{S'} G_{R20} G_{X20} ds' \qquad \text{(B-1)}$$

125

where G_{R20} can be found in [16]

$$G_{R20} = (2/\pi^3 R^2)\int_0^\infty \exp(-\beta^2\lambda)[\beta(J_1^2(\beta)+Y_1^2(\beta))]^{-1}d\beta \qquad (B-2)$$

where $\qquad \lambda=\alpha(t-\tau)/R^2 \qquad\qquad\qquad\qquad\qquad (B-3)$

The integral form of G_{R20} is not easy to manipulate. For simple analysis the time domain of G_{R20} is subdivided into two parts, which are small time domain and large time domain. For each time domain there is a simple expression that can approximate (B-2). In this case the time domain is divided at dimensionless time $\lambda=6$.

For $\lambda<6$, by the least square error method with the polynomial model, the best one is given as

$$G_{R20}=(2\pi R^2)^{-1}[\ (\pi\lambda)^{-1/2} - .5 + .413434\lambda^{1/2} - .299877\lambda$$
$$+ .154483\lambda^{3/2} -.045263\lambda^2 +.005484\lambda^{5/2}] \qquad (B-4)$$

The values of (B-4) and (B-2) can be compared to check the accuracy of the approximate expression of G_{R20} for the small time domain. For example,

at $\lambda=1$ the value of (B-2) is 0.2926330

the value of (B-4) is 0.2924500

the relative error is .0625%

at $\lambda=6$ the value of (B-2) is .0680578

the value of (B-4) is .0682995

the relative error is .355%

For the case of $\lambda > 6$, G_{R20} can be expressed [16] by

$$G_{R20} = [1 - L(1+3(1-L)/4\lambda)/2\lambda - (\pi^2+4)/32\lambda]/(4\pi R^2\lambda) \qquad \text{(B-5)}$$

where

$L = \log(4\lambda) - \gamma$

$\gamma = .57722$, which is called Euler number.

G_{X20} can be found [17] to be

$$G_{X20} = [\exp((z-z')^2/4\alpha(t-\tau)) + \exp((z+z')^2/4\alpha(t-\tau))]$$
$$/(4\pi\alpha(t-\tau))^{1/2} \qquad \text{(B-6)}$$

Since G_{R20} is not function of z, (B-1) can be rewritten as

$$\int_S G_{R20}G_{X20}ds' = 2\pi R G_{R20}\int_a^b G_{X20}dz' \qquad \text{(B-7)}$$

where $\int_a^b G_{X20}dz'$ can be obtained by (A-17)

Define $\int_a^b G_{X20}dz' = F \qquad \text{(B-8)}$

Substituting (B-8) into (B-7) and changing the time variable obtains

$$\Theta_{ji}^2 = 2\pi R/k \int_0^{t^+} FG_{R20} d\lambda \tag{B-9}$$

The time domain λ in (B-9) can be subdivided into two region. One is from 0 to 6; The other is from 6 to t^+. (B-9) can be rwwritten as

$$\Theta_{ji} = 2\pi R/k \int_0^6 FG_{R20} d\lambda + 2\pi R/k \int_6^{t^+} FG_{R20} d\lambda \tag{B-10}$$

For the case of $\lambda < 6$, only the first term of the right hand side (B-10) is needed to calculate. This term contains the integration of expressions of the combination of polynomial and complemetery error function, which can be solved by the following relations.

$$\int_a^b U^{(2n-3)/2} erfc(aU^{-1/2}) dU = 2t^{(2n-1)/2} [erfc(at^{-1/2}) -$$
$$aE_n(a^2/t)(\pi t)^{-1/2}]/(2n-1) \quad n=1,2,3... \tag{B-11}$$

$$\int_a^b U^n erfc(aU^{-1/2}) dU = [t^{n+1}/(n+1) + (-1)^n 2^{n+1} a^{2n+2}/$$
$$(n+1)(2n+1)(2n-1)...1] erfc(at^{-1/2}) + \sum [(-1)^{n-k}$$
$$2^{n-k+2} a^{3+2n-2k} t^{(2k-1)/2} exp(-a^2/t)]/(n+1)(2n+1)(2n-1)...$$
$$(2k-1)\pi \quad n=1,2,3,.... \tag{B-12}$$

where E_n ie the exponential integral function with order n

$$E_n(z) = \int_1^\infty exp(-zt)/t^n dt \tag{B-13}$$

The value and formulas of (B-13) can be found in [19]

For the case of $\lambda > 6$, it is difficult to calculate the second term of the right hand side of (B-10) analytically. Since the value is very small compared with that of the first term, (B-10) can be approximated as

$$\theta_{ji} = 2\pi R/k \int_0^6 FG_{RO2} d\lambda + \sum_{h=1}^{m} 2\pi R/k [FG_{RO2}] \Delta t \qquad (B-14)$$

where $FG_{RO2}(h) = FG_{RO2}[6+(h-1/2)\Delta t]$ $\qquad$ (B-15)

GENERAL EXPRESSION OF $\theta^1_{n+1,i}$

$\theta^1_{n+1,i}$ is the temperature rise at the n+1th node, the center point of the bottom surface, of the solid cylinder due to unit heat flux over the element i, which is from $z_{i-1}=a$ to $z_i=b$, and is shown in Figure C-1.
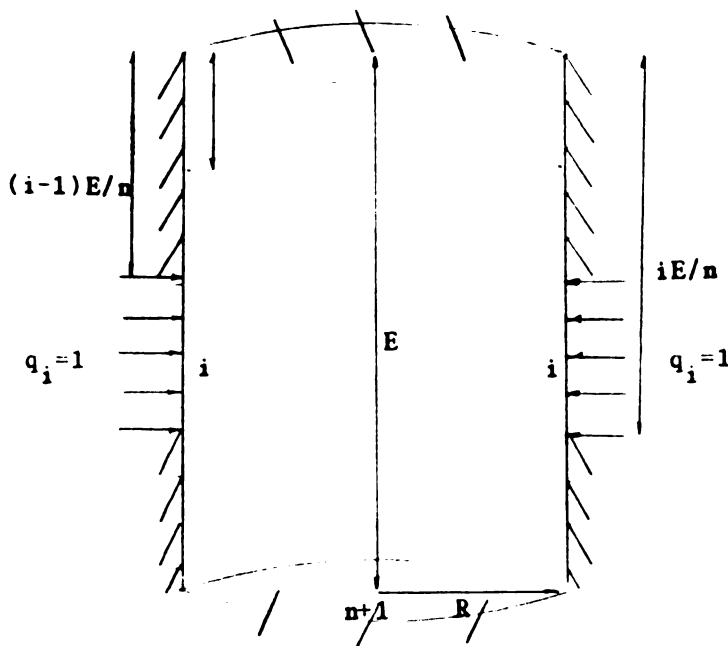

Firgue C-1 Geometry representation of $\theta^1_{n+1,i}$

From the multiplication method of Green's function $\theta^1_{n+1,i}$ can be expressed as

$$\theta^1_{n+1,i}=\alpha/K\int_{=0}^{t}d\tau\int_{S}G_{R02}G_{X22}ds' \qquad (C-1)$$

where $ds'=2\pi R dz'$; α and k are the thermal conductivity and thermal diffusivity of the material.

$$G_{R02} = [\; 1+\sum_{m=1}^{\infty}\exp(-\alpha(t-\tau)\beta_m^2/R^2)/J_0(\beta_m)\;]/\pi R^2 \qquad (C-2)$$

where $J_1(\beta_m)=0$, J_1 is the Bessel function of the first kind with order one and J_0 is the Bessel function of the first kind with order zero.

$$G_{X22} = [\; 1+2\sum_{n=1}^{\infty}\cos(n\pi z'/E)\exp(n^2\pi^2\alpha(t-\tau)/E^2)\;]/E \qquad (C-3)$$

Substituting (C-2) and (C-3) into (C-1), one obtains

$$\theta_{n+1,i}^{1+} = 2t_{/n}^{+} + C_{n+1,i}^{1} - A_1 - A_2 - A_3 \qquad (C-4)$$

where n is the number of equally-spaced surface elements on the radial surface of the solid cylinder

$$A_1 = \sum_{m=1}^{\infty} 2\exp(-\beta_m^2 t^+)\; /n\beta_m^2 J_0(\beta_m) \qquad (C-5)$$

$$A_2 = 4\sum_{n=1}^{\infty}[\; \sin(n\pi b/E)-\sin(n\pi a/E)\;]\exp(-n^2\pi^2 g^2 t^+)/(n^3\pi^3 g^2) \qquad (C-6)$$

$$A_3 = 4\sum_{n=1}^{\infty}\sum_{m=1}^{\infty}[\; \sin(m\pi b/E)-\sin(m\pi a/E)\;]\exp[-(\beta_n^2+m^2\pi^2 g^2)t^+]$$
$$/(m\pi(\beta_n^2+m^2\pi^2 g^2)J_0(\beta_n)) \qquad (C-7)$$

For very small times $t^+ <.01$, $\theta_{n+1,i}^{1}$ is approximately 0.

$$\theta^1_{n+1,i} = a/K \int_0^{.01} d\tau \int_S G_{R02} G_{X22} ds'$$
$$+ a/k \int_{.01}^t d\tau \int_S G_{R02} G_{X22} ds' \qquad (C-8)$$

$$\theta^1_{n+1,i} = 0 + a/K \int_{.01}^t d\tau \int_S G_{R02} G_{X22} ds' \qquad (C-9)$$

$$\theta^{1+}_{n+1,i} = C^1_{n+1,i} - f(t^+) \qquad (C-10)$$

The value of $C^1_{n+1,i}$ can be obtained by substituting (C-2) and (C-3) into (C-9). So, (C-4) is suitable for the case of t^+ greater than 0.01.

LIST OF REFERENCE

1. Keltner, N. R. and Beck, J. V., "Unsteady Surface Element Method," Journal of Heat Transfer, Vol. 103, pp. 759-764, 1981.

2. Beck, J. V. and Keltner, J. V., "Transient Thermal Contact of Two Semi-Infinite Bodies over a Circular Region," AIAA paper No. AIAA-81-1162.

3. B. Litouhi and Beck. J. V., "Multinode Unsteady Surface Element Method with Application to Contact Conductance Problem,"

4. B. Lithouhi and Beck, J. V., "Intrinsic Thermocouple Analysis Using Multinode Unsteady Surface Element Method," AIAA paper No. AIAA-83-1437.

5. Beck, J. V. and H. Hurwicz, "Effect of Thermocouple Cavity on Heat Sink Temperature," Journal of Heat Transfer, Vol. 82, No. 1, pp. 27-36, Febrary 1960.

6. M. Necati Ozisik, Heat Conduction, John Wiley and Sons, New York, 1980

7. Carslaw and Gaeger, Conductance of Heat in Solid, Cambridge University Press, Cambridge, 1959.

8. Beck, J. V. and Keltner, N. R., "Influence Function for Unsteady Surface Element Method,"

9. Master, J. L. and Stein, S., "Effect of an Axial Cavity on the Temperature History of a Surface Heated Solid," Review of Scientific Instrumentation, Vol. 27, pp. 1065-1069, 1956.

10. Bussell, B., "Analog Study of a Thermocouple Instrumentation Error," Dept. of Engineering, University of California, Los Angeles, August 1957.

11. Chin Jen Chen and Peter, Li, "Minimization of Temperature Distortion in Thermocouple Cavity,"

12. , "Standard Method for Measuring Extreme Heat-Transfer Rate from High-Energy Enviroments Using a Transient Null-Point Calorimeter," ANSI-ASTM E593-77

13. Beck, J. V., David H., Y. Yen and Bryan Johnon, "Steady state Temperature Distribution for Infinite Region Outside a Partially Heated Cylinder," ASME paper No. 82-HT-24 and Chem. Eng. Comm., Vol 26, Nos 4-6, pp. 355-367.

14. Beck, J. V., "Green's Function Solution for Transient Heat Conduction Problem," *Int. J. Heat and Mass Transfer*, Vol. 27, No. 8, pp.1235-1244, 1984

15. Beck, J. V., "Green's Function and Numbering System for transient Heat Conduction," AIAA 19th Thermophysics Conference, June 25-28 1984, Snowmass, Colorado. AIAA-84-1741.

16. Beck, J. V., "Radial Direction Green's Function-Cylindrical Coordinate," Dept. of Engineering, Michigan State University, Heat Transfer Group, Nov. 1982.

17. Beck, J. V., "Green's function-Rectangular Coordinate," Dept. of Engineering, Michigan State University, Heat Transfer Group, Aug. 1982.

18. Beck, J. V., "Green's Function for Radial Spherical Coordinate," Dept. of Engineering, Michigan State University, Heat transfer Group,

19. Abramowitz, M. and Stegun, T. A., *Handbook of Mathematical Functions, with Formulas, Graphes and Mathematical Tables*, National Bureau of Standards, Applied Kathematics Series, Vol. 55, 1964.